# DEVELOPMENT OF MULTILAYER PLA/GRAPHENE NANOCOMPOSITES WITH HIGH OXYGEN BARRIER PROPERTIES

Ву

Xinyi Wang

# A THESIS

Submitted to
Michigan State University
in partial fulfillment of the requirements
for the degree of

Packaging—Master of Science

2019

#### **ABSTRACT**

# DEVELOPMENT OF MULTILAYER PLA/GRAPHENE NANOCOMPOSITES WITH HIGH OXYGEN BARRIER PROPERTIES

Ву

#### Xinyi Wang

Poly(lactic acid) (PLA) films were coated with chitosan and chitosan-graphene (chitGRH) layers. To prepare the coating layers, first, graphite was added directly into chitosan acid solution. After 30 min of ultrasonication, graphene layers in graphite were dispersed evenly in the solution due to the similar surface energies between chitosan and graphene. Chitosan acid solution was also ultrasonicated for 30 min. Before coating, PLA films were treated with oxygen plasma at 300 Watt for 10 min on both sides to enable evenly coating of chitosan solution distribution on PLA's surface. Then, a roll coating machine was used to apply 3 or 10 layers of chitosan or chitGRH solution on each side of the PLA films. Thicknesses of the coating layers were determined by a scanning electron microscope. Thermal gravimetric analysis and differential scanning calorimetry studies showed that the coating layers did not affect PLA's bulk properties (i.e., glass transition and melting temperatures, and crystallinity). Oxygen permeability (OP) tests were conducted at 23°C and 0, 30, 60, and 90% relative humidity (RH). Oxygen plasma treatment did not affect the OP of the coated PLA films. The addition of both chitosan and chitGRH layers reduced the OP of PLA films by three order of magnitude at 0% RH. The effectiveness of chitosan on reducing the OP of the multilayer structure depended on the test RH due to chitosan hydrophilicity. ChitGRH was more effective to reduce OP at 60% RH. The development of PLA- chitGRH multilayer films open the possibility of producing compostable high oxygen barrier multilayer films.

Copyright by XINYI WANG 2019



#### **ACKNOWLEDGEMENTS**

I would like to express my deepest appreciation to my major advisor, Dr. Rafael Auras. He is the most supportive, most patient, kindest, and sharpest advisor that a graduate student can ever get. His gave me much freedom to work on the directions that I wanted to, and at the pace I felt comfortable with. Meanwhile, he always corrected me and provided me suggestions when I got lost. During my thesis writing, Dr. Auras's professionalism urged me to think about my thesis in a deeper way, and his encouragement helped me to finish it on time. He is not only an advisor in research, but also in life. My experience working with Dr. Auras changed my way of thinking and doing things a lot in a good way. I hope in the future we can work together again.

I want to say thank you to my colleagues, Uruchaya and Ilke, for their help and guidance in my research. Whenever I asked Uruchaya a question, she always answered me in a very detailed way that I could quickly understand. When she was not the correct person to go to, she would navigate me to the person that I can get the answer. Also, Uru's review paper inspired and guided me a lot on my thesis. Ilke was the one that taught me everything at the very beginning of my research, including experimental methods, critical thinking, data analysis, etc. The coating solution preparation method in this thesis was also retrieved from her study.

I wish to thank my friends that significantly affected me during these three years, Pengfei, Zhao, Suihan, Jin, Sonal, Wanwarang, Vijay, Kexin, Amrut, Anibal. Thanks to Pengfei and Zhao for being my roommates. They both listened to me a lot for my happy things, sad things, complaints on different things, or just nonsense. This intensively relaxed me when I was stressful due to the study or the research. Thanks to Suihan for being a "teacher" and a "prosecutor" of me. Suihan

has more experience than me in both life and research. She never hesitated to share her experience with me and guided me to the correct way. I totally trust her and believe that every single piece of suggestion from her was due to her consideration of me. Thanks to Jin for always taking care of me. Jin is the person who told me how nice Dr. Auras was, and indirectly lead me to join his group. She is very good at doing follow-up job. I asked for much help from her, sometimes she could help me, sometimes not. However, she always doublecheck if her solutions helped me or if my problems got solved, which was very sweet. Thanks for Sonal and Yuzhu for being my officemates and giving me advices on mass transfer mechanism and experimental design within the first two years. Thank you to Wanwarang for always consider me as her friend. She always told me the solutions of a potential problem that I would face, even though I hadn't asked her yet. This saved me a lot of time during my thesis writing and submission. Thank you to Vijay and Amrut for taking care of me during my internship. They also texted and called me a lot telling me "Write fast, you have to graduate in May." Without their continuous encouragement, I could not finish everything on time. Thanks to Kexin for being such an incredibly relaxing friend. All the time I spent with her was fulfilled with "HAHAHA", which relaxed me during the struggling times in research and study. Last but not the least, thanks to Anibal for caring about me, providing suggestions, and being my mental support in the first two years.

I owe my most sincere gratitude to my parents, Song Wang, and Changyan Xu. It was them that convinced me to come to the U.S. for graduate study, which lead me to know such many good friends. Also, they are always my mental support that I know they will protect me no matter what happened. I have made a lot of willful decisions without discussing with them in these 3

years, thanks for all the understanding and still being supportive. Thinking about them, I felt I am invincible.

I know it is a big wish, but I still want to wish everyone that I met a bright future, wish everything happen to them is good thing, and every good thing happens to them. I will never know how I would be if I haven't met them here and there. However, even though I am not perfect, I am always improving and learning from each one of them. Most importantly, I like myself right now. I believe that it was all the experience that I had with everyone, good or bad ones, that made me become a Xinyi now. Thus, I want to thank everyone for showing up in my life and again, wish you all the best.

# TABLE OF CONTENTS

LIST OF TABLES	x
LIST OF FIGURES	xi
KEY TO SYMBOLS AND ABBREVIATIONS	xiii
1. INTRODUCTION	1
1.1 Background and Motivation	1
1.2 Overall Goal and Objectives	3
REFERENCES	4
2. LITERATURE REVIEW	9
2.1 Oxygen Permeability	9
2.1.1 Food Packaging	9
2.1.2 Principle of Permeation	9
2.1.3 Factors affecting permeation	12
2.2 Poly(lactic acid)	13
2.2.1 Introduction	13
2.2.2 Oxygen Barrier	14
2.2.3 Surface Modification	17
2.2.4 PLA Coated Films	18
2.3 Graphene	20
2.3.1 Introduction	20
2.3.2 Production	21
2.3.3 Oxygen Barrier Improvement	22
2.4 Chitosan	25
2.4.1 Introduction	25
2.4.2 Production	25
2.4.3 Properties	27
2.4.4 Chitosan/Graphene Composite	30
REFERENCES	31
3. MATERIALS AND METHODS	41
3.1 Materials	41
3.2 Methods	41
3.2.1 Home-Made PLA Films Production	41
3.2.2 Preparation of Chitosan Water Solution	42
3.2.3 Production of Chitosan-Graphene Water Solution	42
3.2.4 Plasma Treatment	42
3.2.5 Preparation of HPLA-Coating-HPLA-HP Film	43

3.2.6 Preparation of LLDPE-Coating	ng-LLDPE-HP Film44
	Film45
3.2.8 Preparation of Coating-PLA-	Coating Film46
	47
3.2.10 Film Thicknesses	48
3.2.11 Characterization of the m	ultilayer structures48
3.2.12 Thermal Properties	49
3.2.13 Oxygen Permeability	49
3.2.14 Statistical Analysis	50
REFERENCES	51
4. RESULTS AND DISCUSSION	53
4.1 Preliminary Study	53
4.1.1 HPLA-Coating-HPLA-HP Film	53
4.1.2 LLDPE-Coating-LLDPE-HP Fil	m56
4.2 PLA-Coating Film	59
4.2.1 Morphology	59
4.2.2 Thermal Properties	62
4.3 Coating-PLA-Coating Film	72
4.3.1 Thermal Properties	72
4.3.2 Oxygen Barrier Properties	72
APPENDIX	83
REFERENCES	95
5. CONCLUSION AND RECOMMENDAT	FIONS99
5.1 Conclusions	99
5.2 Recommendations	102
REFERENCES	104

# LIST OF TABLES

<b>Table 2-1. Tentative PLA crystalline structures below</b> $T_g$ , adapted from [5]	15
Table 2-2. Oxygen permeability of PLA and other common packaging materials under	various
temperatures and RH conditions.	15
Table 2-3. Oxygen and water barrier properties of chitosan films.	28
Table 2-4. Physical properties of chitosan film.	30
Table 4-1. OP value of HPLA-coating-HPLA-HP films at 23°C, 0% RH.	55
Table 4-2. OP value of LLDPE-coating-LLDPE-HP films at 23°C, 0% RH	57
Table 4-3. TGA results of PLA, chitosan, and graphite	65
Table 4-4. TGA results of coated PLA films.	66
Table 4-5. DSC parameters of PLA and coated PLA films	68
Table 4-6. Thickness and OP value of PLA and chit coated PLA films at 23°C, 0% or 50%	<b>RH.</b> 70
Table 4-7. OP values of coating-PLA-coating films, control films, and chit coating films	at 23°C.
	73

# LIST OF FIGURES

Figure 2-1. Steady state of permeation through a membrane
Figure 2-2. Synthesis of high molecular weight (MW) PLA, adapted from [11]14
Figure 2-3. Arrhenius plot of OP at 70% RH, adapted from [27]
<b>Figure 2-4. Effects of coating on PLA film on OP value.</b> References: <sup>a</sup> [16], <sup>b</sup> [22], <sup>c</sup> [25], <sup>d</sup> [39], <sup>e</sup> [26], <sup>f</sup> [38] The numbers on bottom of the bar are <i>P</i> x 10 <sup>-20</sup> kg m m <sup>-2</sup> s <sup>-1</sup> Pa <sup>-1</sup> of pure PLA film used in corresponding experiments except in reference <sup>a</sup> ( <i>P</i> of PLA-PLA film). Number in PLA multilayer coating names are numbers of coating been applied in corresponding experiments. Abbreviations GO = graphene oxide, rGO = reduced graphene oxide, MMT = montmorillonite, polyGalA = pectin (polygalacturonic acid), NFC <sup>d</sup> = cationic cellulose nanofiber, PEI = polyethyleneimine, NFC <sup>e</sup> = polyethyleneimine, CMC = carboxymethyl cellulose, ALG = sodium alginate, N/A = not available.
Figure 2-5. Illustration of graphene structure, adapted from [40]
<b>Figure 2-6. Effects of graphene on OP value.</b> References: a [60], b [17], c [54], d [57], e [61]24
Figure 2-7. Extraction of chitin and fabrication of chitosan, adapted from [68]26
Figure 2.8. Preparation of HPLA-Coating-HPLA film
Figure 2.9. Preparation of LLDPE-Coating-LLDPE film45
Figure 2.10. Preparation of PLA-Coating film46
Figure 2.11. Preparation of Coating-PLA-Coating film47
Figure 2.12. Preparation of coating film48
<b>Figure 4-1. OP distribution of HPLA-coating-HPLA-HP films at 23°C, 0% RH.</b> Same color name corresponds to same color data. One data represents one measurement
Figure 4-2. (a) HPLA film sample used for HPLA-coating-HPLA-HP, (b) HPLA film with colored chit coating.

Figure 4-3. Single layer LLDPE films with or without coating
<b>Figure 4-4. OP distribution of LLDPE-coating-LLDPE-HP films at 23°C, 0% RH.</b> Same color name corresponds to same color data
Figure 4-5. Cross-sections of (a) PLA film, (b) PLA-20chit film, (c) 20chit coating part on PLA film, and (d) curvature of PLA-20chit film. PLA and coating part were labeled. The unlabeled part in (d) is the bottom surface of PLA film
<b>Figure 4-6. EDX line scan of N, O, and C distribution of PLA-20chit.</b> (a) N distribution, (b) O distribution, (c) C distribution, and (d) SEM image of PLA-20chit61
Figure 4-7. TGA thermograms of tested samples.
Figure 4-8. DSC plots of the second heating cycle of PLA and coated PLA films67
<b>Figure 4-9. OP distribution of PLA and chit coated PLA films at 23°C, 0% or 50% RH.</b> Same color name corresponds to the same color data71
<b>Figure 4-10. Effect of relative humidity to OP value at 23°C and various RH.</b> (a) PLA, (b) PLA-2p. A Data in the same plot sharing the same capital letter had no significant difference
<b>Figure 4-11. Effect of relative humidity to OP value at 23°C and various RH.</b> (a) 3chit-PLA-3chit, (b) 10chit-PLA-10chit, (c) 3chitGRH-PLA-3chitGRH, (d) 10chitGRH-PLA-10chitGRH. A Data in the same plot sharing the same capital letter had no significant difference
<b>Figure 4-12. Effect of numbers of coating layers to OP value at 23°C and various RH.</b> A Data sharing the same capital letter with the same relative humidity in one plot were had no significant difference.
<b>Figure 4-13.</b> Effect of graphene in coating layers to OP value at 23°C and various RH. A Data sharing the same capital letter with the same relative humidity in one plot had no significant difference.
<b>Figure 4-14. Effect of storage condition on OP of 3chit-PLA-3chit at 23°C.</b> A Data sharing the same capital letter with the same relative humidity had no significant difference. Data in "with condition" or "without condition" series sharing the same lowercase letter were not significantly difference.
Figure 4-15. Comparison of calculated and experimental OP values of 3chit-PLA-3chit at 23°C

#### **KEY TO SYMBOLS AND ABBREVIATIONS**

CF crystalline fraction chitosan acid solution chit chitGRH chitosan-graphene acid solution DSC differential scanning calorimeter Ер activation energy EVA = ethylene-vinyl alcohol GRH graphene ΗP Hot-pressed Home-made PLA film HPLA = LLDPE linear low-density polyethylene MAF Mobile amorphous fraction OP oxygen permeability Ρ permeability PLA poly(lactic acid) = rigid amorphous fraction RAF RMS root mean square SEM scanning electron microscope temperature Τ =  $T_e$ end decomposition temperature

$T_g$	=	glass transition temperature
TGA	=	thermogravimetric analysis
$T_m$	=	melting temperature
T <sub>max</sub>	=	maximum temperature
$T_{o}$	=	onset temperature
wt%	=	weight percentage
wtL	=	weight loss
$X_c$	=	degree of crystallinity
$\Delta H_c$	=	crystallization enthalpy
$\Delta H_m$	=	melting enthalpy

#### 1. INTRODUCTION

# 1.1 Background and Motivation

Plastics are wildly being used everywhere in people's lives since they are lightweight, cheap, versatile, and mass producible [1]. Rochman *et al.* estimated that the amount of plastic produced by 2050 will be 33 billion tonnes [2]. In 2015 in the U.S., among the total of 34.5 millions of tons plastic generated in municipal solid waste (MSW), only 9.1% was recycled [3]. These facts, as well as the immense use of petrobased plastics such as polyolefins, poly(ethylene terephthalate), and nylon, urged researchers to study their effects on the environment [2] and search for substitutes of these plastics.

Carbon is the main building block of all plastics. After disposal, they are producers of CO<sub>2</sub> emissions. So, reducing CO<sub>2</sub> emissions due to the use and disposal of fossil plastics is crucial to slow down climate change. Biobased plastics have gaining attention from researchers due to their low carbon footprint value since the amount of CO<sub>2</sub> that biobased plastics emitted during their end of life (e.g., decomposition or incineration) is equal to the amount of carbon that they absorbed during the growing of the biobased resources [1].

Among the many biobased and biodegradable plastics, poly(lactic acid) (PLA) has been extensively studied so far [4]. Some of the advantages that PLA provides are: 1) PLA is derived from renewable sources including corn and sugar canes [5]; 2) PLA can be mass produced [4]; 3) PLA has comparable mechanical properties, heat sealing properties, as well as CO<sub>2</sub> and O<sub>2</sub> barrier properties as PS [6]. PLA has been extensively studied in the area of food packaging materials

[7,8], sustainable barrier applications [9,10], and medicine [11,12]. The U.S. Food and Drug Administration has already approved PLA to be used as food packaging material [13].

Oxygen barrier property is important for food packaging materials and applications since food spoilage can readily happen due to the reaction between oxygen and food [14]. Reactions between lipids and oxygen can drastically influence the flavor of food products, shorten their shelf life, and produced aldehydes and derivatives that are toxic to human bodies [14,15]. Oxygen permeability (OP) is the main parameter used to describe the permeation of oxygen molecules through packaging materials from one side to another side. OP of a material depends on several factors including the amount of oxygen molecules permeated per unit time, area that permeation occurred, thickness of the membrane, oxygen partial pressure at two sides of the material [4], composition of the membrane [16], morphological structure of the membrane, and oxygen barrier testing conditions [17]. An OP that is smaller than 5 x 10<sup>-20</sup> kg m m<sup>-2</sup> s<sup>-1</sup> Pa<sup>-1</sup> for films with a thickness of 20 μm at 23°C and 1 atm is considered high oxygen barrier for packaging materials [18]. OP of pure PLA films at 5-58°C are aggregated around 0.5  $\pm$  0.7 x 10<sup>-17</sup> kg m m<sup>-2</sup> s<sup>-1</sup> Pa<sup>-1</sup> [4– 6,8,19–23]. Thus, researchers have worked on improving PLA's oxygen barrier property. Among all the methods, coating technique stands out due to the precision on thickness control [24], and the protection that coating layers provide to the substrate films.

Graphene has attracted a lot attention in the last decade due to its extraordinary properties, including Young's modulus (1,100 GPa), fracture strength (125 GPa), and electrical conductivity (1,000 S cm<sup>-1</sup>) [25]. Graphene and graphene-containing materials are strong oxygen barrier material due to: 1) graphene flakes can add tortuosity for oxygen molecules to diffuse during permeation; and 2) the lattice constant of graphene (0.245 nm) [26] is smaller than the

kinetic diameter of the oxygen molecules (0.346 nm) [27]. However, the high specific surface area (2,630 m $^2$  g $^{-1}$ ) of graphene [25] causes it to aggregate when added to hydrophobic materials. Chitosan has been shown to enhance the dispersion of graphene in materials and solvents [28,29]. Graphene can be well dispersed in chitosan acid aqueous solution after ultrasonication [28]. The dispersed chitosan graphene can be introduced into PLA and improve its oxygen permeability since OPs of pure chitosan films (10-25°C, 0-75% RH) range from 0.7 x  $10^{-20}$  to  $56 \times 10^{-20}$  kg m m $^{-2}$  s $^{-1}$  Pa $^{-1}$  [30–35]. Chitosan is an abundant natural resource from shells of crustaceans [36].

PLA is a good candidate of food packaging materials; however, it has lower OP. Chitosan and graphene can reduce oxygen molecules permeation. The use of PLA and graphene dispersed in chitosan can open the doors to the exploration of new materials, allowing researchers to fill the knowledge gap of the oxygen permeation mechanism of chitosan-graphene coated on PLA.

#### 1.2 Overall Goal and Objectives

The overall goal of this thesis is to understand how chitosan-graphene coating affects oxygen barrier properties of PLA films over a wide range of relative humidity. The specific objectives are:

- 1) To develop an effective way to apply chitosan-graphene coating on PLA films.
- 2) To create multilayer chitosan-graphene coating layers on PLA films.
- To understand the effect of adding the coating layers on the thermal properties of PLA films.
- 4) To understand the effect of the coating layers and compositions on the oxygen permeability of PLA and PLA coated films at different temperatures and relative humidity.

**REFERENCES** 

#### REFERENCES

- [1] Narayan R. Carbon footprint of bioplastics using biocarbon content analysis and life-cycle assessment. MRS Bull 2011:716–21. doi:10.1557/mrs.2011.210.
- [2] Rochman CM, Browne MA, Halpern BS, Hentschel BT, Hoh E, Karapanagioti HK, et al. Classify plastic waste as hazardous. Nature 2013;494:169–71. doi:10.1021/es303700s.
- [3] Environmental Protection Agency U, of Land O, Management E, of Resource Conservation O. Advancing Sustainable Materials Management: 2015 Fact Sheet Assessing Trends in Material Generation, Recycling, Composting, Combustion with Energy Recovery and Landfilling in the United States. 2018.
- [4] Sonchaeng U, Iñiguez-Franco F, Auras R, Selke S, Rubino M, Lim LT. Poly(lactic acid) mass transfer properties. Prog Polym Sci 2018;86:85–121. doi:10.1016/j.progpolymsci.2018.06.008.
- [5] Auras R, Harte B, Selke S. An Overview of Polylactides as Packaging Materials. Macromol Biosci 2004;4:835–64. doi:10.1002/mabi.200400043.
- [6] Auras RA, Harte B, Selke S, Hernandez R. Mechanical, physical, and barrier properties of poly(lactide) films. J Plast Film Sheeting 2003;19:123–35. doi:10.1177/8756087903039702.
- [7] Goh K, Heising JK, Yuan Y, Karahan HE, Wei L, Zhai S, et al. Sandwich-Architectured Poly(lactic acid)—Graphene Composite Food Packaging Films. ACS Appl Mater Interfaces 2016;8:9994–10004. doi:10.1021/acsami.6b02498.
- [8] Ambrosio-Martín J, López-Rubio A, José Fabra M, Angel López-Manchado M, Sorrentino A, Gorrasi G, et al. Synergistic effect of lactic acid oligomers and laminar graphene sheets on the barrier properties of polylactide nanocomposites obtained by the in situ polymerization pre-incorporation method. J Appl Polym Sci 2016;133:1–11. doi:10.1002/app.42661.
- [9] Meriçer Ç, Minelli M, Angelis MGD, Giacinti Baschetti M, Stancampiano A, Laurita R, et al. Atmospheric plasma assisted PLA/microfibrillated cellulose (MFC) multilayer biocomposite for sustainable barrier application. Ind Crops Prod 2016;93:235–43. doi:10.1016/j.indcrop.2016.03.020.
- [10] Byun Y, Rodriguez K, Han JH, Kim YT. Improved thermal stability of polylactic acid (PLA) composite film via PLA–β-cyclodextrin-inclusion complex systems. Int J Biol Macromol

- 2015;81:591-8. doi:10.1016/J.IJBIOMAC.2015.08.036.
- [11] Park S, Choi D, Jeong H, Heo J, Hong J. Drug Loading and Release Behavior Depending on the Induced Porosity of Chitosan/Cellulose Multilayer Nanofilms. Mol Pharm 2017;14:3322–30. doi:10.1021/acs.molpharmaceut.7b00371.
- [12] Lopes MS, Jardini AL, Filho RM. Poly (Lactic Acid) Production for Tissue Engineering Applications. Procedia Eng 2012;42:1402–13. doi:10.1016/J.PROENG.2012.07.534.
- [13] Conn RE, Kolstad JJ, Borzelleca JF, Dixler DS, Filer LJ, Ladu BN, et al. Safety assessment of polylactide (PLA) for use as a food-contact polymer. Food Chem Toxicol 1995;33:273–83. doi:10.1016/0278-6915(94)00145-E.
- [14] Oudjedi K, Hassissen N, Zaidi F, Nerin C, Manso S. New active antioxidant multilayer food packaging films containing Algerian Sage and Bay leaves extracts and their application for oxidative stability of fried potatoes. Food Control 2018;98:216–26. doi:10.1016/j.foodcont.2018.11.018.
- [15] O'Sullivan M, Dowling DP, Contini C, Gargan SÓ, Álvarez R, Monahan FJ. Effect of an active packaging with citrus extract on lipid oxidation and sensory quality of cooked turkey meat. Meat Sci 2013;96:1171–6. doi:10.1016/j.meatsci.2013.11.007.
- [16] Dhieb F Ben, Dil EJ, Tabatabaei SH, Frej M, Abdellah A. Effect of nanoclay orientation on oxygen barrier properties of LbL nanocomposite coated films 2019;9:1632–41. doi:10.1039/c8ra09522a.
- [17] Muramatsu M, Okura M, Kuboyama K, Ougizawa T, Yamamoto T, Nishihara Y, et al. Oxygen permeability and free volume hole size in ethylene-vinyl alcohol copolymer film: temperature and humidity dependence. Radiat Phys Chem 2003;68:561–4. doi:10.1016/S0969-806X(03)00231-7.
- [18] Helmke R. Oxygen-Barrier Packaging: How to Prevent Food Spoilage | Plastic Ingenuity. Plast Ingen 2017. https://www.plasticingenuity.com/blog/oxygen-barrier-packaging-methods (accessed April 11, 2019).
- [19] Laufer G, Kirkland C, Cain AA, Grunlan JC. Clay-chitosan nanobrick walls: Completely renewable gas barrier and flame-retardant nanocoatings. ACS Appl Mater Interfaces 2012;4:1643–9. doi:10.1021/am2017915.
- [20] Rocca-Smith JR, Pasquarelli R, Lagorce-Tachon A, Rousseau J, Fontaine S, Aguié-Béghin V, et al. Toward Sustainable PLA-Based Multilayer Complexes with Improved Barrier Properties. ACS Sustain Chem Eng 2019;7:3759–71. doi:10.1021/acssuschemeng.8b04064.

- [21] Moazeni N, Mohamad Z, Dehbari N. Study of silane treatment on poly-lactic acid(PLA)/sepiolite nanocomposite thin films. J Appl Polym Sci 2015;132:1–8. doi:10.1002/app.41428.
- [22] Svagan AJ, Åkesson A, Cárdenas M, Bulut S, Knudsen JC, Risbo J, et al. Transparent films based on PLA and montmorillonite with tunable oxygen barrier properties. Biomacromolecules 2012;13:397–405. doi:10.1021/bm201438m.
- [23] Aulin C, Karabulut E, Tran A, Waisgberg L, Lindström T. Transparent nanocellulosic multilayer thin films on polylactic acid with tunable gas barrier properties. ACS Appl Mater Interfaces 2013;5:7352–9. doi:10.1021/am401700n.
- [24] Mølgaard SL, Henriksson M, Cárdenas M, Svagan AJ. Cellulose-nanofiber/polygalacturonic acid coatings with high oxygen barrier and targeted release properties. Carbohydr Polym 2014;114:179–82. doi:10.1016/j.carbpol.2014.08.011.
- [25] Yoo BM, Shin HJ, Yoon HW, Park HB. Graphene and graphene oxide and their uses in barrier polymers. J Appl Polym Sci 2014;131:1–23. doi:10.1002/app.39628.
- [26] Galpaya D, Liu M, Motta N, Waclawik E, Yan C, Wang M. Recent Advances in Fabrication and Characterization of Graphene-Polymer Nanocomposites. Graphene 2012;01:30–49. doi:10.4236/graphene.2012.12005.
- [27] Hirschfelder JO, Curtiss CF, Brid RB. Molecular theory of gases and liquids. New York City: New York: Wiley; 1954.
- [28] Unalan IU, Wan C, Trabattoni S, Piergiovanni L, Farris S. Polysaccharide-assisted rapid exfoliation of graphite platelets into high quality water-dispersible graphene sheets †. R Soc Chem 2015;5:26482–90. doi:10.1039/c4ra16947f.
- [29] Lotya M, Hernandez Y, King PJ, Smith RJ, Nicolosi V, Karlsson LS, et al. Liquid Phase Production of Graphene by Exfoliation of Graphite in Surfactant/Water Solutions. J Am Chem Soc 2009;131:3611–20. doi:10.1021/ja807449u.
- [30] Crouvisier-Urion K, Bodart PR, Winckler P, Raya J, Gougeon RD, Cayot P, et al. Biobased Composite Films from Chitosan and Lignin: Antioxidant Activity Related to Structure and Moisture. ACS Sustain Chem Eng 2016;4:6371–81. doi:10.1021/acssuschemeng.6b00956.
- [31] Yan N, Capezzuto F, Lavorgna M, Buonocore GG, Tescione F, Xia H, et al. Borate cross-linked graphene oxide-chitosan as robust and high gas barrier films. Nanoscale 2016;8:10783–91. doi:10.1039/c6nr00377j.
- [32] Giannakas A, Patsaoura A, Barkoula N-M, Ladavos A. A novel solution blending method for

- using olive oil and corn oil as plasticizers in chitosan based organoclay nanocomposites. Carbohydr Polym 2017;157:550–7. doi:10.1016/j.carbpol.2016.10.020.
- [33] Aljawish A, Muniglia L, Klouj A, Jasniewski J, El Scher J€, Desobry S. Characterization of films based on enzymatically modified chitosan derivatives with phenol compounds. Food Hydrocoll 2016;60:551–8. doi:10.1016/j.foodhyd.2016.04.032.
- [34] Hu D, Wang H, Wang L. Physical properties and antibacterial activity of quaternized chitosan/carboxymethyl cellulose blend films. LWT Food Sci Technol 2016;65:398–405. doi:10.1016/j.lwt.2015.08.033.
- [35] Perdones Á, Vargas M, Atarés L, Chiralt A. Physical, antioxidant and antimicrobial properties of chitosan-cinnamon leaf oil films as affected by oleic acid. Food Hydrocoll 2014;36:256–64. doi:10.1016/j.foodhyd.2013.10.003.
- [36] Agulló E, Rodríguez MS, Ramos V, Albertengo L. Present and Future Role of Chitin and Chitosan in Food. Macromol Biosci 2003;3:521–30. doi:10.1002/mabi.200300010.

#### 2. LITERATURE REVIEW

This literature review starts with the characterization of oxygen barrier properties for food packaging applications, following by an introduction of mass transfer, production, properties, and applications of PLA, chitosan, and graphene. Multilayer coating technique is explained. Finally, the current and relevant research about chitosan and graphene coating is discussed.

#### 2.1 Oxygen Permeability

# 2.1.1 Food Packaging

Packaging serves multiple functions, such as protection, preservation, transportation, presentation, and communication. The integrity of food packaging is essential since it protects the product inside from ambient conditions and helps to deliver high quality products to the consumers. Food deteriorates when it lost its quality and safety [1]. The reaction between oxygen and food compounds can easily diminish food quality [1–3]. For example, lipid oxidation is one of the main reasons of food deterioration affecting flavor and shortening the shelf life as well as generating deleterious aldehydes and derivatives [1,4]. Thus, it is important to decrease the oxygen permeability (OP) of food packaging materials under various environment to preserve and to extend the quality of oxygen sensitive food products.

# 2.1.2 Principle of Permeation

Permeation is the process when a component (the permeant) is transported through a solid medium from a high permeant concentration fluid phase to a low permeant concentration fluid phase [5]. Permeability is identified as the main parameter describing permeation. In general, a

large value of permeability means that the solid material has small resistance to the transportation of permeants, and vice versa. In this thesis, the solid material refers to a polymer or polymer-based membrane. According to Ghosal and Freeman [6], permeation of a permeant molecule through a polymer membrane consists of three main steps: ad/absorption, diffusion, and desorption. Permeation can be expressed as:

$$P = D \times S \tag{2-1}$$

where *P* is the permeability, *D* is the diffusion coefficient, and *S* is the solubility coefficient, and when the diffusion process can be described as the Fick's first law and the sorption process follows Henry's law. Functionally, *P* quantifies permeation at steady state, *D* describes how fast permeant molecules are moving in a membrane, and *S* represents how much permeant molecules are sorbed on the surface and bulk of the membrane.

Permeation can also be expressed as:

$$F = \frac{Q}{t \times A} \tag{2-2}$$

where *F* is the flux of permeant, *Q* is the amount of permeant, *t* is the permeation time, and *A* is the area that permeation occurred.

Fick's 1<sup>st</sup> Law is based on the hypothesis that "the rate of transfer of a diffusing substance through unit area of a section is proportional to the concentration gradient measured normal to the section" [7], as expressed by the following equation:

$$F = -D\frac{dc}{dx} (2-3)$$

where *c* is the concentration of the permeant, and *x* is the space or distance measured normal to the section.

At steady state of permeation, the concentration gradient remains constant at all positions throughout the film. **Figure 2-1** shows the permeation through a membrane at steady state, where:

$$\frac{c - c_1}{c_2 - c_1} = \frac{x}{L} \tag{2-4}$$

which represents the linear concentration profile of permeant through a membrane. c represents permeant concentration,  $c_1$  is the concentration at high concentration side, and  $c_2$  is the concentration at low concentration side.

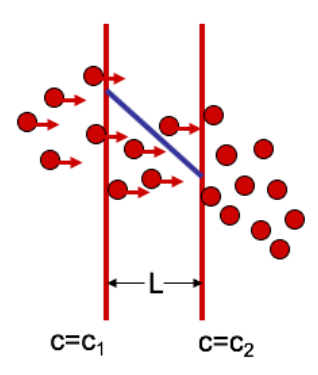


Figure 2-1. Steady state of permeation through a membrane.

If equation 2-4 is replaced in equation 2-3, the following expression can be obtained:

$$F = D \frac{c_1 - c_2}{L} (2-5)$$

The Henry's Law can be applied when the permeant pressure is low (<<1 atm) and no chemically interaction between the permeant and polymer membrane occurs. Equation 2-6 represents this relationship as:

$$c = Sp (2-6)$$

where p is the permeant partial pressure at the interphase. Rearranging equations 2-2, 2-5, and 2-6, the permeation can be expressed as:

$$P = \frac{Q \times L}{t \times A \times (p_1 - p_2)} \tag{2-7}$$

where  $p_1$  and  $p_2$  are permeant partial pressure at two sides of the material  $(p_1 > p_2)$ , Q is the amount of permeant, L is distance that permeation happens, t is the permeation time, and A is the area that permeation occurred.

# 2.1.3 Factors affecting permeation

According to equation 2-7, OP depends on the amount of oxygen permeated, thickness of the membrane, permeation time, area that permeation occurred, and oxygen partial pressure at both sides of the membrane. Other than these, OP is also dependent on the composition of the membrane, *e.g.*, tortuosity [8]. For example, a 0.031 mm high density polyethylene membrane has a high OP of 1.5 x 10<sup>-14</sup> kg m m<sup>-2</sup> s<sup>-1</sup> Pa<sup>-1</sup> at 25°C, 75% RH due to the low resistance to the passage of oxygen [2]. Also, relative humidity can affect OP considerably for water-sensitive polymers such as ethylene-vinyl alcohol [9]. OPs of several polymer films were found to increase significantly at 25°C with an increase of the relative humidity from 75 to 98%. For example, EVA/polyvinylidene chloride (PVDC)/EVA had a 6% increase, nylon/ionomer/polyethylene increased for 136%, and PVDC/EVA had an increase of 100% [2]. The commonly agreed explanation of this phenomenon is that water molecules act as "plasticizer" making paths for oxygen molecules to easily move through the membranes [9]. According to the Arrhenius relationship (as shown in equation 2-8), polymers OP is affected by temperature

$$P = P_o \exp\left(-\frac{E_p}{RT}\right) \tag{2-8}$$

where  $P_0$  is the pre-exponential factors for P,  $E_p$  is the activation energy of permeation, R is the universal gas constant, and T is the temperature. Netramai et al. compared the activation energy of poly (ethylene terephthalate) - PET - and poly (lactic acid) films and found that a higher activation energy for PLA indicating more temperature dependence during mass transfer. OP of PLA film ( $E_p = 129 \pm 2$  kJ mol  $^{-1}$ ) increased 165% from 23°C to 40°C, while OP of PET ( $E_p = 51 \pm 4$  kJ mol  $^{-1}$ ) only increased 21% [10].

# 2.2 Poly(lactic acid)

# 2.2.1 Introduction

PLA is derived from lactic acid (2-hydroxy propionic acid) [11,12], as shown in **Figure 2-2**. PLA is a biobased polymer since it is produced from renewable plant resources, such as corn and sugar cane [5,11] and it is biodegradable and compostable in industrial facilities due to the presence of a hydrolysable ester bond in the constitutional unit. Among all renewable packaging materials, PLA has the highest potential to be adapted for commercial productions [13]. PLA has been widely studied in medicine [14,15], food packaging materials [16,17], and sustainable barrier applications [18,19]. PLA has already been approved for using as packaging materials by the U.S. Food and Drug Administration [20].

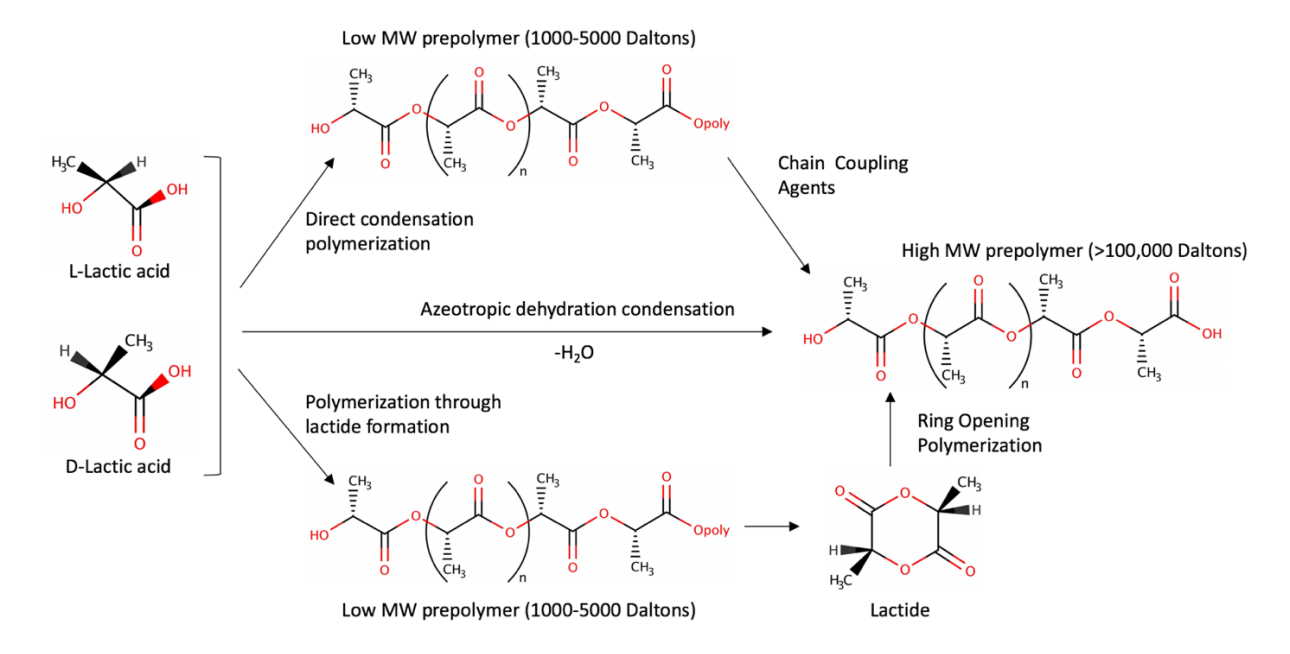


Figure 2-2. Synthesis of high molecular weight (MW) PLA, adapted from [11].

# 2.2.2 Oxygen Barrier

As mentioned in Section 2.1.3, the OP is affected by the nature of the PLA as well as external factors. Commercial PLA are fabricated from L-lactide and D,L-lactide [11,12], while the final percentage of D-lactic acid is always lower than 12% [5]. Sonchaeng *et al.* suggested a three-phase model in semicrystalline PLA including (1) a crystalline fraction (CF); (2) a mobile amorphous fraction (MAF); and (3) a rigid amorphous fraction (RAF) [5]. The relation between the tentative crystalline structures of PLA and amount of D-lactide below the glass transition temperature ( $T_g$ ) is shown in **Table 2-1**. A decrease in melting temperature and glass transition temperature was observed with an increasing amount of D-lactide [5]. Additionally, increasing amount of D-lactide disrupted the regular L-lactide structure translating into a decrease in crystallinity. Since crystalline domains in PLA will hinder oxygen molecules to diffuse [21],

increasing the amount of D-lactide will increase the OP value. Thus, knowing the composition of PLA helps understand the oxygen transfer mechanism.

Table 2-1. Tentative PLA crystalline structures below  $T_g$ , adapted from [5].

Amount of D-lactide	Structure	Possible crystallinity model
8-12%	MAF	One phase
2-8%	MAF, RAF, and CF	Three-phase
<1%	MAF, RAF, and CF	Three-phase

**Table 2-2** shows the OP of PLA and some other commonly used packaging materials under different temperatures and RH conditions. OP value of PLA varies from 1.21 x 10<sup>-18</sup> to 5.35 x 10<sup>-18</sup> kg m m<sup>-2</sup> s<sup>-1</sup> Pa<sup>-1</sup> when testing temperature is around 23 to 25°C. However, there is no trend showing any correlation between % RH and OP value. This was also explained by Sonchaeng *et al.* that OP of PLA is not affected by a short-term exposure to moisture [5].

Table 2-2. Oxygen permeability of PLA and other common packaging materials under various temperatures and RH conditions.

Temperature	RH	Polymer	<i>P</i> x 10 <sup>-20</sup>	Ref.
	%	Polymer	kg m m <sup>-2</sup> s <sup>-1</sup> Pa <sup>-1</sup>	
5	0	PLA (98% L-lactide)	350	[12]
		PLA	233	[22]
	0	PLA	199	[5]
		PLA	$535\pm79$	[23]
23-25		PLA	$484 \pm 52$	[24]
_	20	PLA	270	[25]
<del>-</del>	50	PLA	255	[25]
		PLA	258	[26]

Table 2-2 (cont'd)

	70	PLA (4030-D resin)	121 ± 7	[27]
	70	PLA (4040-D resin)	$\textbf{139} \pm \textbf{14}$	[27]
	80	PLA	238 ± 7	[17]
30		PLA (4030-D resin)	169 ± 9	
		PLA (4040-D resin)	$\textbf{159} \pm \textbf{13}$	- _ [27]
25	_	PLA (4030-D resin)	246 ± 9	
35	_ 70	PLA (4040-D resin)	$\textbf{197} \pm \textbf{14}$	
40	_ /0	PLA (4030-D resin)	$288\pm11$	_ [27]
40		PLA (4040-D resin)	$\textbf{231} \pm \textbf{15}$	_
45	_	PLA (4030-D resin)	$\textbf{354} \pm \textbf{14}$	
43		PLA (4040-D resin)	$293 \pm 22$	
		Poly (ethylene terephthalate) (PET)	29	[28]
	0	Poly (vinylidene chloride) (PVDC)	0.5	
23-25	U	Polypropylene (PP)	647	
		Nylon 6,6	18	
		Poly (vinyl alcohol)	0.3	
	50	Ethylene vinyl alcohol	0.5	[29]
		High-density polyethylene	651	
		PET	29	[28]
	80	PVDC	0.5	
	80	PP	647	
		Nylon 6,6	88	

Auras *et al.* studied the oxygen barrier properties of PLA films made from two resins at 70% RH under different temperatures (25, 30, 35, 40, 45°C). The results are shown in **Table 2-2** and

plotted in **Figure 2-3**. As described by the Arrhenius equation (equation 2-8), increasing temperature leads to an increase in OP value.

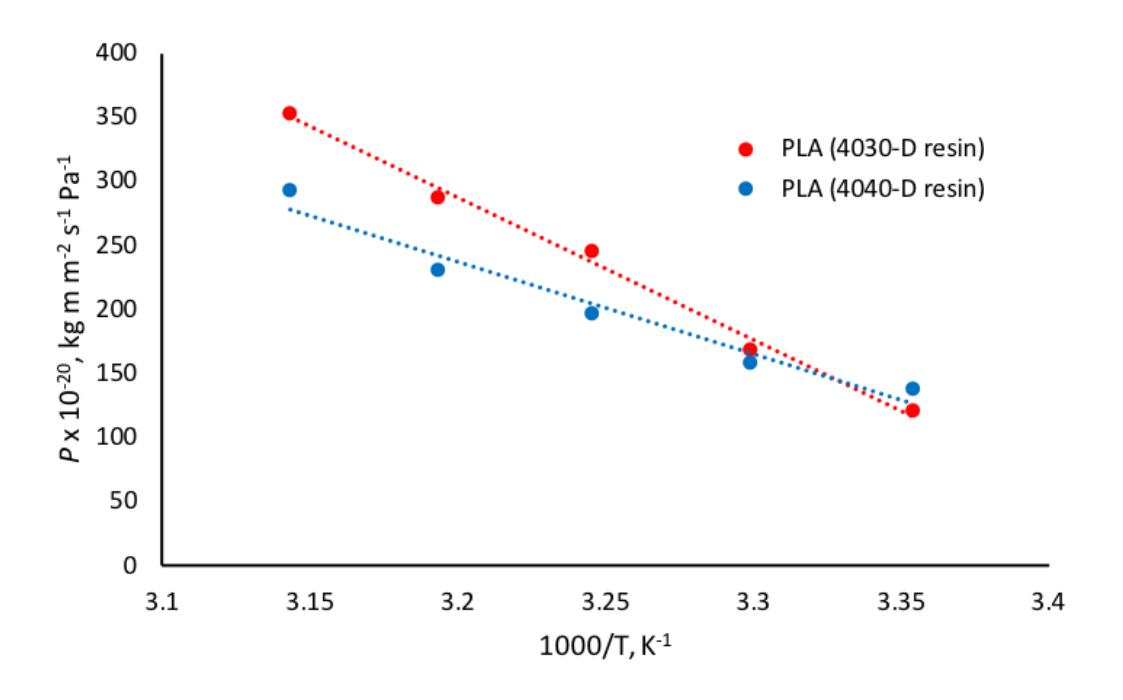


Figure 2-3. Arrhenius plot of OP at 70% RH, adapted from [27].

#### 2.2.3 Surface Modification

Due to the increasing potential of PLA in packaging applications, surface hydrophilicity is required for certain applications such as printing and adhesion [30]. From **Figure 2-2**, high molecular weight PLA consists of ester and methyl groups. Methyl group is non-polar since the bond dipoles in carbon-hydrogen bonds are all cancelled out [31], while the ester group is polar which can participate in hydrogen bonds with water [32]. Thus, even though PLA is susceptible to hydrolysis [5], its intrinsical surface hydrophobicity needs to be decreased for surface functionalization and novel packaging and material applications [30].

Among the different kinds of physical or chemical surface modification methods, plasma treatment is environmentally friendly as well as only treating the most surface of a substrate without affecting the bulk characteristics of a polymer [30,33]. Surface activation and surface abrasion are two major plasma acting mechanisms. Surface activation means that the species created during plasma are replaced or recombined with the substrate polymer and then form new functional groups. Surface abrasion caused by surface micro-abrasion are produced on the polymer surface when oxygen plasma is used [30]. Chaiwong et al. found an increasing hydrophobicity of PLA film after an Ar plasma treatment at 25 W and 100 mTorr. The water contact angle increased from 60.4° to 101.3° after the treatment, which was due to the attached polar groups decreasing the surface energy of PLA, and thus increased water contact angle [34]. Hollahan et al. claimed that oxygen or helium plasma treatment can improve adhesion and wettability of various polymers, such as polyethylene and Teflon [33]. Wan et al. observed a decreasing water contact angle from 78° to 45° after 2-min oxygen plasma treatment at an electrical power of 13.56 Hz on poly(lactide-co-glycolide) films [35]. Pankaj et al. studied OTRs of PLA film before and after dielectric barrier discharge (70 and 80 kV, 0.5, 1.5, 2.5, and 3.5 min) while no significant difference was found for all voltage and time [36].

#### 2.2.4 PLA Coated Films

Many studies reported improved gas barrier properties of PLA film with coatings [16,22,25,26,37–39]. Coating techniques enable researchers to precisely control film structure and thickness [39] and provide a good protection to the substrate. **Figure 2-4** shows recent studies on effects of coating on PLA film OP values. Test conditions fall into the range of 23-25°C and 0-50% RH. The number of coating layers varies between 1 to 70, depending on the different

coating materials. The efficiency of coating on the PLA substrate film on oxygen barrier property improvement is clearly shown by the reduction of OP.

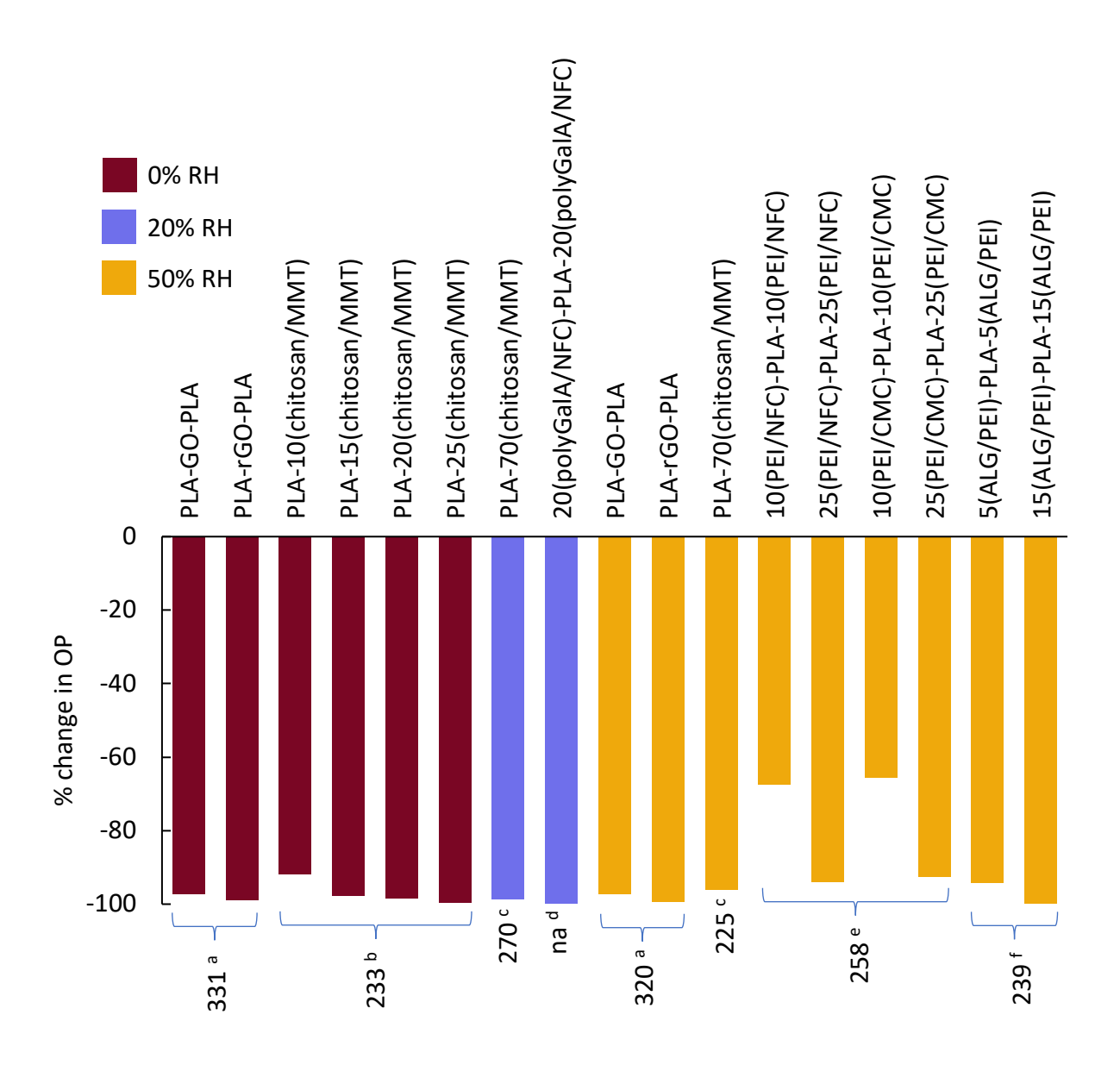


Figure 2-4. Effects of coating on PLA film on OP value. References: a [16], b [22], c [25], d [39], e [26], f [38]. The numbers on bottom of the bar are P x 10<sup>-20</sup> kg m m<sup>-2</sup> s<sup>-1</sup> Pa<sup>-1</sup> of pure PLA film used in corresponding experiments except in reference a (P of PLA-PLA film). Number in PLA

multilayer coating names are numbers of coating been applied in corresponding experiments.

Abbreviations: GO = graphene oxide, rGO = reduced graphene oxide, MMT = montmorillonite, polyGalA = pectin (polygalacturonic acid), NFC <sup>d</sup> = cationic cellulose nanofiber, PEI = polyethyleneimine, NFC <sup>e</sup> = polyethyleneimine, CMC = carboxymethyl cellulose, ALG = sodium alginate, N/A = not available.

# 2.3 Graphene

# 2.3.1 Introduction

Graphene is a single layer of sp<sup>2</sup>-hybridized carbon atoms packed into a honeycomb network. **Figure 2-5** shows the basic structural element of graphene. Single layer graphene forms into 0D fullerenes by wrapping, 1D nanotubes by rolling, and 3D graphite by stacking [40]. The carbon-carbon bond length is 0.142 nm [41], thus the lattice is calculated as 0.245 nm by:

Lattice constant = 
$$\sqrt{3} \times 0.142 \, nm = 0.245 \, nm$$
 (2-9)

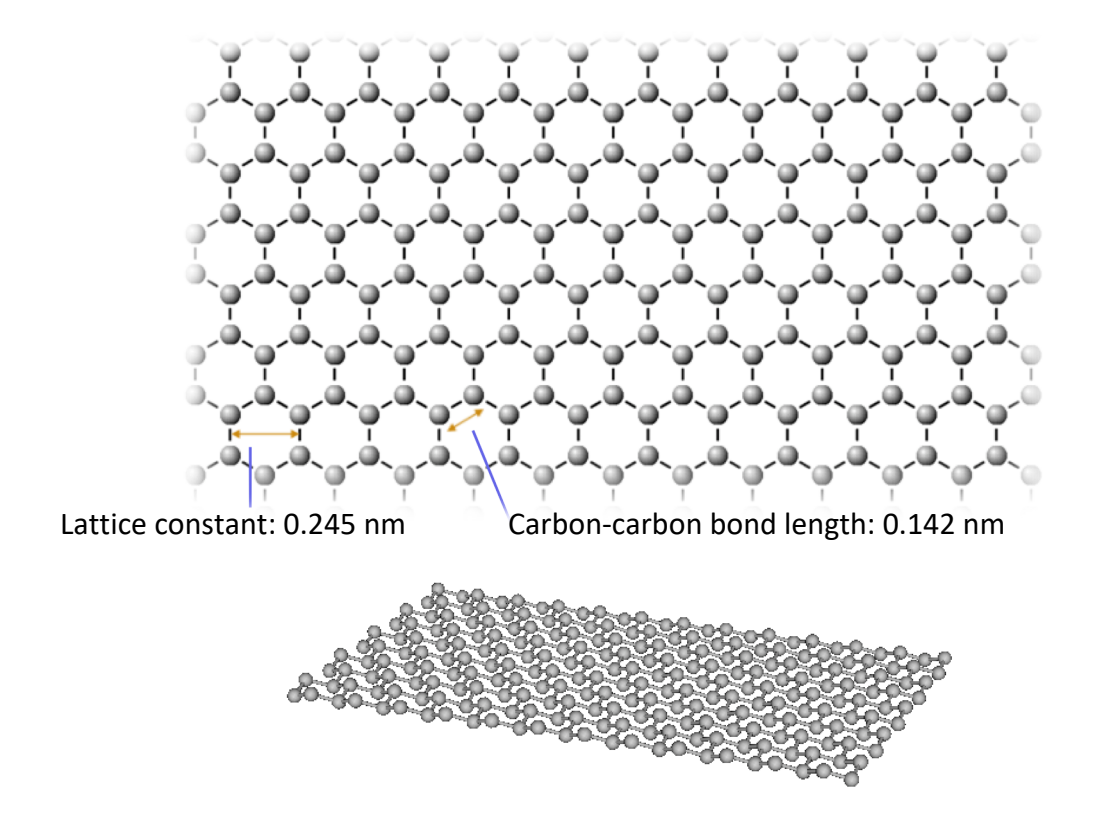


Figure 2-5. Illustration of graphene structure, adapted from [40].

Graphene has a high Young's modulus of approximately 1,100 GPa, a fracture strength of 125 GPa, a theoretical specific surface area of 2,630 m<sup>2</sup> g<sup>-1</sup>, and an electrical conductivity of 1,000 S cm<sup>-1</sup> [42].

# 2.3.2 Production

Many methods have been developed to synthesize graphene, including chemical vapor deposition [43,44], mechanical exfoliation of graphite [45], micromechanical cleavage [46], liquid phase exfoliation [47], oxidation from graphene oxide [48], etc. Among them, the reduction of graphene oxide from graphite is the easiest and most common way to exfoliate graphite in a labscale [49]. However, due to the disadvantage of being low-yielding and expensive with the usage

of strong acid and alkaline, some researchers explored new ways to exfoliate graphene from graphite with less defects and environmental issues [50,51]. Lotya *et al.* obtained graphene flakes of <5 layers, among which ~3% of flakes consisted of monolayers, at an efficiency of 40% by ultrasonicating graphite in sodium dodecylbenzene sulfonate water solution for 30 min. Graphene flakes stayed stable without sediment for approximately 6 weeks [50]. Unalan *et al.* ultrasonicated graphite with chitosan solution for 30 min and achieved a yield of graphene of 5.5 mg mL<sup>-1</sup>, during which ~8.5 wt% of chitosan was adsorbed on the graphene surface. This is due to the fact that the surface free energy of chitosan, after ultrasonication (~47 mJ m<sup>-2</sup>), is very close to that of graphene (46.7 mJ m<sup>-2</sup>). This indicates that single graphene layers are likely to aggregate with chitosan components [51].

# 2.3.3 Oxygen Barrier Improvement

Multiple studies showed that laminar nanomaterials can improve gas barrier properties when being coated on or incorporated into polymer [42,52–57]. For graphene, such a layer structure can make the path for gas molecules more tortuous [17]. An oxygen molecule has a kinetic diameter of 0.346 nm [58], which is larger than the lattice constant of graphene (0.245 nm) discussed in Section 2.3.1. This indicates that a perfect graphene layer should be able to significantly improve oxygen barrier property once it is incorporated in a polymer or in a polymer coating layer in the perpendicular direction of the oxygen flow. However, since graphene tends to aggregate due to its high specific surface area, effective dispersion and orientation of graphene is crucial to achieve high oxygen barrier [55].

Evenly dispersing a small amount of nano-scale inorganic phase in a polymer matrix can significantly improve gas barrier properties of the substrate [17,59]. Another common method is

to form a uniform coating with an inorganic phase to maximize the blocking effect, and thus improve barrier properties of the polymer [54]. Figure 2-6 shows the changes in polymer OP with addition of graphene [17,54,57,60,61]. Test temperature varied from 23 to 35°C and relative humidity ranged from 0% to 80%. The increase in OP with addition of graphene varied from -44.2% to 492% when it was added into the polymer matrix, while -99.9% to -82.7% when graphene was incorporated into the coating layer(s). Here a negative % change means a decrease in OP, indicating an improvement in oxygen barrier, and vice versa. It shows that applying coating with graphene tends to decrease OP more than incorporating graphene into matrix. These data supported Pierleoni *et al.*'s statement that more aggregation of graphene sheets takes place and thus the filler aspect ratio decreases significantly in the polymer phase, leading to an inefficient usage of graphene [54].

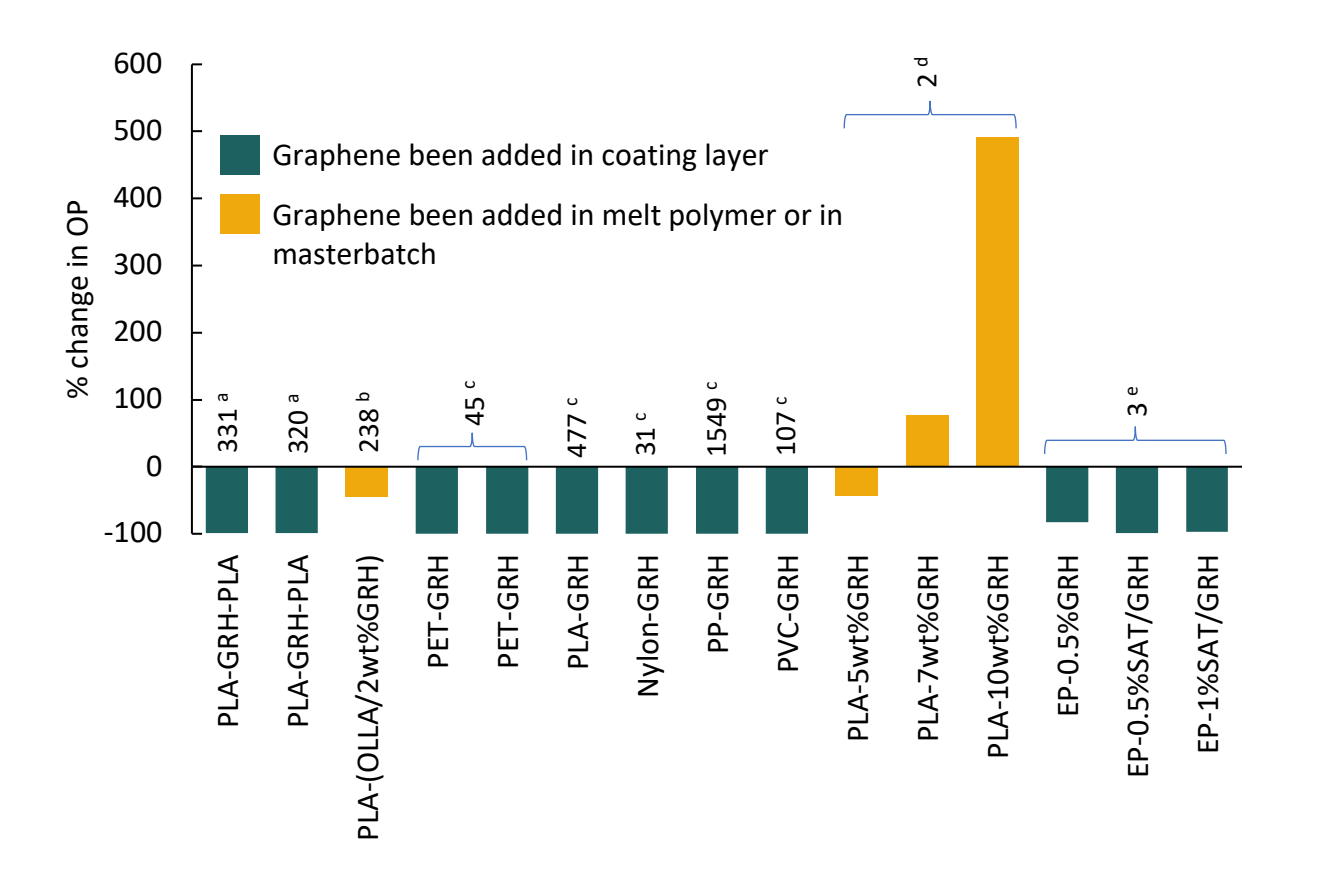


Figure 2-6. Effects of graphene on OP value. References: a [60], b [17], c [54], d [57], e [61]. The numbers on top of the bar are  $P \times 10^{-20}$  kg m m<sup>-2</sup> s<sup>-1</sup> Pa<sup>-1</sup> of polymer film without graphene used in corresponding experiments. Abbreviations: GRH = graphene, OLLA = lactic acid oligomers, PET = polyethylene terephthalate, PP = polypropylene, PVC = poly (vinyl chloride), EP = epoxy, SAT = salinized aniline trimer. Positive change means increasing OP and negative change means reduction of OP.

# 2.4 Chitosan

# 2.4.1 Introduction

Chitosan is an abundant and naturally-occurring polysaccharide derived from deacetylation of chitin, which is extracted from shells of crustaceans such as crab and shrimp [62–65]. It has received raising attention as packaging materials due to its biocompatibility, biodegradability[65], water solubility [66], and film-forming ability [67]. As aforementioned, chitosan has good biocompatibility and biodegradability, which make it a potential food packaging material for products such as fruits, vegetable and meat [81].

# 2.4.2 Production

Chitin is obtained by conducting acid treatment and alkaline treatment to crustaceans. Then partial deacetylation is done on chitin to get chitosan [68]. Brief illustration of extraction of chitin and production of chitosan is shown in **Figure 2-7**.

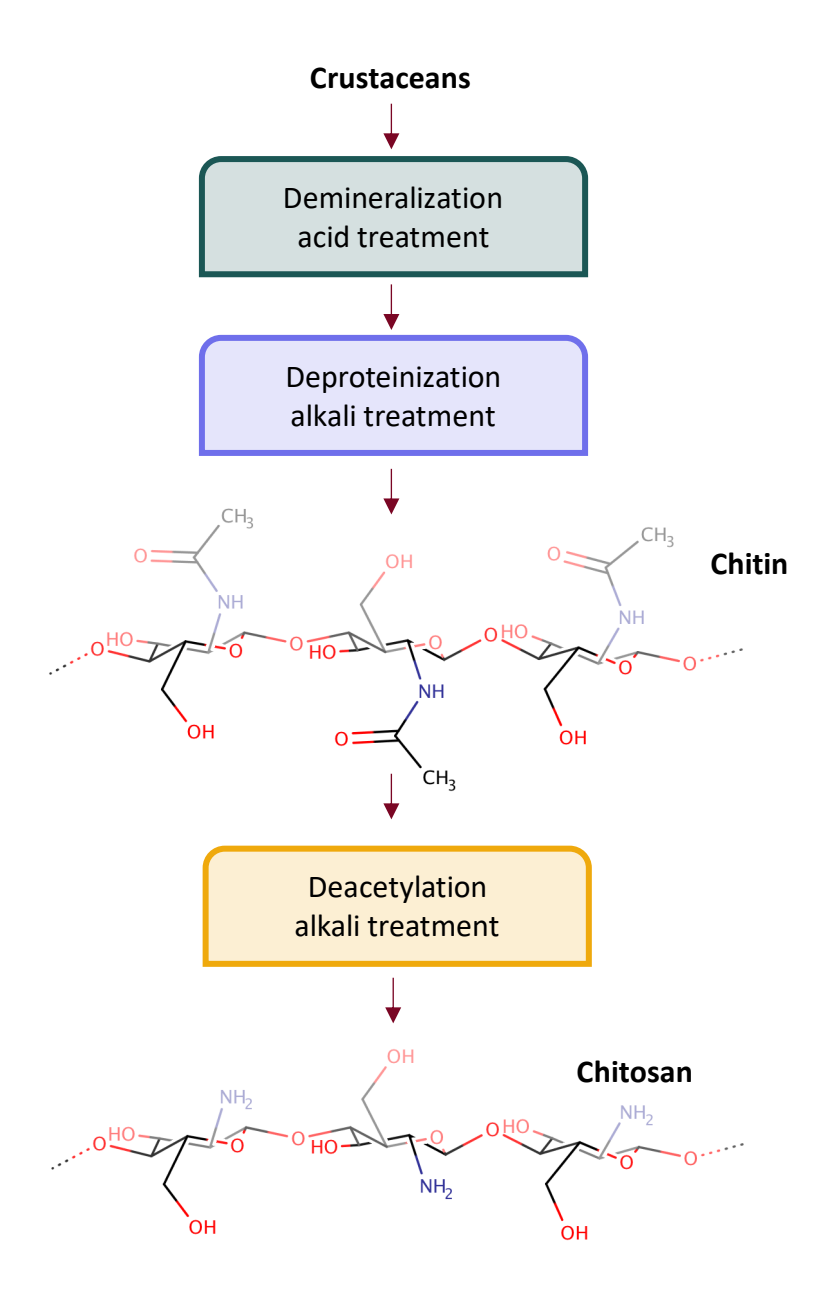


Figure 2-7. Extraction of chitin and fabrication of chitosan, adapted from [68].

# 2.4.3 Properties

Chitosan is widely being used as an antimicrobial agent due to its high chelating capacity for metal ions such as  $Cu^{2+}$ ,  $Ni^{2+}$ ,  $Co^{2+}$ ,  $Fe^{2+}$ , etc. [69]. Such chelation can take place in both acid [70] and neutral conditions [71].

As shown in **Figure 2-7**, the presence of functional groups including hydroxyl and amino groups in chitosan allows for structural modifications [72]. The free amino groups provide a positive charge to chitosan and make it soluble in acidic solutions [68]. Chitosan can easily be coated on negatively charged surfaces [64], such as on polymer membranes after oxygen plasma treatment.

Table 2-3. Oxygen and water barrier properties of chitosan films.

Test parameter	DD	M <sub>w</sub>	Temperature	RH	_ Test value	Ref.
	%	kg mol <sup>-1</sup>	°C	%		
	90	274	25	75	39	[73]
	>75	Low	23	0	32	[74]
OP x 10 <sup>-20</sup>	>75	na	23	75	56	[74]
kg m m <sup>-2</sup> s <sup>-1</sup> Pa <sup>-1</sup>	>75	190-310	23	0	$\textbf{1.9} \pm \textbf{0.2}$	[75]
ng III III 5 Fa	>75	190-310	23	50	$2.0 \pm 0.2$	[75]
	na	239	23	50	$32,940 \pm 2,635$	[76]
	91	na	23	0	$2\pm 2$	[77]
	22	na	10	58	0.7	[78]
	22	na	20	54	2	[78]
	90	274	25	30	33	[73]
	na	239	38	50	58	[76]
	>75	Low	38	90	8	[79]
	>75	High	38	90	9	[79]
WVP x 10 <sup>-14</sup>	91	na	23	60	$(4 \pm 0.3) \times 10^8$	[77]
kg m m <sup>-2</sup> s <sup>-1</sup> Pa <sup>-1</sup>	22	na	5	100-58	$(2\pm0.5) \times 10^{13}$	[78]
	22	na	20	100-54	$(2\pm0.2) \times 10^{13}$	[78]
	85	165	25	30-100	$40\pm3$	[80]
	85	165	25	30-85	$30\pm2$	[80]
	85	165	25	30-75	$\textbf{20}\pm\textbf{1}$	[80]

Abbreviation: DD = Deacetylation degree,  $M_w$  = average molecular weight, WVP = water vapor permeability.

Table 2-3 listed some recent studies on water vapor and oxygen barrier properties of chitosan films. There are several unexpected large permeability values, which might be due to errors in test methods or sample defects. Other data varies from 0.7 to 56 x 10<sup>-20</sup> kg m m<sup>-2</sup> s<sup>-1</sup> Pa<sup>-1</sup> for OP and 8 to 58 x 10<sup>-14</sup> kg m m<sup>-2</sup> s<sup>-1</sup> Pa<sup>-1</sup> for WVP. Results of some studies on mechanical properties and water contact angle are also shown in Table 2-4. The variation in data shows that deacetylation degree and average molecular weight influence chitosan's inherent properties. Deacetylation degree determines the amount of free amino group and average molecular weight represents the average length of chitosan chains.

Table 2-4. Physical properties of chitosan film.

DD M <sub>w</sub> _		Mechanical properties				Water contact	
		Test RH	EM x 10 <sup>9</sup>	Elongation	TS x 10 <sup>7</sup>	angle	Ref.
%	kg mol <sup>-1</sup>	%	Pa	%	Pa	o	-
90	274	33	3 ± 0.6	7 ± 4	8 ± 3	85	[73]
90	274	75	0.1 0.05	$54 \pm 12$	2 ±0.2	na	[73]
>75	Low	na	na	20	2	na	[74]
75	190-310	na	3	8	10	na	[75]
na	239	50	3.1	na	7	na	[76]
>75	Low	na	na	$5\pm0.5$	$6\pm3$	105	[79]
>75	High	na	na	$5\pm0.4$	$5\pm3$	105	[79]
75-85	50-190	na	na	na	na	86	[82]
91	na	na	na	$246 \pm 0.6$	$\textbf{0.2} \pm \textbf{0.01}$	na	[77]
22	na	na	$2\pm0.05$	$20\pm 5$	$4\pm0.6$	na	[78]
na	na	50	(5 $\pm$ 0.8) x 10 <sup>-3</sup>	$65\pm17$	$\textbf{4}\pm\textbf{1}$	na	[80]

Abbreviations: EM = Young's modulus, TS = tensile strength.

# 2.4.4 Chitosan/Graphene Composite

Researchers are focusing on developing chitosan/graphene derivative composites [74,83–90]. Applications for chitosan/graphene composites are electrode sensor [91], chemicals removal [92,93], biosensing [94,95], and water purification [96]. In recent years, it has been reported that graphene or few layers of graphene (<5 layers) can stably exist in chitosan acid aqueous solution after ultrasonication as mentioned in Section 2.3.2 [51]. However, there is a lack of studies and understanding on considering chitosan/graphene as coatings on packaging materials and its gas barrier property mechanisms.

REFERENCES

#### REFERENCES

- [1] Oudjedi K, Hassissen N, Zaidi F, Nerin C, Manso S. New active antioxidant multilayer food packaging films containing Algerian Sage and Bay leaves extracts and their application for oxidative stability of fried potatoes. Food Control 2018;98:216–26. doi:10.1016/j.foodcont.2018.11.018.
- [2] EUSTACE IJ. Some factors affecting oxygen transmission rates of plastic films for vacuum packaging of meat. Int J Food Sci Technol 1981;16:73–80. doi:10.1111/j.1365-2621.1981.tb00998.x.
- [3] Miller KS, Krochta JM. Oxygen and aroma barrier properties of edible films: A review. Trends Food Sci Technol 1997;8:228–37. doi:10.1016/S0924-2244(97)01051-0.
- [4] O'Sullivan M, Dowling DP, Contini C, Gargan SÓ, Álvarez R, Monahan FJ. Effect of an active packaging with citrus extract on lipid oxidation and sensory quality of cooked turkey meat. Meat Sci 2013;96:1171–6. doi:10.1016/j.meatsci.2013.11.007.
- [5] Sonchaeng U, Iñiguez-Franco F, Auras R, Selke S, Rubino M, Lim LT. Poly(lactic acid) mass transfer properties. Prog Polym Sci 2018;86:85–121. doi:10.1016/j.progpolymsci.2018.06.008.
- [6] Ghosal K, Freeman BD. Gas separation using polymer membranes: an overview. Polym Adv Technol 1994;5:673–97. doi:10.1002/pat.1994.220051102.
- [7] Crank J. The mathematics of diffusion. Clarendon Press; 1975.
- [8] Dhieb F Ben, Dil EJ, Tabatabaei SH, Frej M, Abdellah A. Effect of nanoclay orientation on oxygen barrier properties of LbL nanocomposite coated films 2019;9:1632–41. doi:10.1039/c8ra09522a.
- [9] Muramatsu M, Okura M, Kuboyama K, Ougizawa T, Yamamoto T, Nishihara Y, et al. Oxygen permeability and free volume hole size in ethylene-vinyl alcohol copolymer film: temperature and humidity dependence. Radiat Phys Chem 2003;68:561–4. doi:10.1016/S0969-806X(03)00231-7.
- [10] Netramai S, Rubino M, Auras R, Annous BA. Mass Transfer Study of Chlorine Dioxide Gas Through Polymeric Packaging Materials. J Appl Polym Sci 2009;114:2929–36. doi:10.1002/app.

- [11] Lim LT, Auras R, Rubino M. Processing technologies for poly(lactic acid). Prog Polym Sci 2008;33:820–52. doi:10.1016/j.progpolymsci.2008.05.004.
- [12] Auras R, Harte B, Selke S. An Overview of Polylactides as Packaging Materials. Macromol Biosci 2004;4:835–64. doi:10.1002/mabi.200400043.
- [13] Taylor P, Weber CJ, Haugaard V, Festersen R, Bertelsen G. Production and applications of biobased packaging materials for the food industry Production and applications of biobased packaging materials for the food industry. Food Addit Contam 2002;19:172–7. doi:10.1080/0265203011008748.
- [14] Park S, Choi D, Jeong H, Heo J, Hong J. Drug Loading and Release Behavior Depending on the Induced Porosity of Chitosan/Cellulose Multilayer Nanofilms. Mol Pharm 2017;14:3322–30. doi:10.1021/acs.molpharmaceut.7b00371.
- [15] Lopes MS, Jardini AL, Filho RM. Poly (Lactic Acid) Production for Tissue Engineering Applications. Procedia Eng 2012;42:1402–13. doi:10.1016/J.PROENG.2012.07.534.
- [16] Goh K, Heising JK, Yuan Y, Karahan HE, Wei L, Zhai S, et al. Sandwich-Architectured Poly(lactic acid)—Graphene Composite Food Packaging Films. ACS Appl Mater Interfaces 2016;8:9994–10004. doi:10.1021/acsami.6b02498.
- [17] Ambrosio-Martín J, López-Rubio A, José Fabra M, Angel López-Manchado M, Sorrentino A, Gorrasi G, et al. Synergistic effect of lactic acid oligomers and laminar graphene sheets on the barrier properties of polylactide nanocomposites obtained by the in situ polymerization pre-incorporation method. J Appl Polym Sci 2016;133:1–11. doi:10.1002/app.42661.
- [18] Meriçer Ç, Minelli M, Angelis MGD, Giacinti Baschetti M, Stancampiano A, Laurita R, et al. Atmospheric plasma assisted PLA/microfibrillated cellulose (MFC) multilayer biocomposite for sustainable barrier application. Ind Crops Prod 2016;93:235–43. doi:10.1016/j.indcrop.2016.03.020.
- [19] Byun Y, Rodriguez K, Han JH, Kim YT. Improved thermal stability of polylactic acid (PLA) composite film via PLA–β-cyclodextrin-inclusion complex systems. Int J Biol Macromol 2015;81:591–8. doi:10.1016/J.IJBIOMAC.2015.08.036.
- [20] Conn RE, Kolstad JJ, Borzelleca JF, Dixler DS, Filer LJ, Ladu BN, et al. Safety assessment of polylactide (PLA) for use as a food-contact polymer. Food Chem Toxicol 1995;33:273–83. doi:10.1016/0278-6915(94)00145-E.
- [21] Michaels AS, Bixler HJ. Solubility of gases in polyethylene. J Polym Sci 1961;50:393–412. doi:10.1002/pol.1961.1205015411.

- [22] Laufer G, Kirkland C, Cain AA, Grunlan JC. Clay-chitosan nanobrick walls: Completely renewable gas barrier and flame-retardant nanocoatings. ACS Appl Mater Interfaces 2012;4:1643–9. doi:10.1021/am2017915.
- [23] Rocca-Smith JR, Pasquarelli R, Lagorce-Tachon A, Rousseau J, Fontaine S, Aguié-Béghin V, et al. Toward Sustainable PLA-Based Multilayer Complexes with Improved Barrier Properties. ACS Sustain Chem Eng 2019;7:3759–71. doi:10.1021/acssuschemeng.8b04064.
- [24] Moazeni N, Mohamad Z, Dehbari N. Study of silane treatment on poly-lactic acid(PLA)/sepiolite nanocomposite thin films. J Appl Polym Sci 2015;132:1–8. doi:10.1002/app.41428.
- [25] Svagan AJ, Åkesson A, Cárdenas M, Bulut S, Knudsen JC, Risbo J, et al. Transparent films based on PLA and montmorillonite with tunable oxygen barrier properties. Biomacromolecules 2012;13:397–405. doi:10.1021/bm201438m.
- [26] Aulin C, Karabulut E, Tran A, Waisgberg L, Lindström T. Transparent nanocellulosic multilayer thin films on polylactic acid with tunable gas barrier properties. ACS Appl Mater Interfaces 2013;5:7352–9. doi:10.1021/am401700n.
- [27] Auras RA, Harte B, Selke S, Hernandez R. Mechanical, physical, and barrier properties of poly(lactide) films. J Plast Film Sheeting 2003;19:123–35. doi:10.1177/8756087903039702.
- [28] Yam KL. The Wiley encyclopedia of packaging technology. New Jersey: John Wiley & Sons, Inc.; 2009.
- [29] Hansen NML, Plackett D. Sustainable Films and Coatings from Hemicelluloses: A Review. Biomacromolecules 2008;9:1493–505. doi:10.1021/bm800053z.
- [30] Jordá-Vilaplana A, Fombuena V, García-García D, Samper MD, Sánchez-Nácher L. Surface modification of polylactic acid (PLA) by air atmospheric plasma treatment. Eur Polym J 2014;58:23–33. doi:10.1016/j.eurpolymj.2014.06.002.
- [31] Ophardt CE. Polarity of Organic Compounds. Virtual Chemb 2003. http://chemistry.elmhurst.edu/vchembook/213organicfcgp.html (accessed March 20, 2019).
- [32] Ouellette RJ, Rawn JD. Carboxylic Ester an overview | ScienceDirect Topics. Princ Org Chem 2015. https://www.sciencedirect.com/topics/chemistry/carboxylic-ester (accessed March 20, 2019).
- [33] Hollahan JR, Stafford BB, Falb RD, Payne ST. Attachment of amino groups to polymer surfaces by radiofrequency plasmas. J Appl Polym Sci 1969;13:807–16.

- doi:10.1002/app.1969.070130419.
- [34] Chaiwong C, Rachtanapun P, Wongchaiya P, Auras R, Boonyawan D. Effect of plasma treatment on hydrophobicity and barrier property of polylactic acid. Surf Coatings Technol 2010;204:2933–9. doi:10.1016/j.surfcoat.2010.02.048.
- [35] Wan Y, Qu X, Lu J, Zhu C, Wan L, Yang J, et al. Characterization of surface property of poly(lactide-co-glycolide) after oxygen plasma treatment. Biomaterials 2004;25:4777–83. doi:10.1016/j.biomaterials.2003.11.051.
- [36] Pankaj SK, Bueno-Ferrer C, Misra NN, O'Neill L, Jiménez A, Bourke P, et al. Characterization of polylactic acid films for food packaging as affected by dielectric barrier discharge atmospheric plasma. Innov Food Sci Emerg Technol 2014;21:107–13. doi:10.1016/j.ifset.2013.10.007.
- [37] Ligot S, Benali S, Ramy-ratiarison R, Murariu M, Snyders R, Dubois P. Material Science and Engineering with Advanced Research Mechanical, Optical and Barrier Properties of PLA-layered silicate nanocomposites coated with Organic Plasma Polymer Thin Films 2015;1:20–30.
- [38] Gu C-H, Wang J-J, Yu Y, Sun H, Shuai N, Wei B. Biodegradable multilayer barrier films based on alginate/polyethyleneimine and biaxially oriented poly(lactic acid). Carbohydr Polym 2013;92:1579–85. doi:10.1016/j.carbpol.2012.11.004.
- [39] Mølgaard SL, Henriksson M, Cárdenas M, Svagan AJ. Cellulose-nanofiber/polygalacturonic acid coatings with high oxygen barrier and targeted release properties. Carbohydr Polym 2014;114:179–82. doi:10.1016/j.carbpol.2014.08.011.
- [40] Geim AK, Novoselov KS. The rise of graphene. Nat Mater 2007;6:183–91.
- [41] Galpaya D, Liu M, Motta N, Waclawik E, Yan C, Wang M. Recent Advances in Fabrication and Characterization of Graphene-Polymer Nanocomposites. Graphene 2012;01:30–49. doi:10.4236/graphene.2012.12005.
- [42] Yoo BM, Shin HJ, Yoon HW, Park HB. Graphene and graphene oxide and their uses in barrier polymers. J Appl Polym Sci 2014;131:1–23. doi:10.1002/app.39628.
- [43] Nandamuri G, Roumimov S, Solanki R. Chemical vapor deposition of graphene films. Nanotechnology 2010;21:145604. doi:10.1088/0957-4484/21/14/145604.
- [44] Li X, Cai W, An J, Kim S, Nah J, Yang D, et al. Large-Area Synthesis of High-Quality and Uniform Graphene Films on Copper Foils. New Ser 2009;324:1312–4. doi:10.1126/science.1172104.

- [45] Chang YM, Kim H, Lee JH, Song Y-W. Multilayered graphene efficiently formed by mechanical exfoliation for nonlinear saturable absorbers in fiber mode-locked lasers. Appl Phys Lett 2010;97:211102. doi:10.1063/1.3521257.
- [46] Meyer JC, Geim AK, Katsnelson MI, Novoselov KS, Booth TJ, Roth S. The structure of suspended graphene sheets. Nature 2007;446:60–3. doi:10.1038/nature05545.
- [47] Yang W, Widenkvist E, Jansson U, Grennberg H. Stirring-induced aggregation of graphene in suspension. New J Chem 2011;35:780. doi:10.1039/c0nj00968g.
- [48] Hummers WS, Offeman RE. Preparation of Graphitic Oxide. J Am Chem Soc 1958;80:1339–1339. doi:10.1021/ja01539a017.
- [49] Hatui G, Dhibar S, Das CK, Bhattacharya P, Sahoo S. One Pot Synthesis of Graphene by Exfoliation of Graphite in ODCB. Graphene 2013;2:42–8. doi:10.4236/graphene.2013.21006.
- [50] Lotya M, Hernandez Y, King PJ, Smith RJ, Nicolosi V, Karlsson LS, et al. Liquid Phase Production of Graphene by Exfoliation of Graphite in Surfactant/Water Solutions. J Am Chem Soc 2009;131:3611–20. doi:10.1021/ja807449u.
- [51] Unalan IU, Wan C, Trabattoni S, Piergiovanni L, Farris S. Polysaccharide-assisted rapid exfoliation of graphite platelets into high quality water-dispersible graphene sheets †. R Soc Chem 2015;5:26482–90. doi:10.1039/c4ra16947f.
- [52] Mohd Noh MIC, Mohamed MA, Ismail AG, Ani MH, Majlis BY. Improvement of Gas Barrier Properties of Polyethylene Terephtalate (PET) by Graphene Nanoplatelets (GNP). Mater Today Proc 2019;7:808–15. doi:10.1016/j.matpr.2018.12.079.
- [53] Ren F, Tan W, Duan Q, Jin Y, Pei L, Ren P, et al. Ultra-low gas permeable cellulose nanofiber nanocomposite films filled with highly oriented graphene oxide nanosheets induced by shear field. Carbohydr Polym 2019;209:310–9. doi:10.1016/j.carbpol.2019.01.040.
- [54] Pierleoni D, Xia ZY, Christian M, Ligi S, Minelli M, Morandi V, et al. Graphene-based coatings on polymer films for gas barrier applications. Carbon N Y 2016;96:503–12. doi:10.1016/J.CARBON.2015.09.090.
- [55] Akhina H, Mohammed Arif P, Gopinathan Nair MR, Nandakumar K, Thomas S. Development of plasticized poly (vinyl chloride)/reduced graphene oxide nanocomposites for energy storage applications. Polym Test 2019;73:250–7. doi:10.1016/j.polymertesting.2018.10.015.
- [56] Nguyen ST, Torkelson JM, Compton OC, Kim S, Pierre C. Crumpled Graphene Nanosheets

- as Highly Effective Barrier Property Enhancers. Adv Mater 2010;22:4759–63. doi:10.1002/adma.201000960.
- [57] Park GT, Chang J-H, Park GT, Chang J-H. Comparison of Properties of PVA Nanocomposites Containing Reduced Graphene Oxide and Functionalized Graphene. Polymers (Basel) 2019;11:450. doi:10.3390/polym11030450.
- [58] Hirschfelder JO, Curtiss CF, Brid RB. Molecular theory of gases and liquids. New York City: New York: Wiley; 1954.
- [59] Greco A, Timo A, Maffezzoli A. Development and characterization of amorphous thermoplastic matrix graphene nanocomposites. Materials (Basel) 2012;5:1972–85. doi:10.3390/ma5101972.
- [60] Goh K, Heising JK, Yuan Y, Karahan HE, Wei L, Zhai S. Sandwich-Architectured Poly(lactic acid)—Graphene Composite Food Packaging Films. ACS Appl Mater Interfaces 2016;8:9994–10004.
- [61] Ye Y, Zhang D, Liu T, Liu Z, Pu J, Liu W, et al. Superior corrosion resistance and self-healable epoxy coating pigmented with silanzied trianiline-intercalated graphene. Carbon N Y 2019;142:164–76. doi:10.1016/j.carbon.2018.10.050.
- [62] Agulló E, Rodríguez MS, Ramos V, Albertengo L. Present and Future Role of Chitin and Chitosan in Food. Macromol Biosci 2003;3:521–30. doi:10.1002/mabi.200300010.
- [63] Meyers SP, No HK, Nadarajah K, Bhale S, Farr AJ, Prinyawiwatkul W. Chitosan Coating Improves Shelf Life of Eggs. J Food Sci 2006;68:2378–83. doi:10.1111/j.1365-2621.2003.tb05776.x.
- [64] Puvvada YS, Vankayalapati S, Sukhavasi S, Yateendra \*, Puvvada S, Vankayalapati S, et al. Extraction of chitin from chitosan from exoskeleton of shrimp for application in the pharmaceutical industry. Int Curr Pharm J 2012;1:258–63. doi:10.3329/icpj.v1i9.11616.
- [65] Liu Y, Cai Z, Sheng L, Ma M, Xu Q. Influence of nanosilica on inner structure and performance of chitosan based films. Carbohydr Polym 2019. doi:10.1016/J.CARBPOL.2019.02.079.
- [66] Kurita K, Koyama Y, Nishimura S, Kamiya M. Facile Preparation of Water-Soluble Chitin from Chitosan. Chem Lett 1989;18:1597–8. doi:10.1246/cl.1989.1597.
- [67] Muzzarelli RAA, Aiba S, Fujiwara Y, Hideshima T, Hwang C, Kakizaki M, et al. Filmogenic Properties of Chitin / Chitosan. Chitin Nat. Technol., Boston, MA: Springer US; 1986, p. 389–402. doi:10.1007/978-1-4613-2167-5\_48.

- [68] El Knidri H, Belaabed R, Addaou A, Laajeb A, Lahsini A. Extraction, chemical modification and characterization of chitin and chitosan. Int J Biol Macromol 2018;120:1181–9. doi:10.1016/j.ijbiomac.2018.08.139.
- [69] Kong M, Chen XG, Xing K, Park HJ. Antimicrobial properties of chitosan and mode of action: A state of the art review. Int J Food Microbiol 2010;144:51–63. doi:10.1016/j.ijfoodmicro.2010.09.012.
- [70] Entsar I. Rabea †, Mohamed E.-T. Badawy †, Christian V. Stevens \*, Guy Smagghe † and, Steurbaut† W. Chitosan as Antimicrobial Agent: Applications and Mode of Action. Biomacromolecules 2003;4:1457–65. doi:10.1021/BM034130M.
- [71] Kong M, Chen XG, Liu CS, Liu CG, Meng XH, Yu LJ. Antibacterial mechanism of chitosan microspheres in a solid dispersing system against E. coli. Colloids Surfaces B Biointerfaces 2008;65:197–202. doi:10.1016/J.COLSURFB.2008.04.003.
- [72] Wang Y, Wang E, Wu Z, Li H, Zhu Z, Zhu X, et al. Synthesis of chitosan molecularly imprinted polymers for solid-phase extraction of methandrostenolone. Carbohydr Polym 2014;101:517–23. doi:10.1016/J.CARBPOL.2013.09.078.
- [73] Crouvisier-Urion K, Bodart PR, Winckler P, Raya J, Gougeon RD, Cayot P, et al. Biobased Composite Films from Chitosan and Lignin: Antioxidant Activity Related to Structure and Moisture. ACS Sustain Chem Eng 2016;4:6371–81. doi:10.1021/acssuschemeng.6b00956.
- [74] Yan N, Capezzuto F, Lavorgna M, Buonocore GG, Tescione F, Xia H, et al. Borate cross-linked graphene oxide-chitosan as robust and high gas barrier films. Nanoscale 2016;8:10783–91. doi:10.1039/c6nr00377j.
- [75] Giannakas A, Patsaoura A, Barkoula N-M, Ladavos A. A novel solution blending method for using olive oil and corn oil as plasticizers in chitosan based organoclay nanocomposites. Carbohydr Polym 2017;157:550–7. doi:10.1016/j.carbpol.2016.10.020.
- [76] Aljawish A, Muniglia L, Klouj A, Jasniewski J, El Scher J€, Desobry S. Characterization of films based on enzymatically modified chitosan derivatives with phenol compounds. Food Hydrocoll 2016;60:551–8. doi:10.1016/j.foodhyd.2016.04.032.
- [77] Hu D, Wang H, Wang L. Physical properties and antibacterial activity of quaternized chitosan/carboxymethyl cellulose blend films. LWT Food Sci Technol 2016;65:398–405. doi:10.1016/j.lwt.2015.08.033.
- [78] Perdones Á, Vargas M, Atarés L, Chiralt A. Physical, antioxidant and antimicrobial properties of chitosan-cinnamon leaf oil films as affected by oleic acid. Food Hydrocoll 2014;36:256–64. doi:10.1016/j.foodhyd.2013.10.003.

- [79] Leceta I, Guerrero P, Ibarburu I, Dueñas MT, De La Caba K. Characterization and antimicrobial analysis of chitosan-based films. J Food Eng 2013;116:889–99. doi:10.1016/j.jfoodeng.2013.01.022.
- [80] Benbettaïeb N, Kurek M, Bornaz S, Debeaufort F. Barrier, structural and mechanical properties of bovine gelatin-chitosan blend films related to biopolymer interactions. J Sci Food Agric 2014;94:2409–19. doi:10.1002/jsfa.6570.
- [81] Martínez-Camacho AP, Cortez-Rocha MO, Ezquerra-Brauer JM, Graciano-Verdugo AZ, Rodriguez-Félix F, Castillo-Ortega MM, et al. Chitosan composite films: Thermal, structural, mechanical and antifungal properties. Carbohydr Polym 2010;82:305–15. doi:10.1016/j.carbpol.2010.04.069.
- [82] Bertolino V, Cavallaro G, Lazzara G, Milioto S, Parisi F. Halloysite nanotubes sandwiched between chitosan layers: novel bionanocomposites with multilayer structures. New J Chem 2018;42:8384. doi:10.1039/c8nj01161c.
- [83] Hu X, Han G, Sun Y, Tian M, Zhu S, Du M, et al. Ultraviolet protection cotton fabric achieved via layer-by-layer self-assembly of graphene oxide and chitosan. Appl Surf Sci 2016;377:141–8. doi:10.1016/j.apsusc.2016.03.183.
- [84] Kahya N, Bener S, Kaygusuz H, Evingr GA, Erim FB. Adsorptive removal kinetics of anionic dye onto chitosan films doped with graphene oxide: An in situ fluorescence monitoring. Chem Eng Commun 2018;205:881–7. doi:10.1080/00986445.2017.1423064.
- [85] Salehi H, Rastgar M, Shakeri A. Anti-fouling and high water permeable forward osmosis membrane fabricated via layer by layer assembly of chitosan/graphene oxide. Appl Surf Sci 2017;413:99–108. doi:10.1016/j.apsusc.2017.03.271.
- [86] Fan L, Luo C, Sun M, Li X, Qiu H. Highly selective adsorption of lead ions by water-dispersible magnetic chitosan/graphene oxide composites. Colloids Surfaces B Biointerfaces 2013;103:523–9. doi:10.1016/j.colsurfb.2012.11.006.
- [87] Maddalena L, Carosio F, Gomez J, Saracco G, Fina A. Layer-by-layer assembly of efficient flame retardant coatings based on high aspect ratio graphene oxide and chitosan capable of preventing ignition of PU foam. Polym Degrad Stab 2018;152:1–9. doi:10.1016/j.polymdegradstab.2018.03.013.
- [88] Diode TS, Khairir NS, Mat MR. Chitosan / graphene oxide biocomposite film from pencil rod. J Phys Conf Ser 2018;970:012006.
- [89] Weng SX, Yousefi N, Tufenkji N. Self-Assembly of Ultralarge Graphene Oxide Nanosheets and Alginate into Layered Nanocomposites for Robust Packaging Materials. ACS Appl Nano

- Mater 2019;2:1431–44. doi:10.1021/acsanm.8b02323.
- [90] Wang S, Liu G, Pu J. Enhancement of the Strength of Biocomposite Films via Graphene Oxide Modification. BioResources 2018;13:6321–31. doi:10.15376/biores.13.3.6321-6331.
- [91] Huang B, Zhu Q, Liang B, Ye X, Fang L, Tu T, et al. Layer-by-layer chitosan-decorated pristine graphene on screen-printed electrodes by one-step electrodeposition for non-enzymatic hydrogen peroxide sensor. Talanta 2018;190:70–7. doi:10.1016/j.talanta.2018.07.038.
- [92] Chen J, Ma Y, Wang L, Han W, Chai Y, Wang T, et al. Preparation of chitosan/SiO2-loaded graphene composite beads for efficient removal of bilirubin. Carbon N Y 2019;143:352–61. doi:10.1016/J.CARBON.2018.11.045.
- [93] Wu M, Chen W, Mao Q, Bai Y, Ma H. Facile synthesis of chitosan/gelatin filled with graphene bead adsorbent for orange II removal. Chem Eng Res Des 2019;144:35–46. doi:10.1016/J.CHERD.2019.01.027.
- [94] Shan C, Yang H, Han D, Zhang Q, Ivaska A, Niu L. Graphene/AuNPs/chitosan nanocomposites film for glucose biosensing. Biosens Bioelectron 2010;25:1070–4. doi:10.1016/J.BIOS.2009.09.024.
- [95] Magerusan L, Pogacean F, Coros M, Socaci C, Pruneanu S, Leostean C, et al. Green methodology for the preparation of chitosan/graphene nanomaterial through electrochemical exfoliation and its applicability in Sunset Yellow detection. Electrochim Acta 2018;283:578–89. doi:10.1016/j.electacta.2018.06.203.
- [96] Zhang P, Gong J-L, Zeng G-M, Song B, Fang S, Zhang M, et al. Enhanced permeability of rGO/S-GO layered membranes with tunable inter-structure for effective rejection of salts and dyes. Sep Purif Technol 2019. doi:10.1016/j.seppur.2019.03.041.

#### 3. MATERIALS AND METHODS

#### 3.1 Materials

Poly(lactic acid) resin (PLA 4032D with a D-lactide content of 3.8-4.2%) was supplied by NatureWorks LLC (Minnetonka, MN, U.S.). Co-extruded plain PLA films with a thickness of 20 μm were kindly donated by BI-AX International Inc. (Winham, ON, Canada). Chitosan (448869), graphite (496588, powder, particle size < 150 μm), and desiccant (Drietite <sup>TM</sup>, 238988-454G, 8 mesh) were purchased from Sigma Aldrich (St. Louis, MO, U.S.). Acetic acid (analytically pure) with a flash point of 39°C was obtained from Avantor Performance Materials, LLC. (Radnor, PA, U.S.). Aluminum foil from Reynolds Wrap (Louisville, KY, U.S.) was purchased from a local grocery store. Lab deionized water (DI water) was used throughout the project.

### 3.2 Methods

#### 3.2.1 Home-Made PLA Films Production

The PLA resin was first dried at 50°C in vacuum oven under a pressure of 25 in Hg for 12 h, and then extruded in a Microextruder model RCP-0625 (Randcastle Extrusion Systems, Inc.) (Cedar Grove, NJ, U.S.). The screw diameter was 1.5875 cm, with a 24/1 L/D ratio extruder and a volume of 34 cc. The temperature profile of the extruder was 335-380-390-385-385-385-385 °F (168-193-199-196-196-196 -196 °C) from zone 1, zone 2, zone 3, transfer tube, adapter, feed block, and die, respectively. Films were extruded with a screw rotation speed of 20 rpm. The thickness of the home-made PLA film (HPLA) was measured using a digital micrometer (Testing Machines Inc.) (Ronkonkoma, NY, U.S.).

### 3.2.2 Preparation of Chitosan Water Solution

Chitosan (2 wt%) and acetic acid (1 wt%) was added in DI water and stirred by a magnetic stirrer (MS-H-Pro<sup>+</sup>, Scilogex) (Rocky Hill, CT, U.S.) at a speed of 300 rpm under room temperature for 12 h until the chitosan water solution was clear. Then, the chitosan water solution was ultrasonicated for 30 min using an ultrasonicator (VCX750, Sonics & Materials, Inc.) (Newtown, CT, U.S.) equipped with a tip that had a diameter of 13 mm. The ultrasonicated chitosan water solution was centrifuged for 1 h at 1500 rpm with a centrifuge (5804R, Eppendorf) (Hauppauge, NY, U.S.). The obtained supernatant was chitosan water solution (chit) being used later.

#### 3.2.3 Production of Chitosan-Graphene Water Solution

Chitosan water solution was first prepared as reported per Section 3.2.2. Graphite (10 mg mL<sup>-1</sup>) was added into chitosan water solution and stirred for 5 min at a speed of 300 rpm min<sup>-1</sup>. The mixture was then ultrasonicated by 30 min and further centrifuged for 1 h under 1500 rpm. Supernatant from the centrifugation step was the chitosan-graphene water solution (chitGRH) further used. Additional information about the method can be retrieved from Unalan et al. [1]

#### 3.2.4 Plasma Treatment

To introduce negative charges on the surfaces of the polymer films, a plasma reactor (PS 0500, Plasma Science Inc.) (TN, U.S.) was used to treat the substrate films with an oxygen flow of 50% and a plasma power of 300 Watt for 10 min on both sides. PLA film with both sides treated (PLA-2p) was used as control.

### 3.2.5 Preparation of HPLA-Coating-HPLA-HP Film

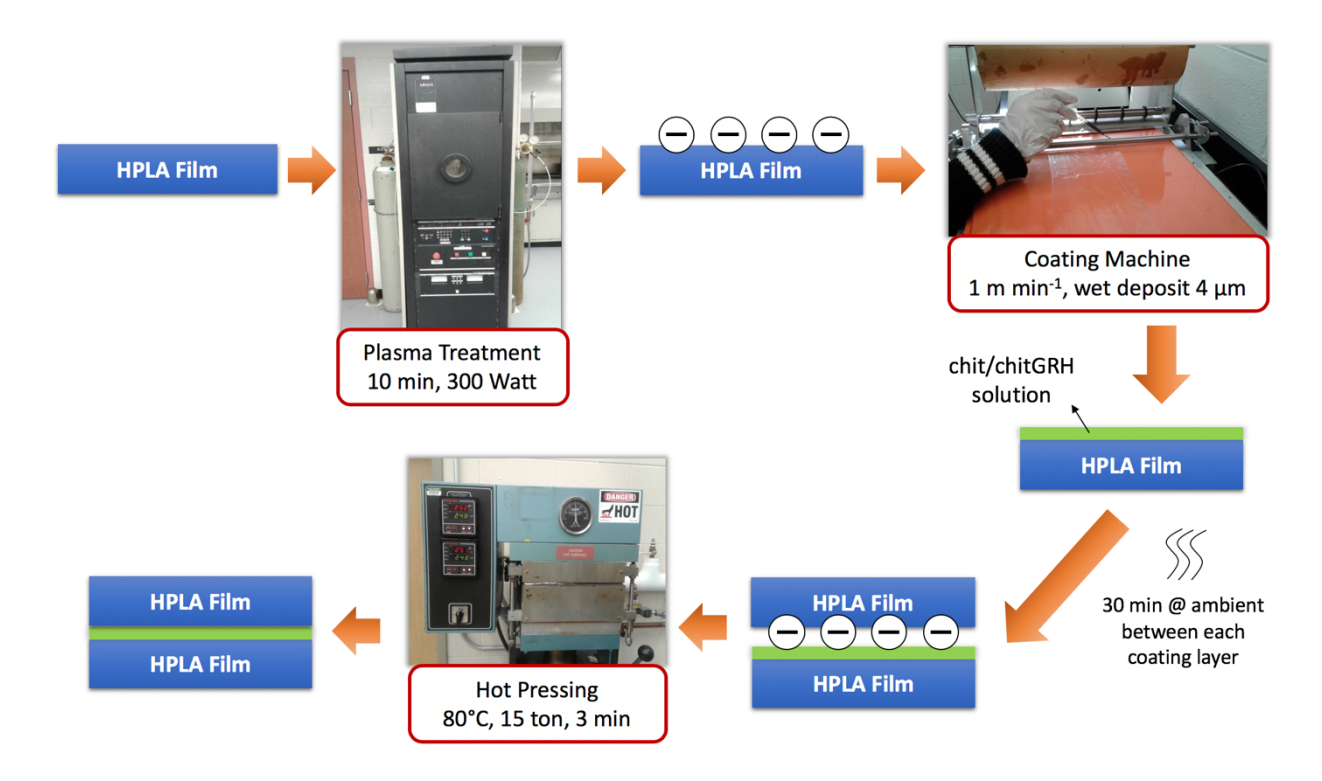


Figure 2.8. Preparation of HPLA-Coating-HPLA film.

HPLA film were first been plasma treated on one side with a 50% oxygen flow under 300 Watt for 10 min. Then, chit or chitGRH were coated on HPLA film using multilayer coating technique by a multicoater (K303 multicoater, RK Printcoat Instruments) (Royston, Hertfordshire, U.K.) with bar #0 (wet film deposit: 4 μm). Coating speed was 1 m min<sup>-1</sup>. There was a 30-min interval between the two consecutive coating layers to let the coating solution dry at room temperature in a hood inside a desiccator with desiccant on the side. After the coating was dry, another plasma treated HPLA film was attached to HPLA-Coating film. Plasma treated side was attached to the coating layer. Then, the multilayer film set was hot pressed (QL438-C, PHI, City of Industry, CA, US) at 80°C under 15 ton of pressure for 3 min. The fabrication process was illustrated in Figure 2.8.

# 3.2.6 Preparation of LLDPE-Coating-LLDPE-HP Film

Chit or chitGRH were coated on LLDPE film by the multicoater with bar #0. Coating speed was 1 m min<sup>-1</sup>. There was a 30-min interval between two coating layers to let the coating solution dry at room temperature in a hood inside a desiccator with desiccant on the side. After the coating was dry, another LLDPE film was being attached to the LLPDE-Coating film. Then, the multilayer film was being compressed at 100°C and 10 ton for 3 min. The fabrication process is illustrated in Figure 2.9.

Seven types of films were produced: (1) LLDPE-LLDPE-HP; (2) LLDPE films with 1-layer chit coating (LLDPE-1chit-LLDPE-HP); (3) LLDPE films with 2-layer chit coating (LLDPE-2chit-LLDPE-HP); (4) LLDPE films with 5-layer chit coating (LLDPE-5chit-LLDPE-HP); (5) LLDPE films with 1-layer chitGRH coating (LLDPE-1chitGRH-LLDPE-HP); (6) LLDPE films with 2-layer chitGRH coating (LLDPE-2chitGRH-LLDPE-HP); (7) and LLDPE films with 5-layer chitGRH coating (LLDPE-5chitGRH-LLDPE-HP).

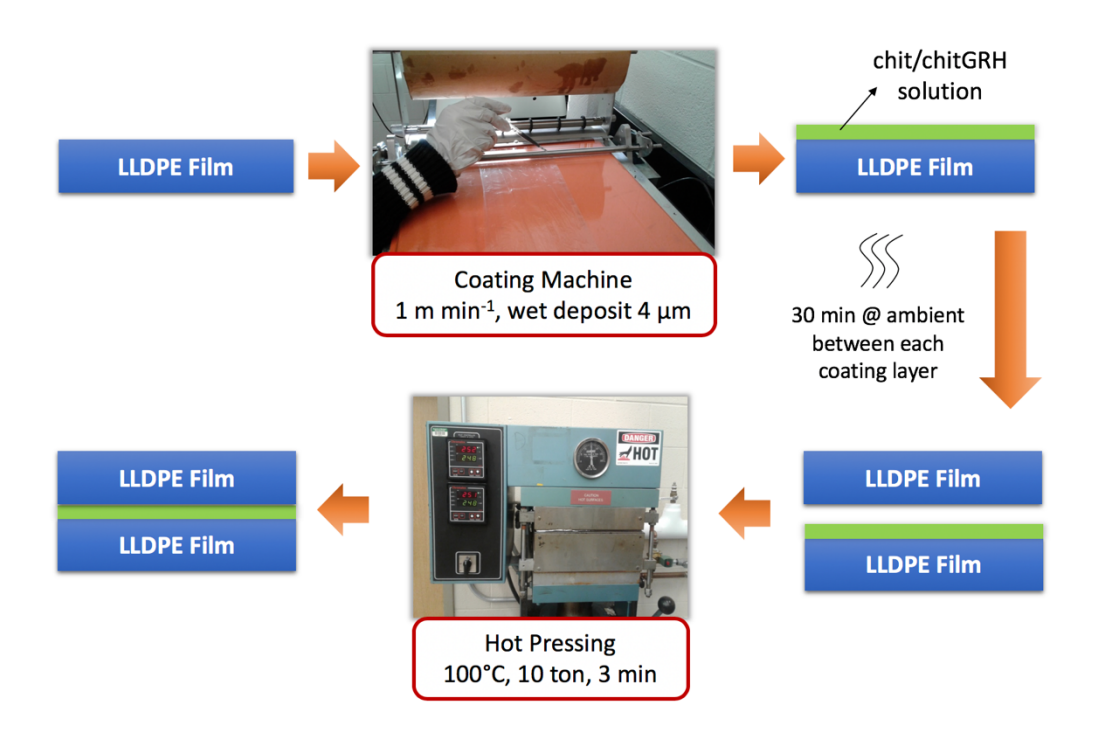


Figure 2.9. Preparation of LLDPE-Coating-LLDPE film.

# 3.2.7 Preparation of PLA-Coating Film

PLA films were first been plasma treated on one side with a 50% oxygen flow under 300 Watt for 10 min. Then chit or chitGRH were coated on PLA film by the multicoater with bar #0. Coating speed was 1 m min<sup>-1</sup>. There was a 30-min interval between two coating layers to let the coating solution dry at room temperature in a hood inside a desiccator with desiccant on the side. Coating process is illustrated in **Figure 2.10**.

Four types of samples were prepared: (1) PLA film with 5-layer chit coating (PLA-5chit); (2) PLA film with 20-layer chit coating (PLA-20chit); (3) PLA film with 5-layer chitGRH coating (PLA-5chitGRH); (4) and PLA film with 20-layer chitGRH coating (PLA-20chitGRH).

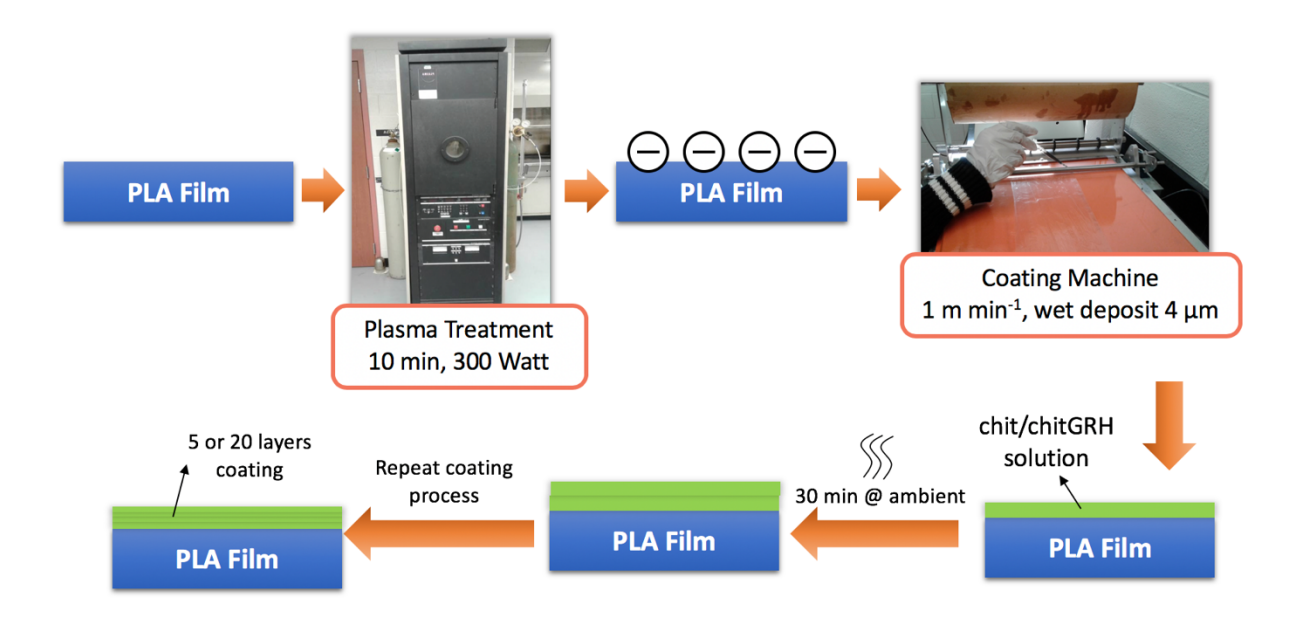


Figure 2.10. Preparation of PLA-Coating film.

# 3.2.8 Preparation of Coating-PLA-Coating Film

PLA films were first been plasma treated with a 50% oxygen flow under 300 Watt for 10 min. Then chit or chitGRH solution were coated by the multicoater with bar #0. Coating speed was 1 m min<sup>-1</sup>. PLA films were alternately coated on each side. There was a 30-min interval between two coating layers to let the coating solution dry at room temperature in a hood inside a desiccator with desiccant on the side. Coating process is illustrated in **Figure 2.11**.

Totally, four samples were prepared: (1) 6-layer chit coated PLA film (3chit-PLA-3chit); (2) 6-layer chitGRH coated PLA film (3chitGRH-PLA-3chitGRH); (3) 20-layer chit coated PLA film (10chit-PLA-10chit); (4) and 20-layer chitGRH coated PLA film (10chitGRH-PLA-10chitGRH).

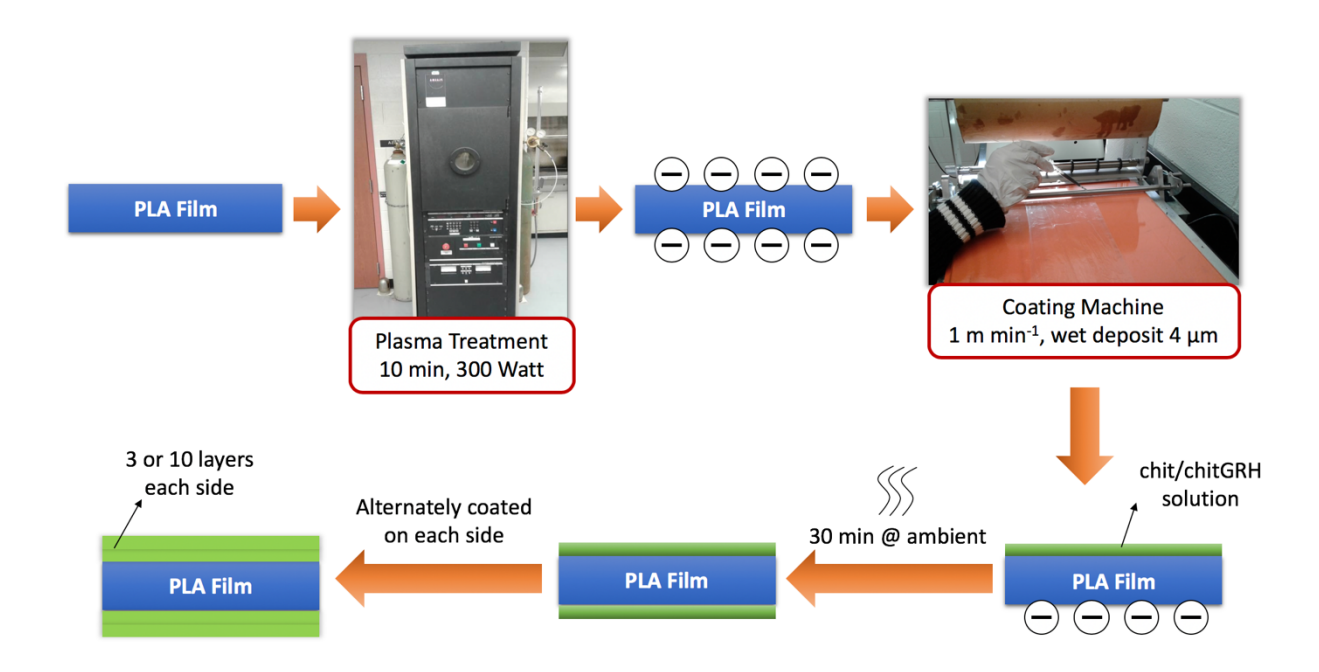


Figure 2.11. Preparation of Coating-PLA-Coating film.

# 3.2.9 Preparation of Coating Film

Aluminum foil was plasma treated with a 50% oxygen flow under 300 Watt for 10 min. Then chitosan or chitGRH solution were coated by the multicoater with bar #0 and a coating speed of 1 m min<sup>-1</sup>. There was a 30-min interval between two coating layers to let the coating solution dry at room temperature in a hood inside a desiccator with desiccant on the side. The coated films were removed carefully from the aluminum foil after they were dried. Coating process is illustrated in **Figure 2.12**. In this step, only 6-layer chit film (6chit) was prepared.

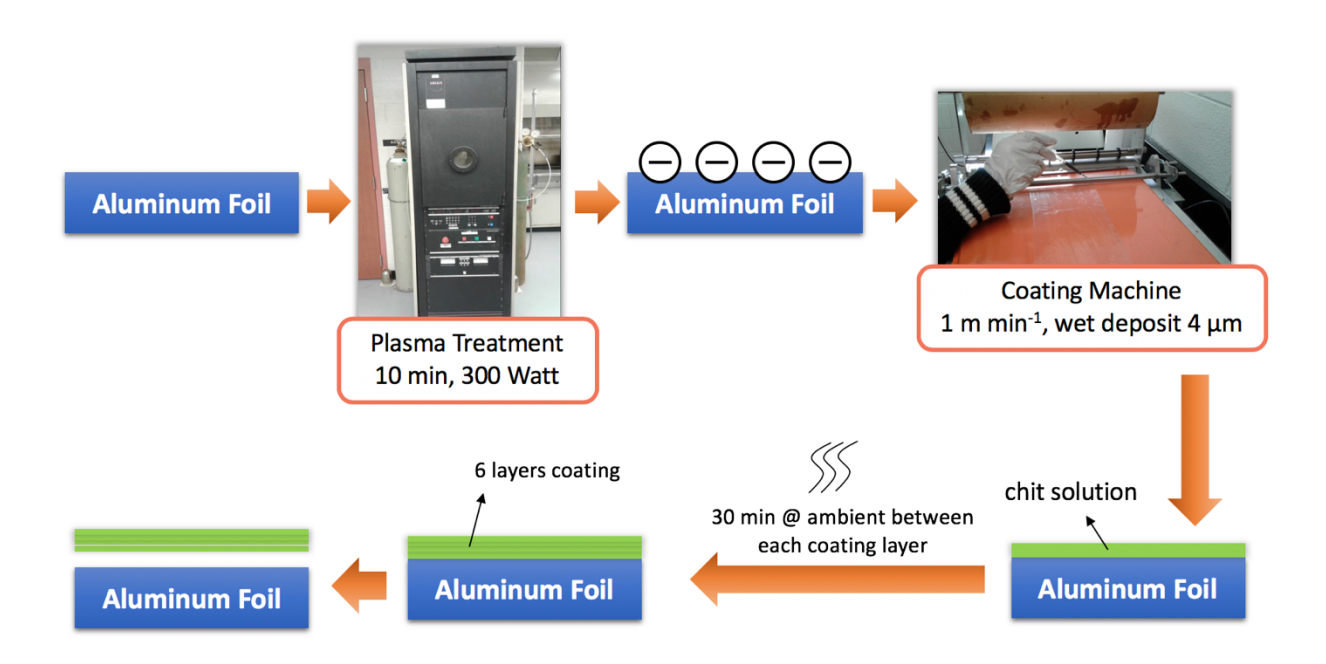


Figure 2.12. Preparation of coating film.

#### 3.2.10 Film Thicknesses

A digital micrometer (49-70-01-0001, Test Machine Inc.) (Ronkonkoma, NY, U.S.) was used to measure the thickness of the films. Resolution of the measured thickness was 0.01 mm.

# 3.2.11 Characterization of the multilayer structures

A scanning electron microscope (SEM) (JEOL 7500F, JEOL Ltd.) (Tokyo, Japan) was used to examine the cross-section of coated PLA films to check the multilayer structure and coating thickness. Coated film samples were first mounted on an aluminum stubs using epoxy glue (System Three Resins, Inc.) (Aubur, WA), and then frozen with liquid nitrogen and cut with a clean double edge razor blade. To prevent being charged by electron beam, film samples were then coated with Iridium for 60 s in a Q150T turbo pumped sputter coater (Quorum Technologies,

Laughton, East Sussex, U.K.) purged with argon gas. Energy dispersive X-ray spectroscopy (EDS) was conducted to distinguish the interface between PLA film and coating layers.

# 3.2.12 Thermal Properties

Thermal degradation properties, including thermogravimetric analysis (TGA) and derivative thermogravimetry (DTG), were determined using a Q50 equipment (TA Instruments) (New Castle, DE, U.S.). PLA, chitosan, graphite, PLA-5chit, PLA-20chit, PLA-5chitGRH, and PLA-20chitGRH were tested. Onset temperature ( $T_o$ ), maximum temperature ( $T_{max}$ ), and end decomposition temperature ( $T_e$ ) were obtained from DTG, and % weight loss (%wtL) during each decomposition stage as determined by TGA. Temperature ramped up to 600°C at a speed of 10°C min<sup>-1</sup>. Data sampling frequency was 1 Hz. A Q100 differential scanning calorimeter (DSC) (New Castle, DE, U.S.) was used to determine the glass transition temperature ( $T_g$ ), melting temperature ( $T_m$ ), crystallization enthalpy ( $\Delta H_c$ ), and melting enthalpy ( $\Delta H_m$ ). Test temperature was set to ramp up from 10°C to 210°C, then decreased back to 10°C, followed by increasing to 210°C again. Temperature was changed at a rate of 10°C min<sup>-1</sup>. Data sampling interval was 5 Hz. Crystallinity of PLA was calculated from enthalpies.

# 3.2.13 Oxygen Permeability

An oxygen permeability tester (Model 2/21 MOCON OX-TRAN, Mocon, Minneapolis, MN, U.S.) was used to test oxygen permeability (OP) of HPLA-Coating-HPLA films, LLDPE-Coating-LLDPE films, and PLA-Coating films based on ASTM F1927-14 [2]. Testing range was 0.05 to 200 cc m<sup>-2</sup> day<sup>-1</sup> with a testing area of 50 cm<sup>2</sup>. A permeation area of 3.14 cm<sup>2</sup> was used. Oxygen concentration was 100%, with a barometric pressure of 0.98 bar. Test temperature was manually

set between 21°C to 23°C. Continuous test mode was used with a 2-h conditioning. Sampling rate was 30 min.

An 8001 Oxygen Permeation Analyzer (Systech Instruments Ltd and Illinois Instruments, Inc.) (Johnsburg, IL, U.S.) was also used to measure oxygen permeability with temperature set as 23°C based on ASTM F1927-14 [2]. Testing range was 0.008 to 432,000 cc m<sup>-2</sup> day<sup>-1</sup> with a testing area of 50 cm<sup>2</sup>. Both bypass time and sampling rate were 10 min. A permeation area of 3.14 cm<sup>2</sup> was used.

An oxygen permeability tester (Model 2/22 MOCON OX-TRAN, mocon) (Minneapolis, MN, U.S.) was used to test OP of coating-PLA-coating films, PLA-coating-PLA films, and coating films based on ASTM F1927-14 [2]. Testing range was 0.05 to 200 cc m<sup>-2</sup> day<sup>-1</sup> with a testing area of 50 cm<sup>2</sup>. Auto Test mode was used, so the test will finish automatically when transmission rate was stable. Tests were run at 23°C without conditioning. Sampling rate was 15 min. Area that permeation occurred for coating-PLA-coating films and PLA-coating-PLA films was 3.14 cm<sup>2</sup>. Since the coating film was very thin and it was difficult to get a single piece of sample, the area for coating film was 0.18 cm<sup>2</sup>. For each test, 2 or 6 replicates were tested for each sample.

# 3.2.14 Statistical Analysis

One-way ANOVA with Tukey's comparison were analyzed using Minitab Express™ from Minitab, LLC (State College, PA, U.S.).

REFERENCES

#### **REFERENCES**

- [1] Unalan IU, Wan C, Trabattoni S, Piergiovanni L, Farris S. Polysaccharide-assisted rapid exfoliation of graphite platelets into high quality water-dispersible graphene sheets †. R Soc Chem 2015;5:26482–90. doi:10.1039/c4ra16947f.
- [2] ASTM International. ASTM F1927-14 Standard Test Method for Determination of Oxygen Gas Transmission Rate, Permeability and Permeance at Controlled Relative Humidity Through Barrier Materials Using a Coulometric Detector. West Conshohocken, PA; ASTM International, 2014. doi: https://doi-org.proxy1.cl.msu.edu/10.1520/F1927-14

# 4. RESULTS AND DISCUSSION

# 4.1 Preliminary Study

Study on type of PLA substrate film and sample preparation method being used are included in this section. HPLA-coating-HPLA-HP was studied first, followed by LLDPE-coating-LLDPE-HP film. By comparing oxygen permeability and OP data distribution, commercial PLA film were tested in the following studies.

# 4.1.1 HPLA-Coating-HPLA-HP Film

PLA films produced in our laboratory were plasma treated (HPLA) coated with chitosan and sandwich with another HPLA film. **Table 4-1** shows the oxygen permeability of HPLA-coating-HPLA-HP films, with OP value distribution plotted in Figure 4-1. Figure 4-2 shows a picture of the HPLA films.

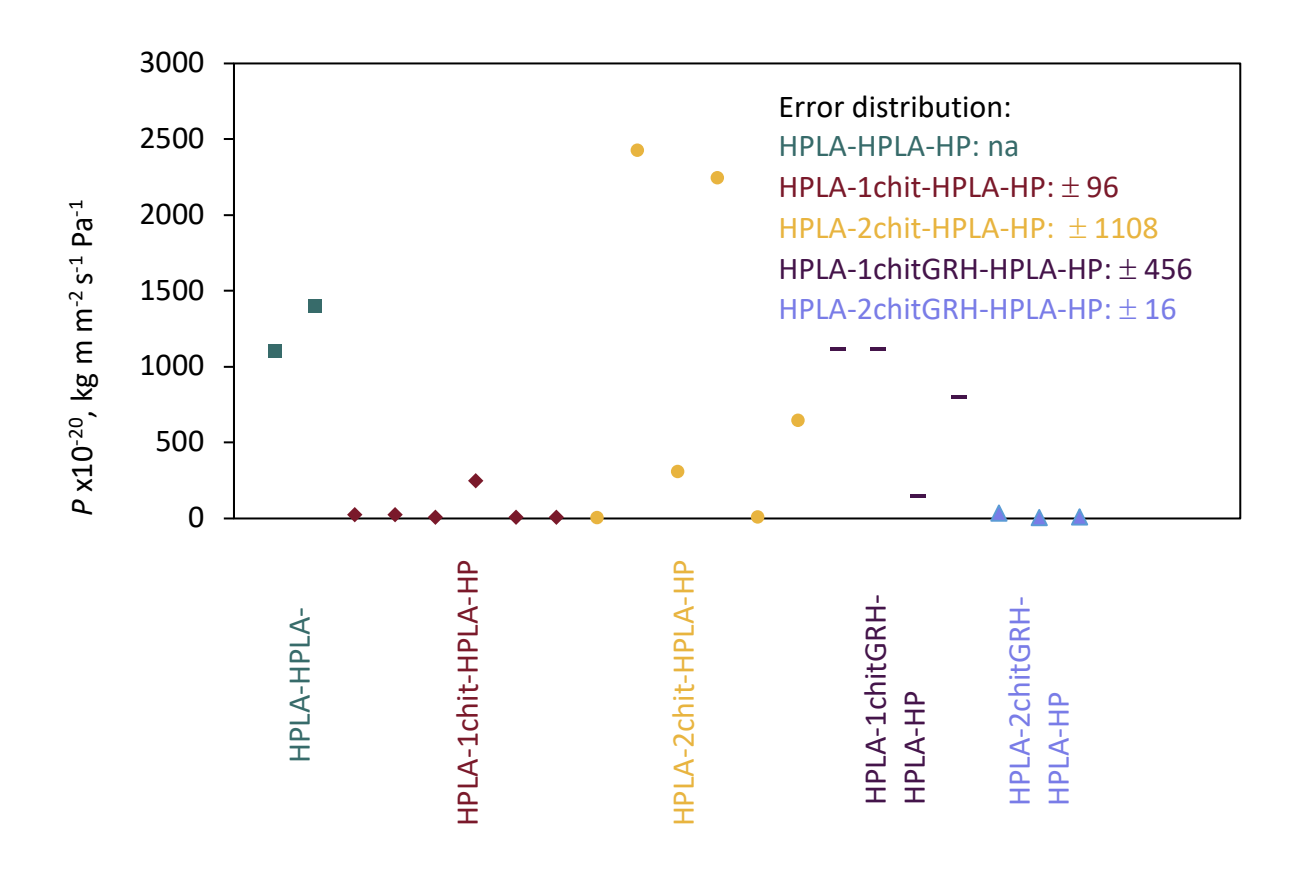


**Figure 4-1. OP distribution of HPLA-coating-HPLA-HP films at 23°C, 0% RH.** Same color name corresponds to same color data. One data represents one measurement.

For this preliminary test, chitosan or chitGRH coating did not improve oxygen barrier property of HPLA film at 23°C, 0% RH. The standard deviations of OP values were very large, which can also be seen from the data points and errors distribution in Figure 4-1, indicating the inconsistency of the samples or tests. This also explained why the OP of HPLA-2chitGRH-HPLA-HP was not significantly different from the OP of HPLA-HPLA-HP. The inconsistency might due to the cracks produced on the HPLA film and its unflattens in **Figure 4-2**. Cracks enabled oxygen to move through the PLA matrix without obstructing O<sub>2</sub> permeation, which triggered the inaccuracy of the tests. On the other hand, equation 2-7 is based on the assumption that the transmission rate of permeant per unit area is measured normal to the test film as mentioned in Section 2.1.2, the

unflattens of the PLA sample film could also make the results imprecise. **Figure 4-2** shows a pictorial view of the samples.

Table 4-1. OP value of HPLA-coating-HPLA-HP films at 23°C, 0% RH.

Type of film	Thickness x 10 <sup>-6</sup> *	<i>P</i> x 10 <sup>-20 *</sup>
туре от пшп	m	kg m m <sup>-2</sup> s <sup>-1</sup> Pa <sup>-1</sup>
HPLA-HPLA-HP	25	1254 <sup>A</sup>
HPLA-1chit-HPLA-HP	$24\pm2$	54 $\pm$ 96 $^{\text{A}}$
HPLA-2chit-HPLA-HP	$25\pm0.5$	943 $\pm$ 1108 $^{\text{A}}$
HPLA-1chitGRH-HPLA-HP	$24\pm2$	$792\pm456$ $^{\text{A}}$
HPLA-2chitGRH-HPLA-HP	$\textbf{24}\pm\textbf{1}$	17 $\pm$ 16 <sup>A</sup>

 $<sup>^{*}</sup>$  Thickness and OP value are shown as average  $\pm$  standard deviation except for HPLA-HPLA-HP, which had two replicates.

<sup>&</sup>lt;sup>A</sup> P values sharing the same capital letter had no significant difference.

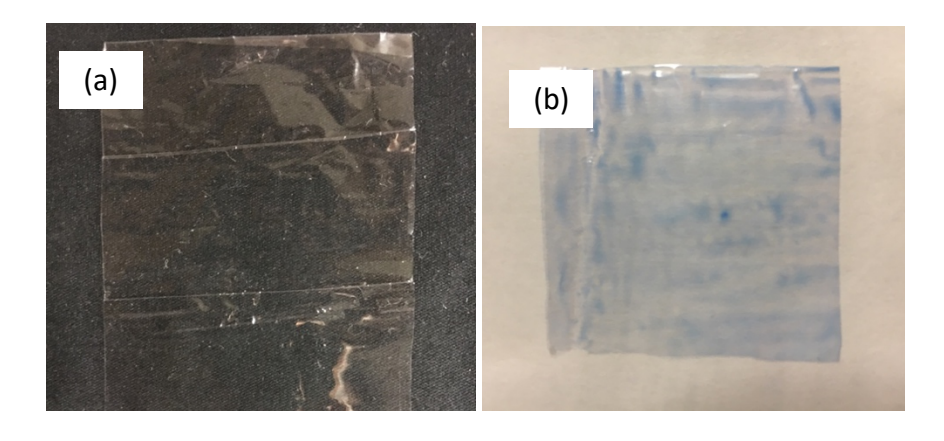


Figure 4-2. (a) HPLA film sample used for HPLA-coating-HPLA-HP, (b) HPLA film with colored chit coating.

#### 4.1.2 LLDPE-Coating-LLDPE-HP Film

Since the coating of HPLA samples did not produce films with improved oxygen barrier, commercial LLDPE films were used to determine if improvement of oxygen barrier can be done with chitosan coatings. Commercial LLDPE films instead of HPLA films were used as substrates.

Figure 4-3 shows LLDPE films before and after chit or chitGRH coating. Transparency decreased in the LLDPE-5chitGRH due to addition of graphene. No cracks or unflattens were observed in the films.

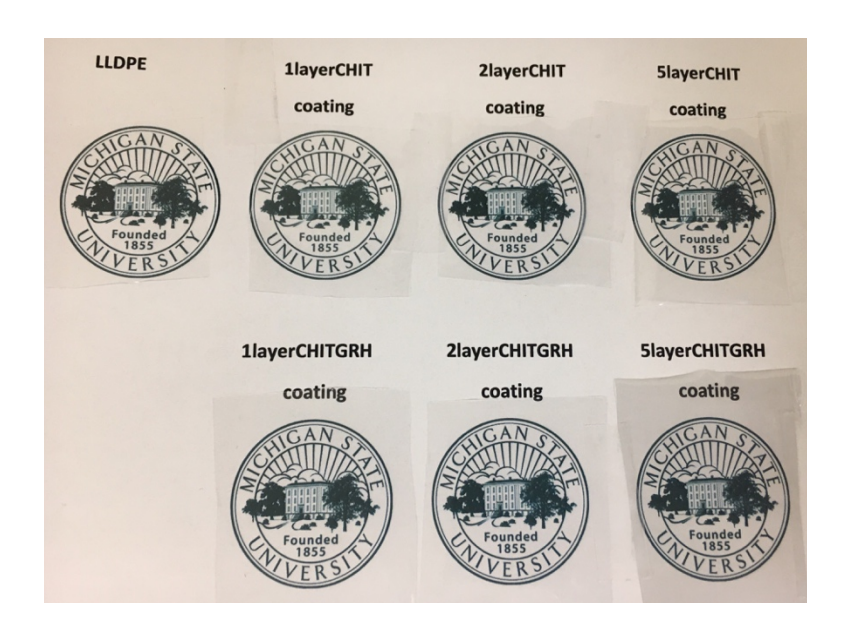


Figure 4-3. Single layer LLDPE films with or without coating.

Table 4-2 shows the oxygen barrier property of the films at 23°C and 0% RH. Large variation of thickness for LLDPE-2chit-LLDPE-HP might be due to wrinkles caused by compression molding. The OP values showed that chit or chitGRH coating can significantly improve oxygen barrier property of LLDPE films although there were unexpected large variations in OP, which could be caused by heat and pressure from compression molding applied during LLDPE-coating-

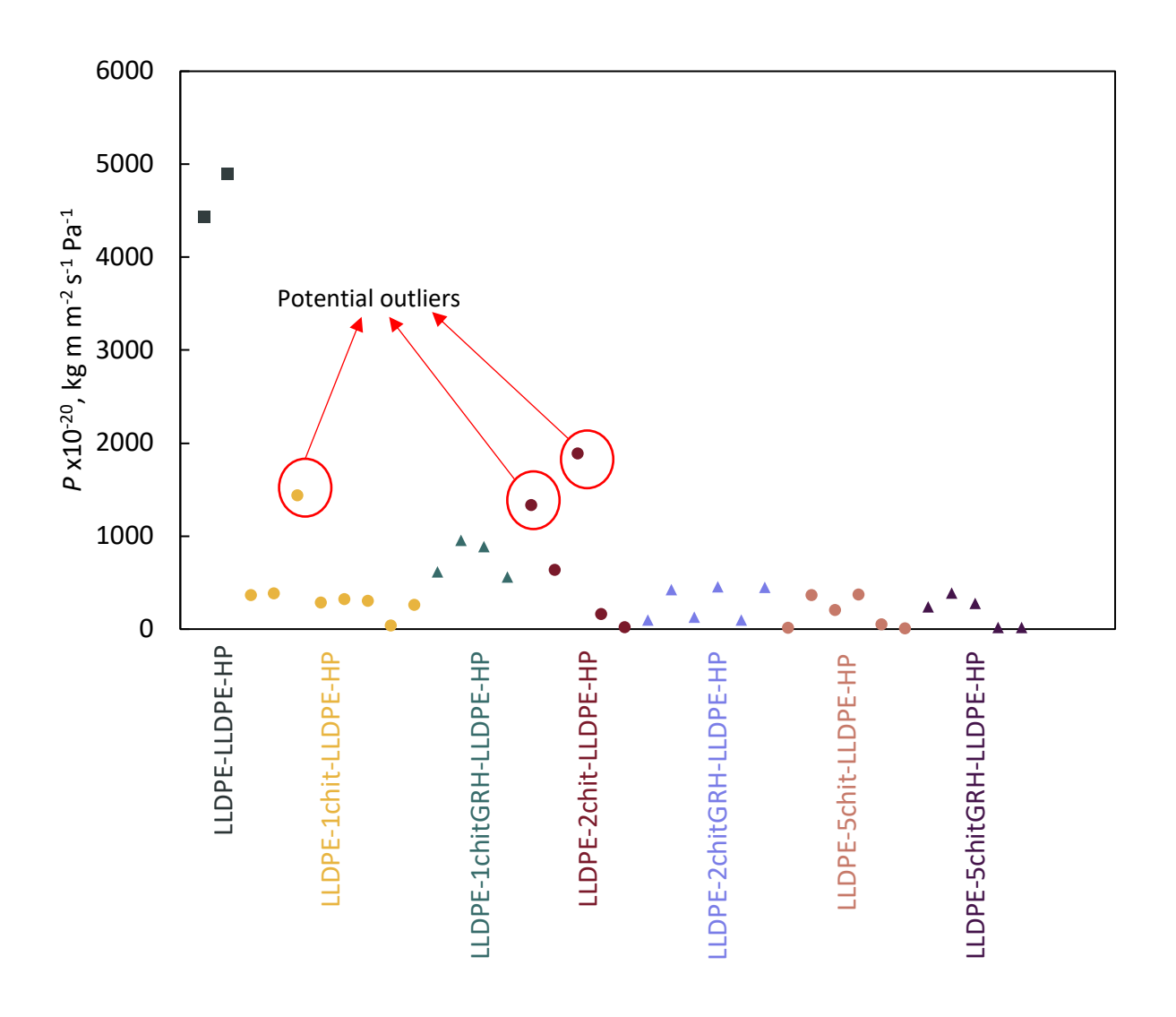
LLDPE production; Also, the presence of data outliers circled in red in Figure 4-4 could be due to experimental errors.

Table 4-2. OP value of LLDPE-coating-LLDPE-HP films at 23°C, 0% RH.

Type of film	Thickness x 10 <sup>-6</sup> *	<i>P</i> x 10 <sup>-20</sup> *
Type of fillin	m	kg m m <sup>-2</sup> s <sup>-1</sup> Pa <sup>-1</sup>
LLDPE-LLDPE-HP	107	4670 <sup>A</sup>
LLDPE-1chit-LLDPE-HP	$\textbf{101} \pm \textbf{2}$	$428\pm423~^{\text{B}}$
LLDPE-2chit-LLDPE-HP	$\textbf{122} \pm \textbf{27}$	$812\pm792$ B
LLDPE-5chit-LLDPE-HP	$\textbf{113}\pm\textbf{1}$	$262\pm202~^{B}$
LLDPE-1chitGRH-LLDPE-HP	$\textbf{119} \pm \textbf{2}$	754 $\pm$ 197 $^{\mathrm{B}}$
LLDPE-2chitGRH-LLDPE-HP	$\textbf{101} \pm \textbf{2}$	$276\pm185$ $^{\text{B}}$
LLDPE-5chitGRH-LLDPE-HP	$106\pm2$	$188\pm164^{\ B}$

 $<sup>^{*}</sup>$  Thickness and OP value are shown as average  $\pm$  standard deviation except for LLDPE-LLDPE-HP, which had two replicates.

<sup>&</sup>lt;sup>A</sup> P values sharing the same capital letter had no significant difference.



**Figure 4-4. OP distribution of LLDPE-coating-LLDPE-HP films at 23°C, 0% RH.** Same color name corresponds to same color data.

All the chitosan coated LLDPE commercial films showed lower OP values than regular LLDPE films with less variations than home-made PLA films. Since hot pressing was not used in the sample preparation since there were multiple parameters that could not easily be controlled easily during the process.

## 4.2 PLA-Coating Film

# 4.2.1 Morphology

Figure 4-5 shows the SEM images of the cross-sections of PLA-Coating films. Thickness was measured using the SEM software. From Figure 4-5 (a) and (b), PLA film and 20chit coating layers have thickness of around 19 and 16 µm, respectively. Figure 4-5 (c) showed clear interface lines between the chitosan coating layers, indicating that the previous dried chitosan coating layers were not attached or dissolved into the newly applied solution. However, a total measured thickness of 20 layers coating (16 µm) was one order of magnitude larger than the estimated from theoretical thickness calculations (0.4 μm for 5 layers coating and 1.6 μm for 20 layers coating). This anomaly could be due to: 1) the unflattens of the coating machine surface and the film surface; 2) the coating rod was not placed parallel to the coating machine surface; 3) the coating bar was not been cleaned enough; 4) the curling of the coated film generated by applying coating only on one side of the substrate, which was due to the fact that the surface of liquid tends to shrink due to surface tension [1]. Figure 4-5 (c) inset shows that there were some cracks found on the chitosan coated layers. The closer to surface of the coated film, the more cracks were present, which could be attributed to the flattening of the dried coated films for further layer application.

**Figure 4-6** shows the EDX line scan results of the PLA-20chit films. More N and O were observed in the chit coating section due to the chemical structures of PLA and chitosan. There was some N signal detected in the PLA films. This might be due to: (1) noise, since at the right end of the line, no element should have been detected there, while still some N was observed;

(2) during the coating process, PLA substrate reacted with chit solution, which enabled amidogen groups in chitosan moving to PLA; (3) the knife cutting from coating part to PLA part during the SEM sample preparation "dragged" some chitosan to PLA section. The highest amount of C was found at the interface, and O was found to concentrate more on both surfaces' chit coating part, which was due to oxygen plasma treatment.

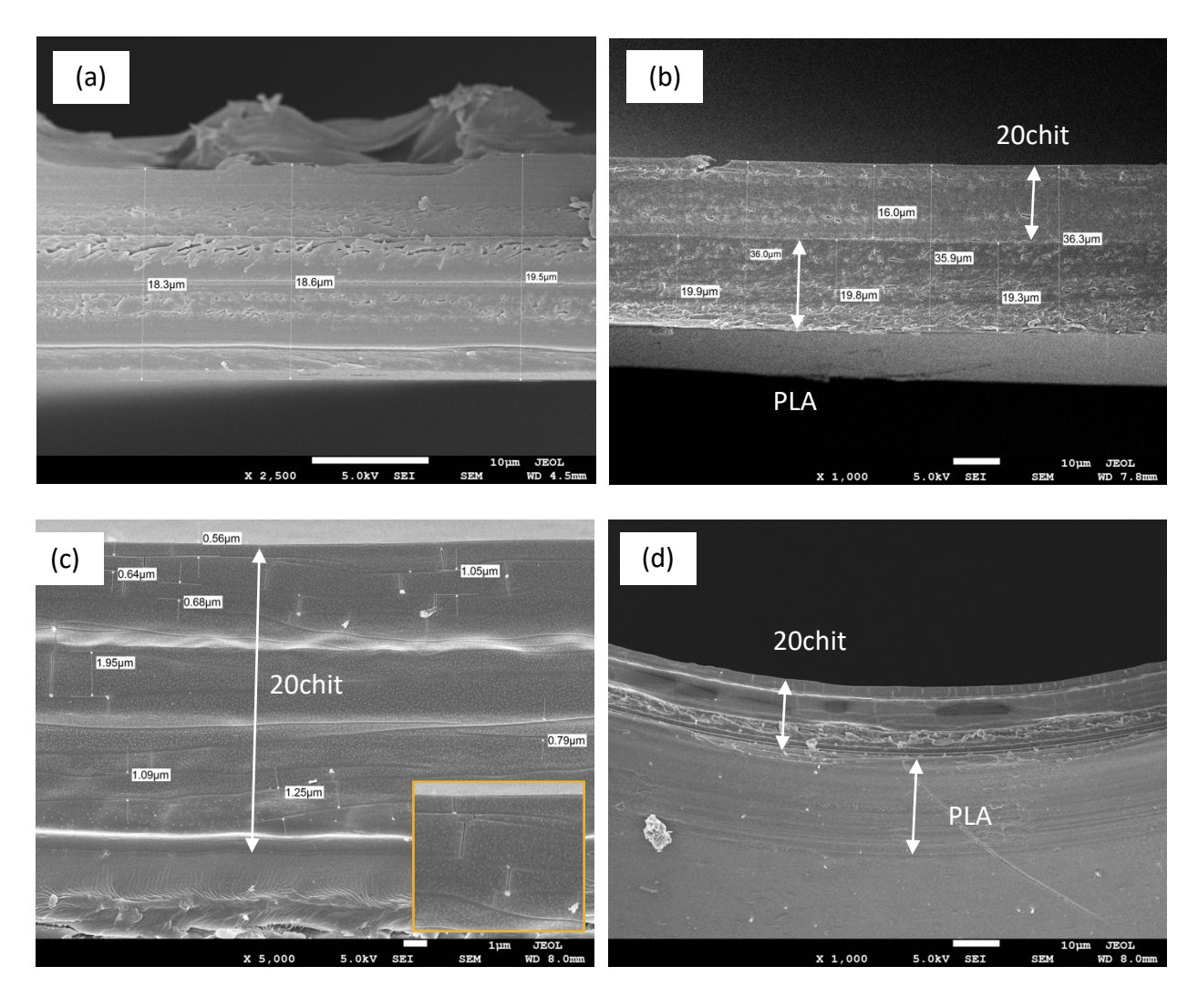
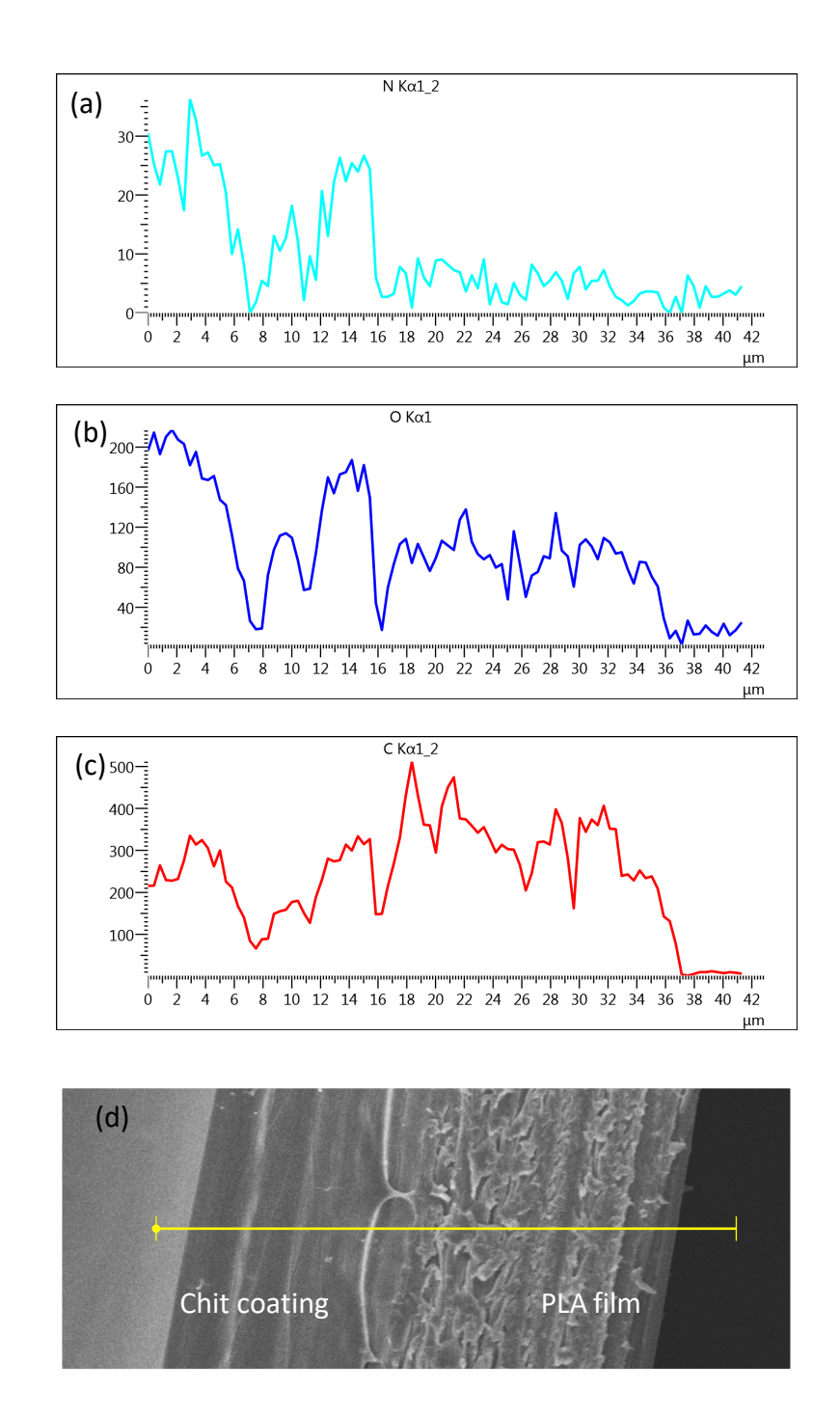


Figure 4-5. Cross-sections of (a) PLA film, (b) PLA-20chit film, (c) 20chit coating part on PLA film, and (d) curvature of PLA-20chit film. PLA and coating part were labeled. The unlabeled part in (d) is the bottom surface of PLA film.



**Figure 4-6. EDX line scan of N, O, and C distribution of PLA-20chit.** (a) N distribution, (b) O distribution, (c) C distribution, and (d) SEM image of PLA-20chit.

# 4.2.2 Thermal Properties

## 4.2.2.1 TGA

**Figure 4-7** shows the thermal stability results of PLA, chitosan, graphite, chitGRH, and coated PLA films, corresponding data was summarized in **Table 4-3** and **Table 4-4**.

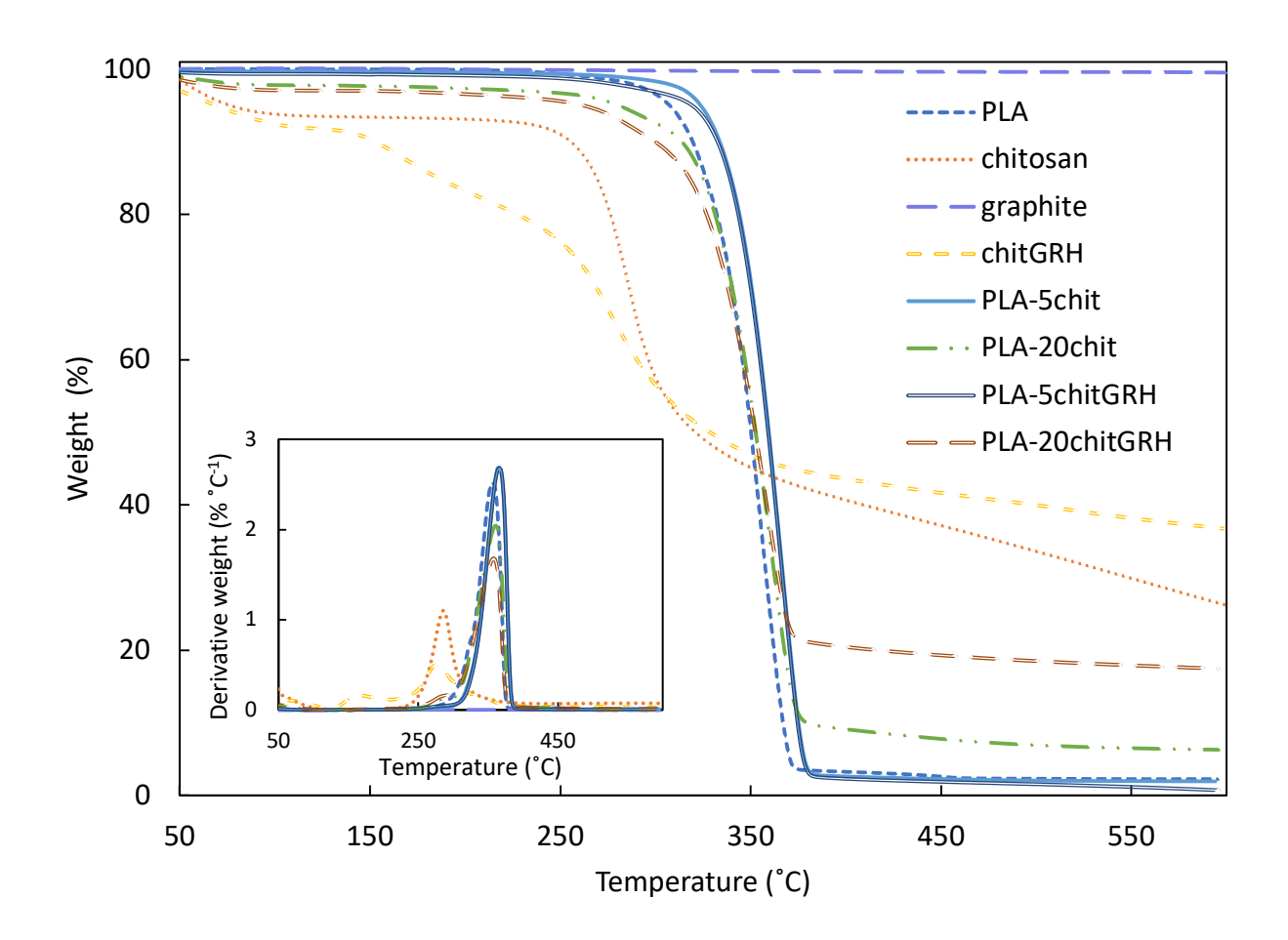


Figure 4-7. TGA thermograms of tested samples.

Tests were done on PLA, chitosan, graphite, and chitGRH first to determine the decomposition temperatures ( $T_o$ ,  $T_{max}$ , and  $T_e$ ), the % weight loss (%wtL), and % residue at one or multiple degradation stage(s). The main degradation of PLA happened at 259-388°C, with peak at 360°C, and weight loss of 98 % after derivative weight was close to 0 % °C-1. Auras *et al.*'s also

showed that the thermal degradation of PLA starts at 300°C and finishes at around 400°C [2]. This difference was due to composition of PLA, since crystallinity of PLA affects its thermal stability [2]. Graphite merely degraded from 0 to 600°C (99.5% residues). Hatui *et al.* prepared stable graphene by first dispersed graphite in orthodichloro benzene solvent, and then evaporated the solvent at 185°C after a 4-h sonication. The group reported a 5% weight loss at 682°C for the obtained graphene [3]. Chitosan had a major degradation (%wtL was 51%) begins at 190°C and lasted until 600°C (derivative weight became stable above zero at 410°C), with a degradation peak at 289°C. The minor degradation from 50 to 126°C can be attributed to the loss of intermolecular H-bonded water [4,5] and moisture absorbed by chitosan powder. Soni *et al.* observed a thermal degradation of chitosan that initiated at 215°C and finished at 350°C [5]. The difference in degradation temperature was due to the difference on the size of the chitosan chains. The smaller the size of a single chitosan chain, the larger the amount of free end chains so that the lower the observed degradation temperature [6].

Causes for different decomposition stages in chitGRH was based on the degradation ranges of chitosan and graphite. Statistical analysis was run to check if the decomposition temperatures in particular stages of chitosan were same as those in chitGRH. Four groups of comparison were run, with only  $T_{e2}$  of chitosan and  $T_{e3}$  of chitGRH showed significantly same. Figure 4-7 shows the change in weight vs. temperature, indicating that the weight of chitGRH and chitosan both gradually decreased from around 260 to 600°C. Figure 4-7 inset shows the derivative of weight vs. temperature plot, showing a peak around 260°C. The derivative weight kept decreasing until about 350°C. With the addition of GRH in chitosan,  $T_o$  increase from 190 to 209°C, while  $T_{max}$  decreased from 289 to 274°C. It has been reported by multiple researchers that

graphene can improve thermal stability of polymer substrate [7–10] due to the strong nanofiller network that well dispersed graphene provided can suppress matrix chains mobility, and thus retard degradation [7,8]. The layered structure of graphene flakes can also hinder the evolution of decomposed gases, which further slowdown the degradation [10,11]. However, Ambrosio-Martín *et al.* reported a decrease in  $T_{max}$  with the addition of functionalized graphene sheet into PLA matrix [12]. Akhina *et al.* did not observe a change in  $T_0$  between PVC and PVC with reduced graphene oxide [11]. On the other hand, Lee *et al.* claimed that a high degradation of graphene could be mainly caused by its defective carbon [13]. Thus, in this study, the dispersion of graphene in chitosan matrix build a network and thus hinder the initiation of degradation. However, after the degradation started and more segmental movement of chitosan chains started to occur, the existence of defective carbon and the high heat conductivity of graphene [12] speeded up the degradation.

In chitGRH, the decomposition from 50 to 119°C may be due to the intermolecular H-bond in water and in acetic acid [4,5]. The decomposition began at 209°C and ended at 423°C with a peak at 274°C corresponded to chitosan. There was another decomposition stage starting at 122°C and finished at 209°C with a peak at 167°C. Similar finding was also reported by Soni *et al.*, and attributed to the existence of acetic acid in the production of chit [6]. The weight percentages of chitosan and GRH in chitGRH was 94 wt% and 6 wt% respectively, obtained from the percentage of chitosan residue, graphite, and chitGRH at 600°C.

The decomposition stages, %wtL, and % residue of each component was also obtained for PLA-5chit, PLA-20chit, PLA-5chitGRH, and PLA-20chitGRH to determine the wt% of PLA in coated films. Data are summarized in **Table 4-4**.

Table 4-3. TGA results of PLA, chitosan, and graphite.

Parameters *	PLA	Chitosan	Graphite	ChitGRH		
	1 <sup>st</sup> decomposition					
T <sub>o1</sub> , °C	259 ± 5	50 ± 0	N/A	50 ± 0		
T <sub>max1</sub> , °C	$360 \pm 6$	N/A	N/A	N/A		
T <sub>e1</sub> , °C	$388 \pm 5$	126 $\pm$ 1 $^{\text{A}}$	N/A	$119\pm2~^{\rm a}$		
%wtL	$98\pm2$	$6\pm1$	N/A	$7\pm 2$		
	2 <sup>nd</sup> decomposition					
T <sub>o2</sub> , °C	N/A	190 ± 1 <sup>B</sup>	N/A	122 ± 3		
T <sub>max2</sub> , °C	N/A	$289\pm6^{\ \text{C}}$	N/A	$167\pm1$		
T <sub>e2</sub> , °C	N/A	$410\pm8$ $^{D}$	N/A	$209\pm4$		
%wtL	N/A	$51\pm2$	N/A	$\textbf{10}\pm\textbf{1}$		
	3 <sup>rd</sup> de	ecomposition				
T <sub>o3</sub> , °C	N/A	N/A	N/A	209 ± 4 <sup>b</sup>		
T <sub>max3</sub> , °C	N/A	N/A	N/A	$274\pm2^{c}$		
T <sub>e3</sub> , °C	N/A	N/A	N/A	423 $\pm$ 11 $^{\text{D}}$		
%wtL	N/A	N/A	N/A	44 ± 4		
Residue, %	$0.5\pm2$	$28\pm2$	99.5	$32\pm4$		

Note:  $T_e$  of chitosan and chitGRH were determined when derivative weight became stable. Degradation was still happening until  $600^{\circ}$ C.

N/A: Not available; the TGA or DTG curves did not show an obvious decomposition stage or a derivative weight peak.

 $<sup>^{*}</sup>$  T, %wtL, and %residue is shown as average  $\pm$  standard deviation except graphite, which had two replicates.

<sup>&</sup>lt;sup>A</sup> Data sharing same letter among A and a, or B and b, or C and c, or D and d were not significantly difference.

Table 4-4. TGA results of coated PLA films.

Parameters *	PLA-5chit	PLA-20chit	PLA-5chitGRH	PLA-20chitGRH		
	1 <sup>st</sup> decomposition					
T <sub>o</sub> , °C	50	50	50	50		
T <sub>max</sub> , °C	N/A	N/A	N/A	N/A		
T <sub>e</sub> , °C	126 <sup>A</sup>	125 <sup>A</sup>	125 <sup>A</sup>	125 <sup>A</sup>		
%wtL	1	2	2	3		
		2 <sup>nd</sup> decomposit	ion			
T <sub>o</sub> , °C	126 <sup>A</sup>	125 <sup>A</sup>	125 <sup>A</sup>	125 <sup>A</sup>		
T <sub>max</sub> , °C	N/A	285 <sup>A</sup>	N/A	285 <sup>A</sup>		
T <sub>e</sub> , °C	292 <sup>A</sup>	294 <sup>A</sup>	296 <sup>A</sup>	294 <sup>A</sup>		
%wtL	1	5	2	6		
		3 <sup>rd</sup> decompositi	ion			
T <sub>o</sub> , °C	292 <sup>A</sup>	294 <sup>A</sup>	296 <sup>A</sup>	294 <sup>A</sup>		
T <sub>max</sub> , °C	366 <sup>A</sup>	361 <sup>B</sup>	367 <sup>A</sup>	359 <sup>B</sup>		
T <sub>e</sub> , °C	395 <sup>A</sup>	394 <sup>A</sup>	393 <sup>A</sup>	392 <sup>A</sup>		
%wtL	93	84	96	71		
Residue, %	5	7	-1	16		

<sup>\*</sup> T, %wtL, and % residue is shown as average value of two replicates.

N/A indicates there was no derivative weight peak for the corresponding decomposition stage.

Weight percentage of PLA in each type of coated film was calculated using %wtL of each component, % residue of PLA, and % residue of chitGRH. Obtained wt% of PLA in PLA-5chit, PLA-20chit, PLA-5chitGRH, and PLA-20chitGRH are 91, 82, 94, and 70% respectively.

<sup>&</sup>lt;sup>A</sup> Data sharing the same capital letter in the same row had no significant difference.

## 4.2.2.2 DSC

**Figure 4-8** shows the DSC results of the second heating cycle of PLA and coated PLA films. Glass transition temperature  $T_g$ , crystallization temperature  $T_c$ , melting temperature  $T_m$ , cold crystallization enthalpy  $\Delta H_c$ , melting enthalpy  $\Delta H_m$ , and degree of crystallinity  $X_c$  of PLA and coated PLA films are summarized in **Table 4-5**. Degree of crystallinity was calculated as expressed [14]:

$$X_c = \frac{\Delta H_c + \Delta H_m}{\Delta H_{ft} \times f} \tag{4.10}$$

where  $\Delta H_{ft}$  is the melting enthalpy for 100% crystalline PLA taken as 93 J g<sup>-1</sup> [15], f is the wt% of PLA in sample films.

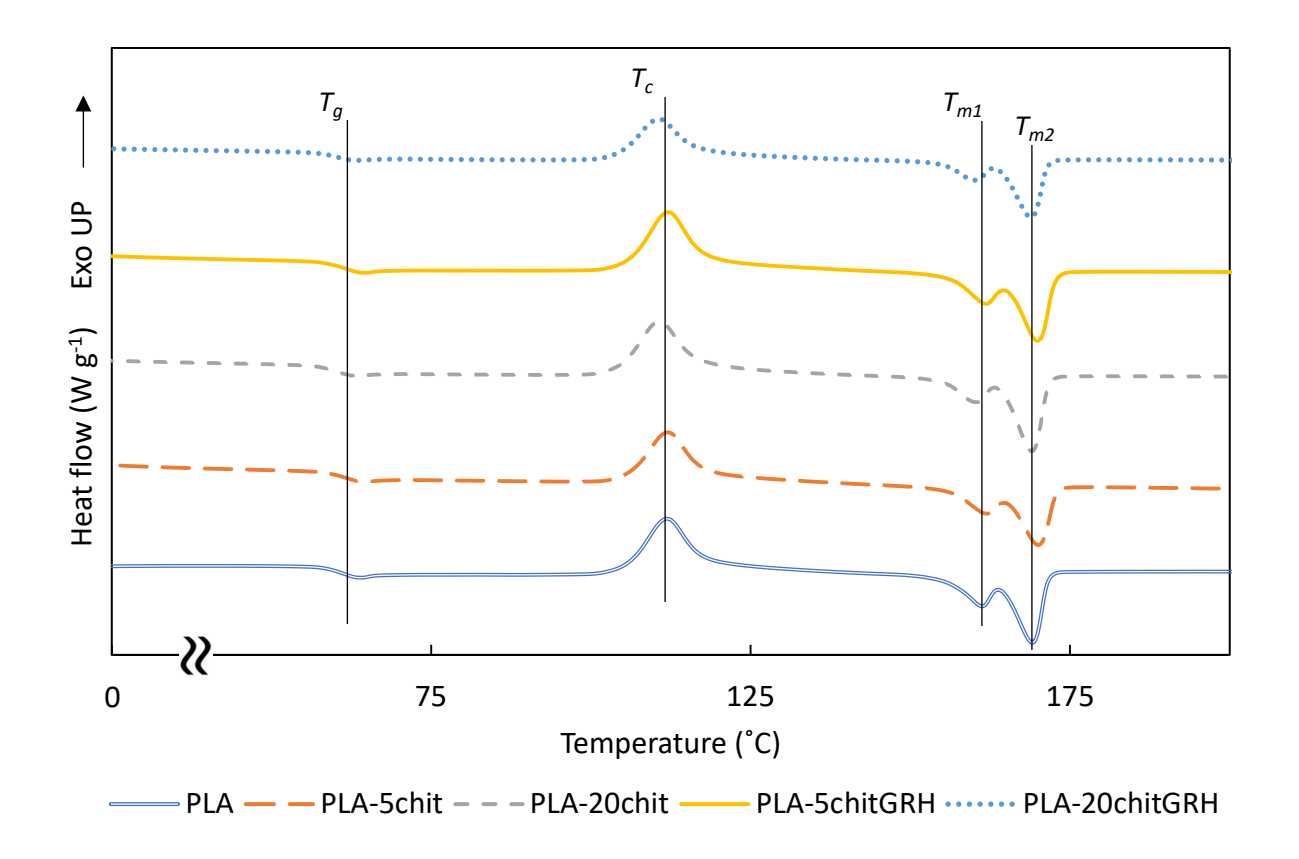


Figure 4-8. DSC plots of the second heating cycle of PLA and coated PLA films.

 $T_g$ 's of PLA and coated PLA films were around 60°C, while 2  $T_m$ 's were observed for each sample, with a small peak at around 161°C and a large peak at around 170°C. The temperatures were within the ranges reported by Auras et~al., that  $T_g$  of PLA ranged from 50 to 80°C, and  $T_m$  within 130 to 180°C [2]. Crystallinity of PLA can be effected by the composition (i.e., D- and LD-lactide) [2]. Sonchaeng et~al. reported a three-phase model for semicrystalline PLA. Rigid amorphous fraction (RAF), mobile amorphous fraction (MAF) and crystalline fraction (CF). RAF has a higher density than MAF, and also the existence of the RAF in the amorphous phase can slow down the relaxation of PLA [16]. The double melting peaks could be attributed to the presence of RAF or the unperfect crystallization of the alpha phase of PLA.

Table 4-5. DSC parameters of PLA and coated PLA films.

Parameters	PLA	PLA-5chit	PLA-20chit	PLA-5chitGRH	PLA-20chitGRH
T <sub>g</sub> , °C *	61 <sup>A C</sup>	62 ± 0.1 <sup>A B</sup>	61 ± 0.5 <sup>c</sup>	62 ± 0.3 <sup>B</sup>	60 ± 0.2 <sup>C</sup>
$T_c$ , °C	111 <sup>A</sup>	112 ± 0.2 <sup>A</sup>	111 ± 0.2 <sup>A</sup>	112 ± 0.1 <sup>A</sup>	$110 \pm 0.2$ <sup>A</sup>
$\Delta H_c$ , J g <sup>-1</sup>	27 <sup>A</sup>	$25\pm0.1$ AB	22 ± 1 <sup>B</sup>	$25 \pm 0.3$ AB	$18 \pm 2$ <sup>C</sup>
<i>T<sub>m1</sub>,</i> °C	161 <sup>A, B</sup>	162 ± 0.5 <sup>A</sup>	161 ± 0.4 <sup>B</sup>	162 ± 0.5 <sup>A</sup>	$160 \pm 0.1$ B
<i>T<sub>m2</sub>,</i> °C	169 <sup>A, C</sup>	$170\pm0.3$ AB	169 $\pm$ 0.2 A <sup>C</sup>	$170 \pm 0.4$ B	169 ± 0.2 <sup>c</sup>
$\Delta H_m$ , J g <sup>-1</sup>	34 <sup>A</sup>	32 ± 1 <sup>A</sup>	$27 \pm 0.3^{B}$	32 ± 0.1 <sup>A</sup>	$23 \pm 3$ <sup>C</sup>
$X_c$ , %	66 <sup>A</sup>	67 ± 1 <sup>A</sup>	65 ± 1 <sup>A</sup>	64 ± 0.3 <sup>A</sup>	63 ± 7 <sup>A</sup>

Note: Data are shown as average  $\pm$  standard deviation except PLA, which had two replicates.

The presence of chit or chitGRH coating did not significantly influence the crystallinity and  $T_c$  of PLA substrate. The presence of graphene did not change glass transition properties of PLA-

<sup>&</sup>lt;sup>A</sup> Data sharing the same capital letter in the same row had no significant difference.

5chit, while decreased  $\Delta H_c$  and  $\Delta H_m$  of PLA-20chit. Without graphene, increasing coating layers from PLA-5chit to PLA-20chit decreased  $T_g$ , both  $T_m$ -s, and  $\Delta H_m$ . With graphene, PLA-20chitGRH has all the thermal transition values lower than PLA-5chitGRH, except  $T_c$  and  $X_c$ . However, the changess in  $T_g$  and  $T_m$  were minor change within 2°C. Thus, it was concluded that the coating solutions did not deteriorate the PLA substrate during the coating process.

# 4.2.2.3 Oxygen Barrier Properties

OP of PLA, PLA-5chit, and PLA-20chit were tested to check the efficiency of coating solutions on one side of PLA. **Table 4-6** summarizes the results. Thickness of the obtained PLA-5chit (24  $\mu$ m) and PLA-20chit (38  $\mu$ m) films were much higher than theoretical thickness mentioned in section 4.2.1. PLA's OP was higher for 50% RH. By comparing OP value, an increase was found in all samples with an increase in relative humidity. This was partially contradictory with the conclusion from Sonchaeng *et al.* that OP of PLA had no relation with % RH [16]. Also, addition of chitosan coating did not reduce the OP for all the samples. The issues in film thickness and OP variations were due to cracks in films resulted from film curvature mentioned in Section 4.2.1.

Table 4-6. Thickness and OP value of PLA and chit coated PLA films at 23°C, 0% or 50% RH.

Type of film	Thickness x 10 <sup>-6</sup> *	<i>P</i> x 10 <sup>-20 *</sup>
	m	kg m m <sup>-2</sup> s <sup>-1</sup> Pa <sup>-1</sup>
PLA-0% RH	20 ± 0	269 $\pm$ 24 $^{\mathrm{A}}$
PLA-5chit-0% RH	$24\pm2$	$28\pm35~^{B}$
PLA-20chit-0% RH	$37\pm2$	$46\pm40~^{B}$
PLA-50% RH	$21\pm0.5$	310 $\pm$ 31 $^{\mathrm{a}}$
PLA-5chit-50% RH	$\textbf{24}\pm\textbf{1}$	185 $\pm$ 115 $^{ab}$
PLA-20chit-50% RH	$39\pm1$	101 $\pm$ 107 $^{\rm b}$

 $<sup>^*</sup>$  Data are shown as average  $\pm$  standard deviation except PLA, which had two replicates.

<sup>&</sup>lt;sup>A</sup> *P* value sharing the same capital letter had no significant difference.

<sup>&</sup>lt;sup>a</sup> *P* value sharing the same lowercase letter do not have significant difference.

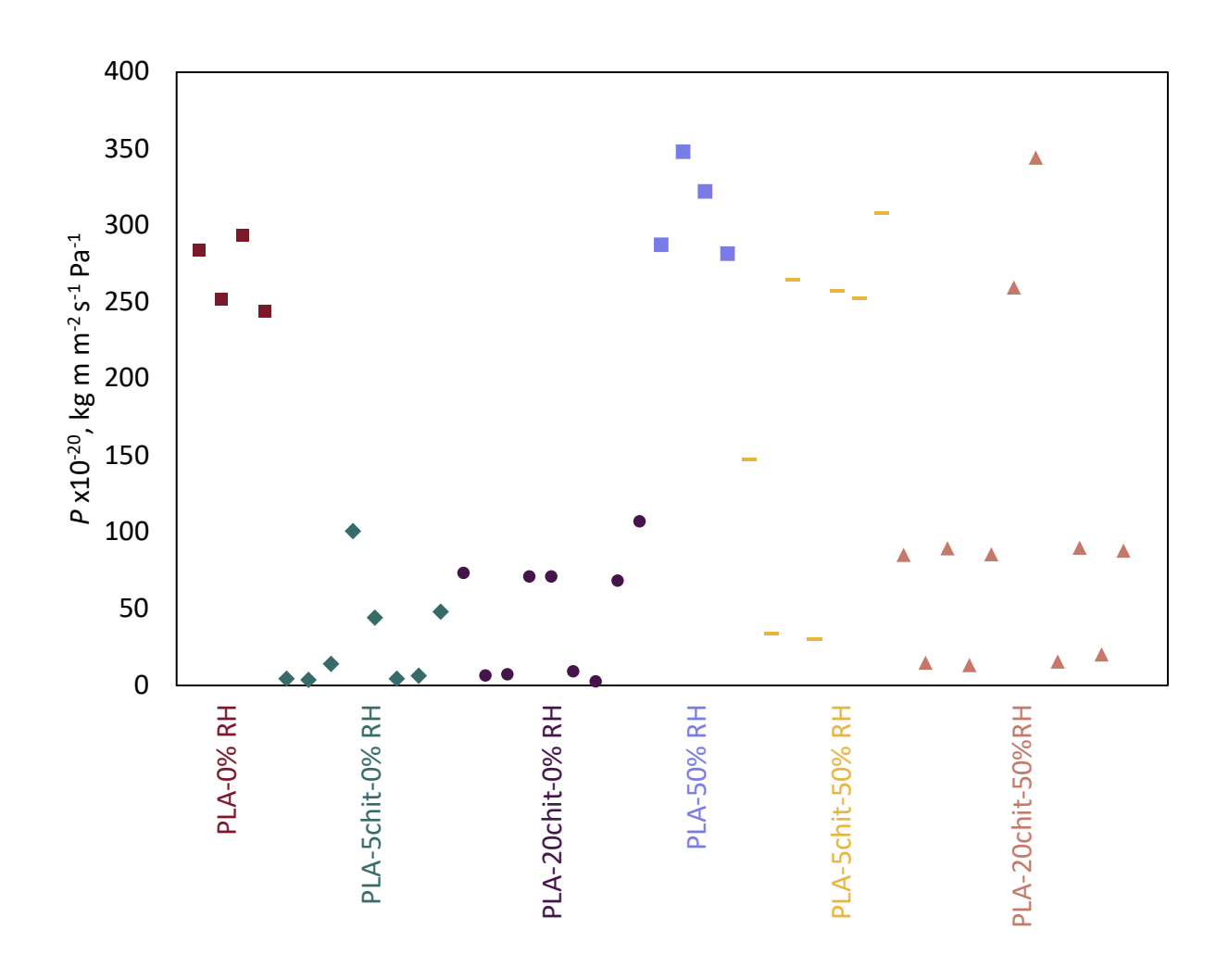


**Figure 4-9. OP distribution of PLA and chit coated PLA films at 23°C, 0% or 50% RH.** Same color name corresponds to the same color data.

# 4.3 Coating-PLA-Coating Film

# 4.3.1 Thermal Properties

DSC and TGA were not repeated for coating-PLA-coating films since only the coating positions changed from PLA-coating films.

# 4.3.2 Oxygen Barrier Properties

To avoid the curvature resulted from only doing coating on one side of the PLA substrate, chitosan was coated both sides of the films. **Table 4-7** shows the OP of PLA, PLA-2p, and 6chit, and PLA with different coating at 23°C and various % RH. Without condition, a total of 6-layer and 20-layer chitGRH coating decreased oxygen permeability of PLA by 98.5% and 99.7% at 0% RH respectively.

Table 4-7. OP values of coating-PLA-coating films, control films, and chit coating films at 23°C.

Type of film	Thickness x 10 <sup>-6</sup> *		<i>P</i> x 10	<sub>)</sub> -20 *	
Type of film		kg m m <sup>-2</sup> s <sup>-1</sup> Pa <sup>-1</sup>			
	- 111	0%	30%	60%	90%
	With	nout condition	**		
PLA	20 ± 0	$269\pm24$ <sup>A</sup>	289 ± 4 <sup>A</sup>	$282\pm12$ <sup>A</sup>	284 ± 6 <sup>A</sup>
PLA-2p	$20\pm0.4$	$289\pm16$ $^{\text{A}}$	$286\pm16^{\text{A}}$	$293 \pm 27$ $^{\text{A}}$	$280\pm8$ $^{\text{A}}$
3chit-PLA-3chit	$20\pm0.5$	$16\pm5$ $^{B}$	$18\pm0.5\ ^B$	141 $\pm$ 10 $^{\text{B}}$	$261\pm8$ $^{AB}$
10chit-PLA-10chit	$25\pm0.5$	$0.7\pm0.7^{B}$	$3\pm0.3^{B}$	$37\pm5$ <sup>C</sup>	221 $\pm$ 12 $^{B}$
3chitGRH-PLA-3chitGRH	$21\pm0.8$	$4\pm0.9$ $^B$	$7\pm0.1~^B$	$72\pm18$ <sup>C D</sup>	$235\pm30^{\ B}$
10chitGRH-PLA-10chitGRH	$\textbf{27} \pm \textbf{1.8}$	$0.9\pm0.1$ $^{\text{B}}$	2 <sup>B</sup>	$24\pm2^{\ D}$	163 $\pm$ 33 <sup>C</sup>
	Wi	ith condition *	*		
3chit-PLA-3chit	21 ± 1	0.5	na	36 ± 7	211
6chit	$8\pm2.5$	$14\pm7$	$6\pm3$	24	$\textbf{107} \pm \textbf{13}$

 $<sup>^{*}</sup>$  Data are shown as average  $\pm$  standard deviation, otherwise the data is reported as an average from two replicates without standard deviation.

<sup>\*\*</sup> Without condition means sample films were kept in sealed PE bags at 23°C. With condition means sample films were kept in sealed PE bags with desiccant at 23°C before testing.

<sup>&</sup>lt;sup>A</sup> Data sharing the same capital letter in a column in "without condition" had no significant difference.

## 4.3.2.1 Effect of Plasma Treatment

**Table 4-7** indicates that 10 min plasma treatment on both side of PLA film will not change its OP value at 0%, 30%, 60%, and 90% RH, confirming that plasma treatment only react with the topmost layer of the PLA film without changing the bulk structure [18,19].

# 4.3.2.2 Effect of Relative Humidity

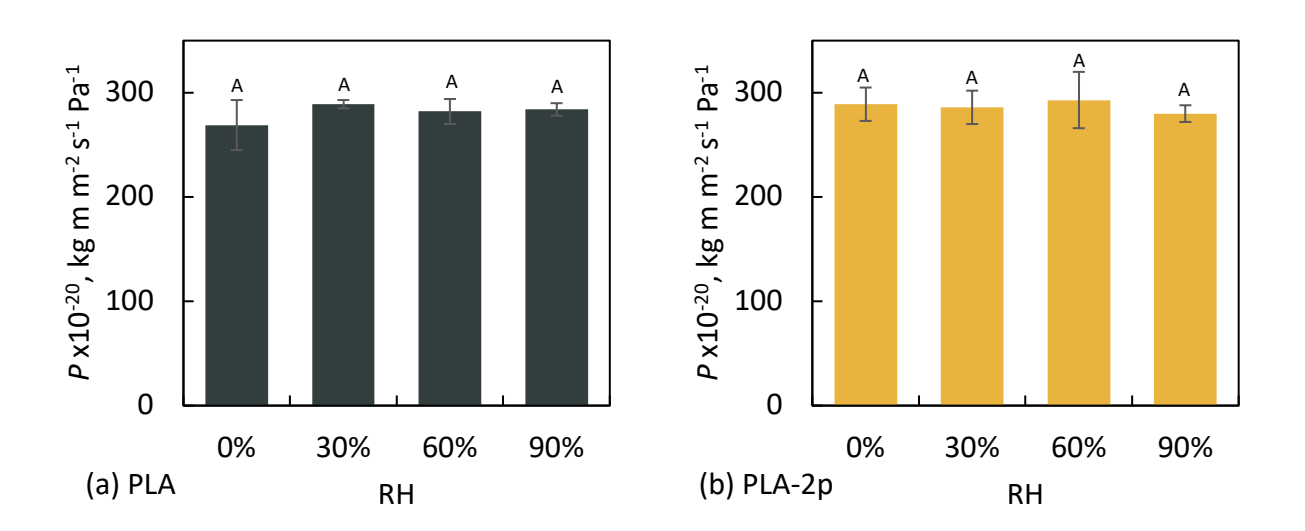


Figure 4-10. Effect of relative humidity to OP value at 23°C and various RH. (a) PLA, (b) PLA-2p.

Figures 4-10 and 4-11 showed the effect of RH on OP value at 23°C for different samples. Relative humidity did not affect OP value for PLA, as also reported by Sonchaeng *et al.* and Auras et al [16,20]. Same thing for PLA-2p, since oxygen plasma treatment do not change bulk properties of the film as previously discussed in Sections 2.2.3 and 4.3.2.1. This is contrary as shown in **Table 4-6** because 1) untested PLA films were not kept in dry condition, thus some degree of hydrolysis might have happened before the test; 2) tests were done with an 8001 Oxygen Permeation Analyzer, while tests in this section were conducted with a MOCON OX-TRAN 2/22. There might

A Data in the same plot sharing the same capital letter had no significant difference.

be accuracy problem on the old 8001 machine, which was also the reason that oxygen permeability analyzer was changed for coating-PLA-coating samples. When RH increased from 0% to 30%, all coated films exhibited no significant change in OP. When RH increase to 60%, 10chitGRH-PLA-10chitGRH still showed no significant increase in OP due to the presence of GRH while OP of all other coated films drastically raised. When RH further increased from 60% to 90%, OP value of all coated films increased significantly. The reasons that OP augmented with increasing RH can be a smaller plasticization effect by water molecules [21,22] but a majority interaction effect of water with the presence of the polysaccharide chitosan [23] as shown in Figure 4-11 (a)-(b). The increase in OP values was only noticeable at 60% and 90% RH with addition of chitosan, indicating the plasticizing effect of water is less effective. The polar amino groups (-NH<sub>2</sub>) interact with water molecules and trigger the chitosan layer plasticization and further enable the swelling of the coating layers. This increases the free volume in chitosan and reduces the intermolecular interactions, which makes it easier for the oxygen molecules to diffuse through the matrix [21]. However, this effect is not significant when RH was below 30% RH. Similar results were reported by Giannakas et al., but for chitosan film OP from 0% to 50% RH [24]. Then, OP showed an exponential increase from 30% to 90% RH. The increase of OP from 30% to 90% RH in Figure 4-11 coincides the Yan et al.'s study that OP value of pristine chitosan film was twice at 75% RH than at 0% RH[25]. Aulin et al. reported a drastically increase in OTR value of microfibrillated cellulose films from 70% to 80% RH while very small increase from 0 to 70% RH [26]. Cellulose has similar chemical structure than chitosan [27,28], but the -NH₂ present in chitosan is replaced by the -OH [29]. So, this result correlates to chitosan. Figure 4-11 (c) and (d) also shows that the presence of graphene affected the OP values.

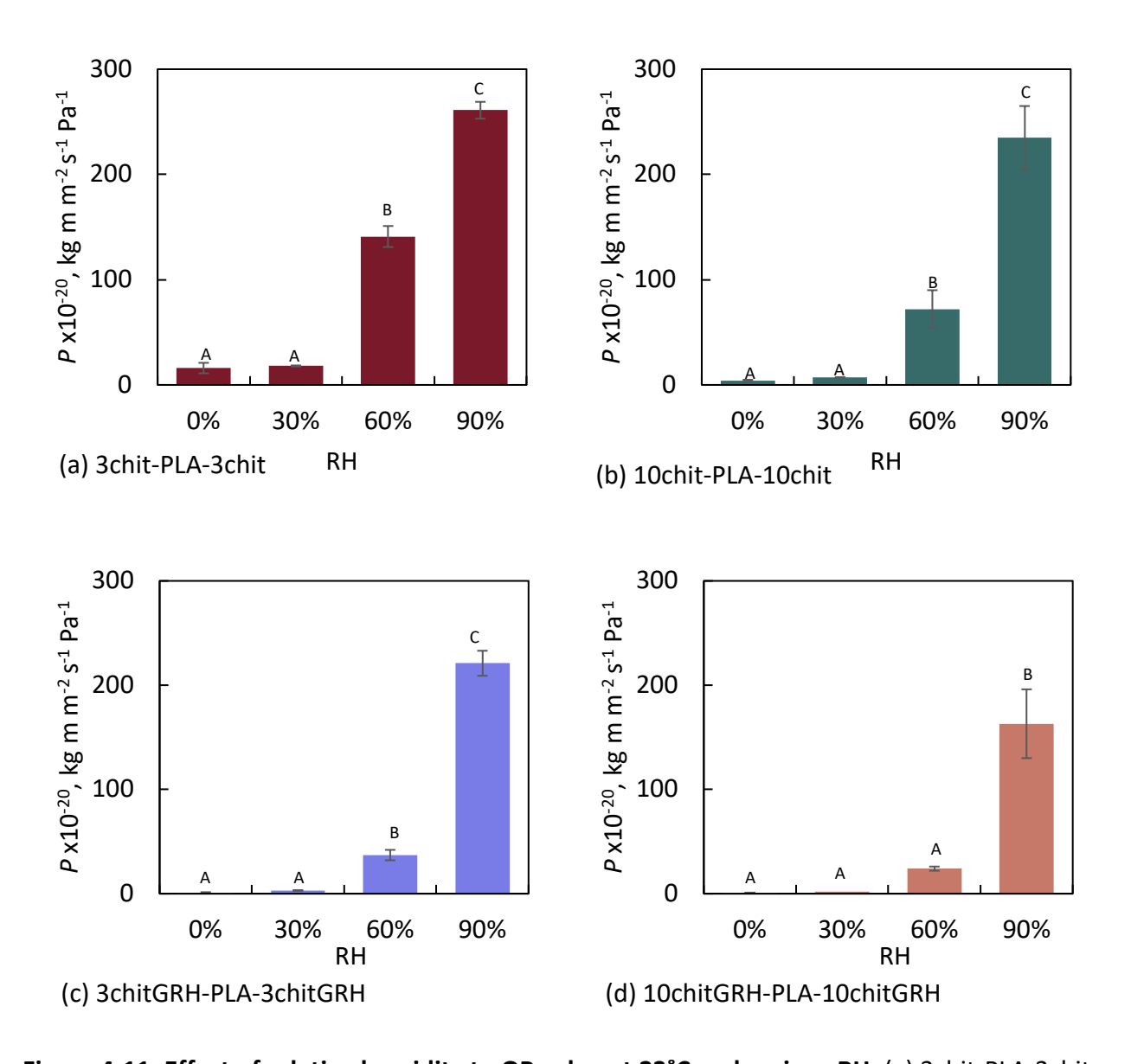


Figure 4-11. Effect of relative humidity to OP value at 23°C and various RH. (a) 3chit-PLA-3chit, (b) 10chit-PLA-10chit, (c) 3chitGRH-PLA-3chitGRH, (d) 10chitGRH-PLA-10chitGRH. A Data in the same plot sharing the same capital letter had no significant difference.

# 4.3.2.3 Effect of Coating Layers

From **Table 4-7**, 6 or 20 layers of chitosan or chitGRH coating can significantly improve oxygen barrier property of PLA films at 0, 30, and 60% RH. At 90% RH, 6 layers chitosan coating did

not decrease the OP of PLA while additional layers could improve the films' oxygen barrier property.

Figure 4-12 shows how the number of coating layers affected the OP value. For PLA film with chitosan coating at 0, 30, 60, and 90% RH, 20 layers coating provides 75, 61, 49, and 10%, lower OP than 6 layers coating. For PLA film with chitGRH coating at 30, 60, and 90% RH, 20 layers coating leads to 33, 35, and 26% lower OP, and 29% higher OP at 0% RH than 6 layers coating. The improvement of the oxygen barrier can be attributed to an increasing coating layer thickness which creates a longer path for oxygen molecules to go through. Similar findings were reported by several researchers [21,30]. Aulin et al. found a 82% decrease in OTR from 20 bilayers to 50 bilayers of PEI/NFC coating on PLA [30]. Rocca et al. reported a non-linear relation between wheat gluten coating thickness with OP value of coated PLA film. OP decreased more than 94% with the coating thickness increased from 0 to 20 μm. When the coating thickness was between 20 μm to 60 μm, OP did not further decrease [21]. 10chitGRH-PLA-10chitGRH had a higher OP than 3chitGRH-PLA-3chitGRH at 0% RH, which could be attributed to: 1) the limitation of the testing machine that a very small amount of permeant been detected could cause the signal received by the machine being small, as well as the signal to noise ratio, and thus lead to the inaccuracy of the test; and 2) the fact that sample films were not kept in dried condition before testing, so 10chitGRH-PLA-10chitGRH could absorb more water molecules due to the hydrophilicity of chitosan.

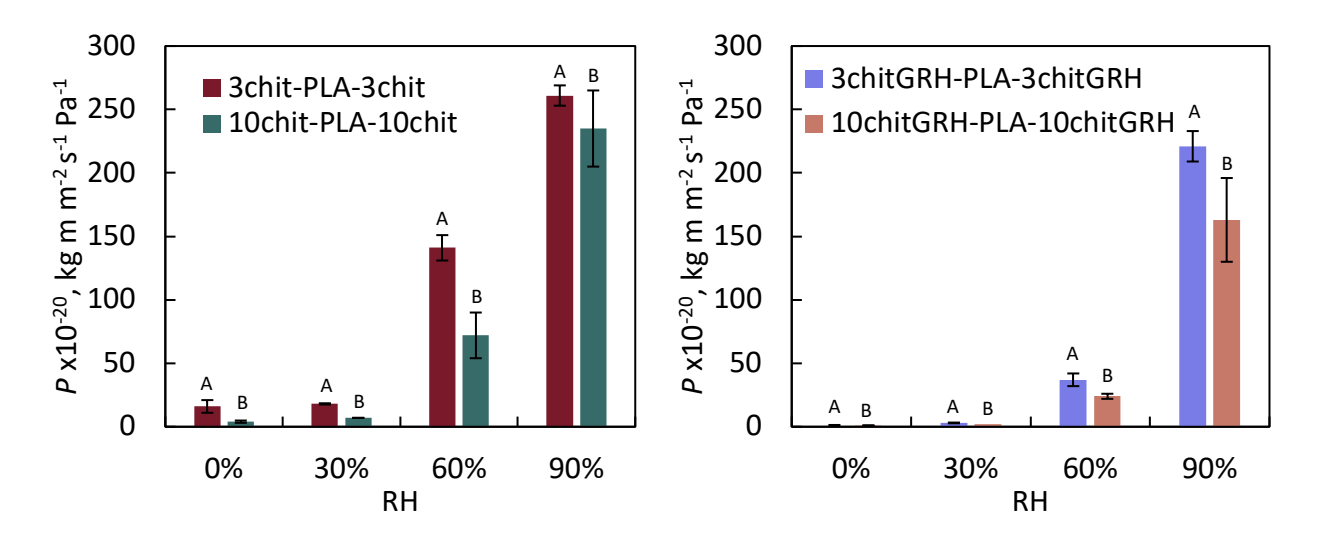


Figure 4-12. Effect of numbers of coating layers to OP value at 23°C and various RH. A Data sharing the same capital letter with the same relative humidity in one plot were had no significant difference.

Figure 4-13 shows the effect of the presence of graphene. Six layers chitGRH coating provided stronger oxygen barrier to PLA films compare to chitosan coating at 0, 30, and 60% RH. No difference was found at 90% RH. For twenty layers coated films, the presence of GRH did not change the OP at 0 or 30% RH but improved the OP at 60 and 90% RH. The shape of graphene flakes can help create a more tortuous path for the oxygen molecules [12] as discussed in Section 2.3.3. However, with a high RH (i.e., abundant water molecules) and a thin coating, it is possible that there was enough plasticization and swelling in the film that the hydrophobicity of GRH became negligible (e.g., 6 layers coated film).

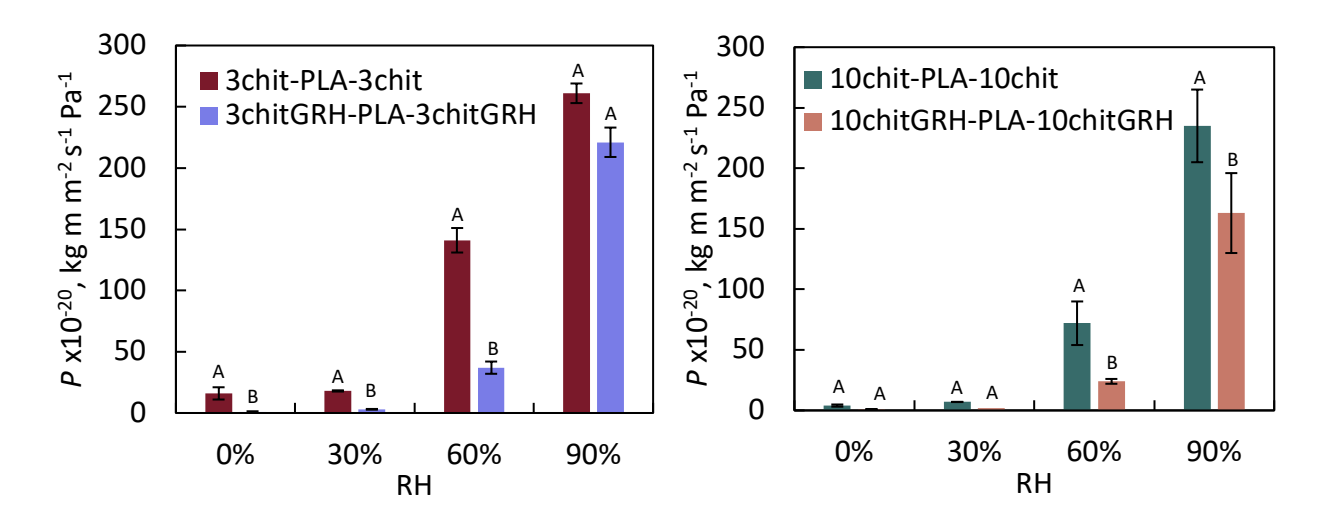


Figure 4-13. Effect of graphene in coating layers to OP value at 23°C and various RH. A Data sharing the same capital letter with the same relative humidity in one plot had no significant difference.

# 4.3.2.4 Effect of Storage Conditions

Influence of storage condition on OP value on 3chit-PLA-3chit at 23°C at 0%, 60%, and 90% was evaluated as shown in **Figure 4-14**. An increase in OP was found with an increase in RH with conditioning, and OP of samples with condition were lower than OP of samples without condition at all three-relative humidity. This is due to the plasticization effect of water molecule by moisture in ambient condition to the film. Without being stored in dry condition, films were tested mostly within two weeks. This implied that conditioning of the films is a critical factor to take into consideration when testing these films and potential future development for commercialization.

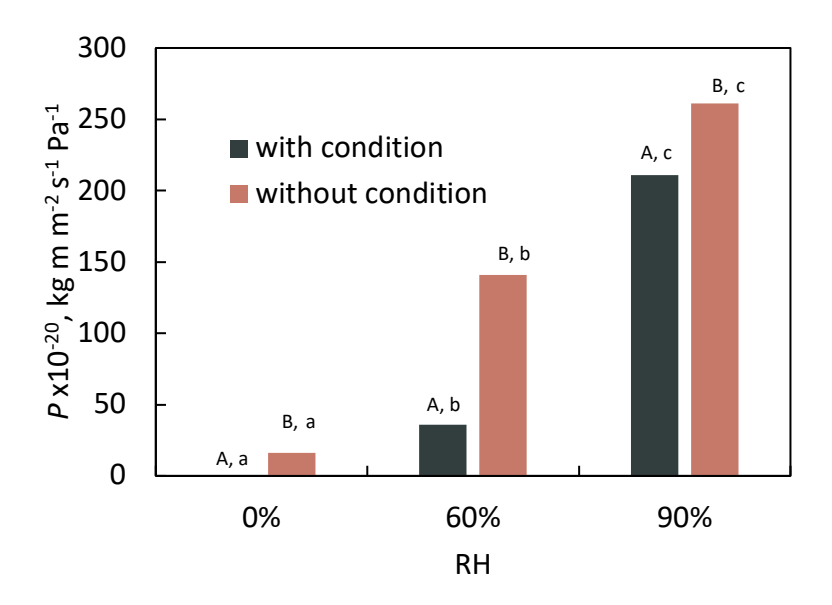


Figure 4-14. Effect of storage condition on OP of 3chit-PLA-3chit at 23°C. A Data sharing the same capital letter with the same relative humidity had no significant difference. Data in "with condition" or "without condition" series sharing the same lowercase letter were not significantly difference.

## 4.3.2.5 Multilayer Structure Permeability Model

Thickness and OP value of 6chit (with condition) and PLA (without condition) was used to calculate the theoretical OP of 3chit-PLA-3chit using equation 4.11.

$$OP_t = \frac{\sum_n l_i}{\sum_n \frac{l_i}{OP_i}} \tag{4.11}$$

where  $OP_i$  and  $I_i$  are OP and thickness of each layer component and  $OP_t$  is the OP of the whole multilayer structure. This equation was based on the assumption that there is no chemically interaction between the oxygen and polymer. Also, permeability of multilayer film is only affected by the thickness and permeabilities of each layer component, but not the order of the

layers. The calculated  $OP_t$  values were compared with OP of 3chit-PLA-3chit obtained from the experiments. A root mean square (RMS) parameter was used to check difference as shown in equation 4.12.

$$RMS = \sqrt{\frac{\sum \left[\frac{OP - OP_t}{OP}\right]^2}{N}}$$
 (4.12)

where *N* is sample size, OP is experimental data, OP<sub>t</sub> is calculated data. **Figure 4-15** shows the variation between calculated and experimental OP values with the RMS values. Negative % variation means experimental value was smaller than calculated value, and vice versa. Smaller RMS means better fit between calculated and experimental data. OP from experimental was lower than from model at 0%, then experimental data became larger. At 0% RH, experimental value was 43% lower than calculated value. At 30% RH, 37% difference was found. Experimental OP was higher than calculated OP for 129 and 65% respectively. The relatively small difference at 0% and 30% while large difference at 60 and 90% RH was attributed to the fact that 6chit sample was stored in dry condition, and PLA-6chit was not. Thus, the calculated OP value should be closer to the OP value of PLA-6chit if the sample was stored in dry condition.

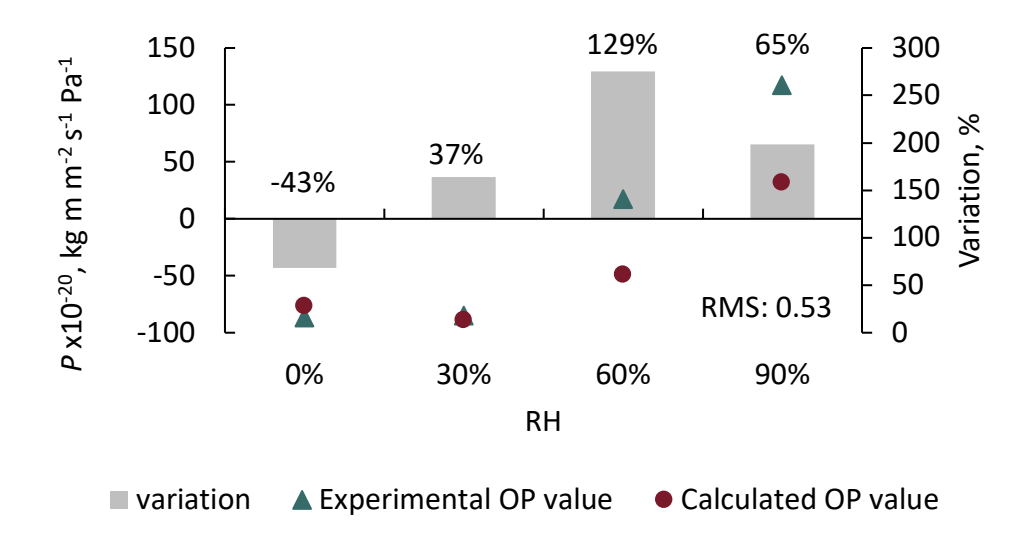


Figure 4-15. Comparison of calculated and experimental OP values of 3chit-PLA-3chit at 23°C and various % RH.

**APPENDIX** 

# **OXYGEN PERMEATION TEST**

# A. HPLA-Coating-HPLA-HP

	Th'	Oxygen Trans	mission Rate	Р	
Type of film	Thickness	cc m <sup>-2</sup> day <sup>-1</sup>		cc mil m <sup>-2</sup>	day <sup>-1</sup>
	μm	0% RH	50%RH	0% RH	50% RH
HPLA-HPLA-HP	25 ±	2981	1879	2934	1850
HPLA-HPLA-HP	25 ±	3789	2809	3729	2765
HPLA-1chit-HPLA-HP	22 ±	673	-	662	-
HPLA-1chit-HPLA-HP	22 ±	93	344	80	298
HPLA-1chit-HPLA-HP	25 ±	21	259	21	255
HPLA-1chit-HPLA-HP	25 ±	22	405	22	399
HPLA-2chit-HPLA-HP	25 ±	842	1613	829	1587
HPLA-2chit-HPLA-HP	25 ±	31	291	31	286
HPLA-1chitGRH-HPLA-HP	25 ±	393	786	387	773
HPLA-1chitGRH-HPLA-HP	26 ±	98	374	100	383
HPLA-2chitGRH-HPLA-HP	25 ±	93	504	91	496
HPLA-2chitGRH-HPLA-HP	23 ±	26	418	23	379
HPLA-2chitGRH-HPLA-HP	24 ±	32	224	30	212

Type of film	Thickness μm	WVTR g m <sup>-2</sup> day <sup>-1</sup>	<i>P</i> (g mil m <sup>-2</sup> day <sup>-1</sup> )
		90% RH 38 °C	90% RH 38 °C
HPLA-HPLA-HP	21 ±	337	279
HPLA-HPLA-HP	21 ±	368	304
HPLA-1chitGRH-HPLA-HP	22 ±	266	230
HPLA-1chitGRH-HPLA-HP	24 ±	243	229
HPLA-2chitGRH-HPLA-HP	25 ±	246	239
HPLA-2chitGRH-HPLA-HP	26 ±	239	244
HPLA-2chitGRH-HPLA-HP	23 ±	283	256
HPLA-2chitGRH-HPLA-HP	24 ±	261	247
HPLA-1chit-HPLA-HP	25 ±	265	261
HPLA-1chit-HPLA-HP	25 ±	199	196
HPLA-2chit-HPLA-HP	25 ±	293	288
HPLA-2chit-HPLA-HP	25 ±	202	199

# B. LLDPE-Coating-LLDPE-HP

Name	Thickness	Transmission rate @ 100%
		(cc/m²-day)
LLDDE LLDDE HD	108 um	2728.759
LLDPE-LLDPE-HP	105 um	3103.368
	97 um	250.9579
	98 um	260.8589
		948.7170
LLDPE-1chit-LLDPE-HP	101 um	191.8760
		215.7679
	102	200.9995
	102 um	29.03462
	120 um	339.5794
LLDPE-1chitGRH-LLDPE-HP	120 um	528.5709
LLDFL-1CIII(GKI1-LLDFL-11F	117 um	504.5454
		317.4806
LLDPE-2chit-LLDPE-HP	147 um	605.4421
LLDFL-ZCIIIC-LLDFL-IIF	130 um	966.3173
	102	64.34452
LLDPE-2chitGRH-LLDPE-HP	103 um	273.7083
LLDFL-2CIIICGKII-LLDFL-IIF	00.00	307.0634
	99 um	64.25926
	114	11.63984
LLDPE-5chit-LLDPE-HP	114 um	216.8162
LLDFL-JUIII-LLDFE-FF	112	224.2276
	112 um	34.04571
	100	148.3359
LLDPE-5chitGRH-LLDPE-HP	108 um	237.1440

	174.4170
105 um	11.43383
	11.03662

## C. PLA-Coating (Sample Data)

#### 1. PLA-5chit

====== SECTION NAME: HEADER INFORMATION ======= MOCON OX-TRAN® 2/21 - Single Test Report for Module System Title of Report: Number 1, Cells and B **User Supplied Header** Information: Exported on: 7/22/2017 6:38:59 AM ===== SECTION NAME: MODULE 1 INFORMATION ======= Serial Number: MH\_01807 Setup Name: (4 BUR)Default Temp Setpoint/Actual: Auto: 23.0 / 23.1 °C. Barometric Pressure: Passed In: 0.98 bar Relative Humidity: Permeant - Man: 25.0%, Carrier - Man: 25.0% Permeant Concentration: 100 % Ambient Temp: Manual: 22.5 °C. ====== SECTION NAME: OPERATOR COMMENTS ======= ====== SECTION NAME: UNUSUAL LOG ENTRIES ======= ===== SECTION NAME: CELL B INFORMATION ======= Test Number: 2 Material ID: 5P4chitM2CBPT Using Method: Default Sample Type: Film: 3.14 cm<sup>2</sup>, 22 μm Test Mode: Continuous Control Params: Infinite ExamMinutes: 30 Individual Zero: No Ind. Zero Conditioning: 1 Hour Cycles Complete: 10 Current Status: Test Done

Started Testing: 7/21/2017 9:25:19 PM

Elapsed Time: 8:30

====== SECTION NAME: TEST RESULTS FOR CELL B =======

**IN SELECTED UNITS** 

Transmission @ 100 % 1170.876 cc / [  $m^2$  - day ] Transmission @ 100% 1170.876 cc / [  $m^2$  - day ]

Permeation: 1014.144 cc - mil / [ m<sup>2</sup> - day ]

====== SECTION NAME: DATA POINTS FROM CELL B =======

Time Rate / Event

0:00 Condition

1:00 Test

2:00 1122.121

3:30 1160.330

4:00 1163.763

4:30 1165.449

5:30 1162.304

6:00 1160.704

6:30 1161.319

7:30 1175.702

8:00 1165.719

8:30 1170.876

9:13 Complete

## 2. PLA-20chit

Illinois Instruments Inc - 8000 results file

START = 11 Jul 2017 11:21:00 PM

**MASK** 

Sample Time (Mins) 1

Temperatures (deg C) 23.0 23.0

Bypass Time 10

Purge Level 160

Sampling rate 1

Stop Band 1	
Wet N2 + 02 1	
Purge 1	
Timed 0	
Auto Stop 0	
RH(O2) values 24.4	24.4
RH(N2) values 25.5	25.7
OTR Data (cc/m2/day	y) 1A 1B
20P6chitM2CBPT41	20P6chitM2CBPT41
20P6chitM2CBPT41 A160	20P6chitM2CBPT41
	20P6chitM2CBPT41
A160	20P6chitM2CBPT41
A160 B160	20P6chitM2CBPT41
A160 B160 A82.4	20P6chitM2CBPT41
A160 B160 A82.4 B192	20P6chitM2CBPT41
A160 B160 A82.4 B192 A11953	20P6chitM2CBPT41

A24254

B13601

A24845

B14087

A25098

- D. Coating-PLA-Coating (Sample Data)
- 1. 3chitGRH-PLA-3chitGRH

#### MOCON OX-TRAN® 2/22 - Single Test Report

Instrument Serial #: 0317FN0197, Instrument Name: Device Name, Instrument #: <no value>

**TEST INFO** 

Sample ID: 6p4chitmgrh12·4b Cell ID: Cell B Test ID: 370 Material ID: User ID: Method: <no value> Anibal

#### **TEST DETAILS**

Temperature: 23.0/22.9 °C Test Gas RH: 60.0/60.0 %RH Carrier Gas RH: 60.0/60.0 %RH ReZero Exam: 20 minutes Sample Area: 3.14 cm<sup>2</sup> Thickness: 0.02200 mm Barometer: 729 mmHg

Test Time: 20.42 hours Exam Minutes: 15 minutes Conditioning: N/A Individual Zero: Off

Turbo Cool: Off Test Mode: Auto Rezero: On ReZero Frequency: 2 High Purge: On Number of Cycles: N/A Compensate: On Concentration: 100.00 % Convergence Hours: N/A Conditioning Time: N/A High Purge Time: 10 minutes Start Date: 11:58 AM, 2/24/2018

#### **TEST RESULTS**

Transmission @100.0% Permeation @100.0% Rezero:

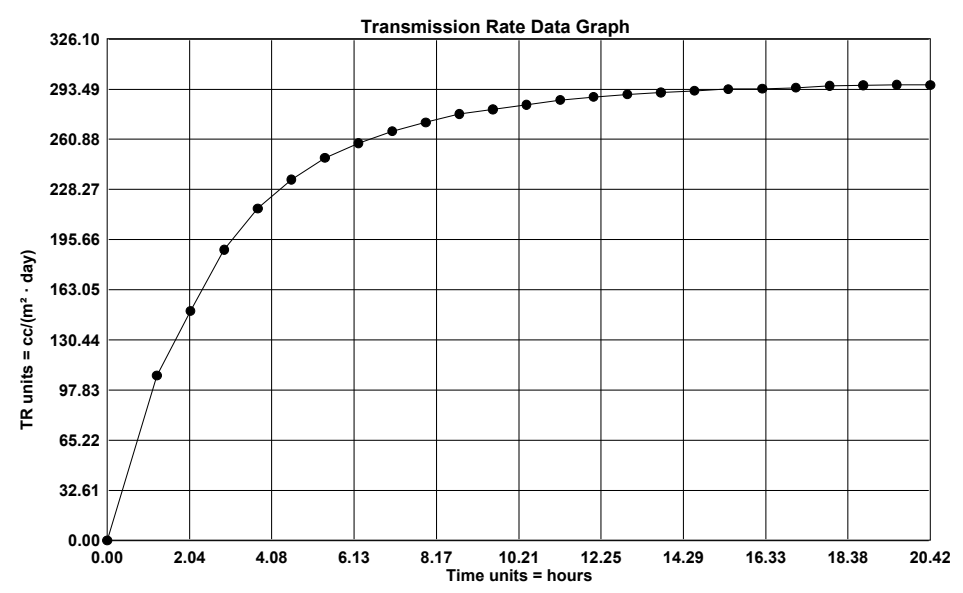
# IN SELECTED UNITS

296.22 cc/(m<sup>2</sup> · day) 6.5168400 cc · mm/(m2 · day)

#### IN STANDARD UNITS

296.22 cc/(m<sup>2</sup> · day) 256.5684 cc · mil/(m² · day) 0.00147 cc/day

#### **OPERATOR COMMENTS:**



#### Auto Test Parameters:

Date/Time 2/24/2018, 12:52 PM 2/24/2018, 1:47 PM

#### **Test Parameters**

Exam Time=20 min, ReZero Freq=2, ReZero Exam=20 min Exam Time=15 min, ReZero Freq=2, ReZero Exam=20 min

## 2. PLA-2p

## MOCON OX-TRAN® 2/22 - Single Test Report

Instrument Serial #: 0317FN0197, Instrument Name: Device Name, Instrument #: <no value>

#### **TEST INFO**

 Cell ID:
 Test ID:
 Sample ID:
 Material ID:
 User ID:
 Method:

 Cell B
 362
 pla2sideb
 <no value>
 xinyi
 Anibal

#### **TEST DETAILS**

Temperature: 23.0/23.0 °C
Test Gas RH: 60.0/60.1 %RH
Carrier Gas RH: 60.0/60.0 %RH
Sample Area: 3.14 cm²
Thickness: 0.02000 mm
Barometer: 735 mmHg

Test Time: 5.74 hours
Exam Minutes: 15 minutes
Carrier Gas RH: 60.0/60.0 %RH
Carrier Gas RH: 60.0/60.1 %RH
Carrier Gas RH: 60.0/60.0 %RH
Carrier Gas RH: 60.0/60.1 %RH
Carrier Gas RH: 60.0/60.0 %RH
Carrier Gas RH: 60.0/

Exam Minutes: 15 minutes

ReZero Exam: 20 minutes

Conditioning: N/A
Individual Zero: Off

ReZero Frequency: 0
High Purge: On
Number of Cycles: N/A

Turbo Cool: Off

Compensate: On Concentration: 100.00 % Convergence Hours: N/A Conditioning Time: N/A High Purge Time: 10 minutes Start Date: 12:26 PM, 2/19/2018

#### **TEST RESULTS**

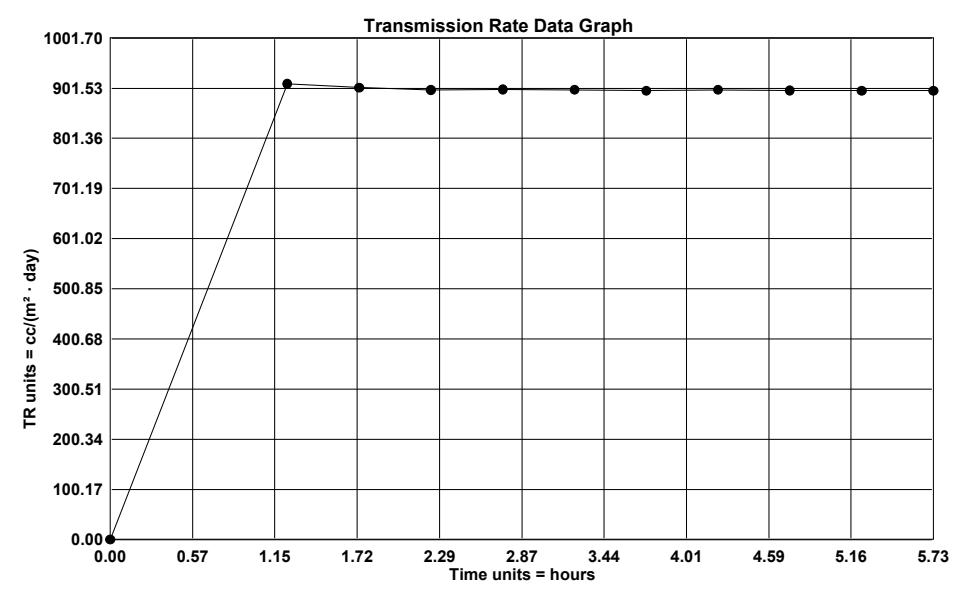
Transmission @100.0% Permeation @100.0% Rezero:

## IN SELECTED UNITS

896.61 cc/(m² · day) 17.932200 cc · mm/(m² · day) IN STANDARD UNITS

896.61 cc/(m² · day) 705.9921 cc · mil/(m² · day) 0.00111 cc/day

#### **OPERATOR COMMENTS:**



### **Auto Test Parameters:**

Date/Time

2/19/2018, 1:20 PM 2/19/2018, 1:55 PM

#### Test Parameters

Exam Time=20 min, ReZero Freq=2, ReZero Exam=20 min Exam Time=15 min, ReZero Freq=0, ReZero Exam=20 min

## 3. 10chit-PLA-10chit

#### MOCON OX-TRAN® 2/22 - Single Test Report

Instrument Serial #: 0317FN0197, Instrument Name: Device Name, Instrument #: <no value>

TEST	

Cell ID: Cell A Sample ID: 20p4chitm5·12a Material ID: Test ID: 483 User ID: Method: <no value>

#### **TEST DETAILS**

Temperature: 23.0/22.9 °C Test Time: 47.38 hours Turbo Cool: Off Compensate: On Test Gas RH: 90.0/89.9 %RH Exam Minutes: 30 minutes Test Mode: Continuous Concentration: 100.00 % Carrier Gas RH: 90.0/90.0 %RH ReZero Exam: 30 minutes Rezero: On Convergence Hours: N/A ReZero Frequency: 3 Sample Area: 3.14 cm<sup>2</sup> Conditioning: Off Conditioning Time: N/A Thickness: 0.02500 mm High Purge Time: 10 minutes Start Date: 1:28 PM, 5/16/2018 Individual Zero: Off High Purge: On Barometer: 742 mmHg Number of Cycles: N/A

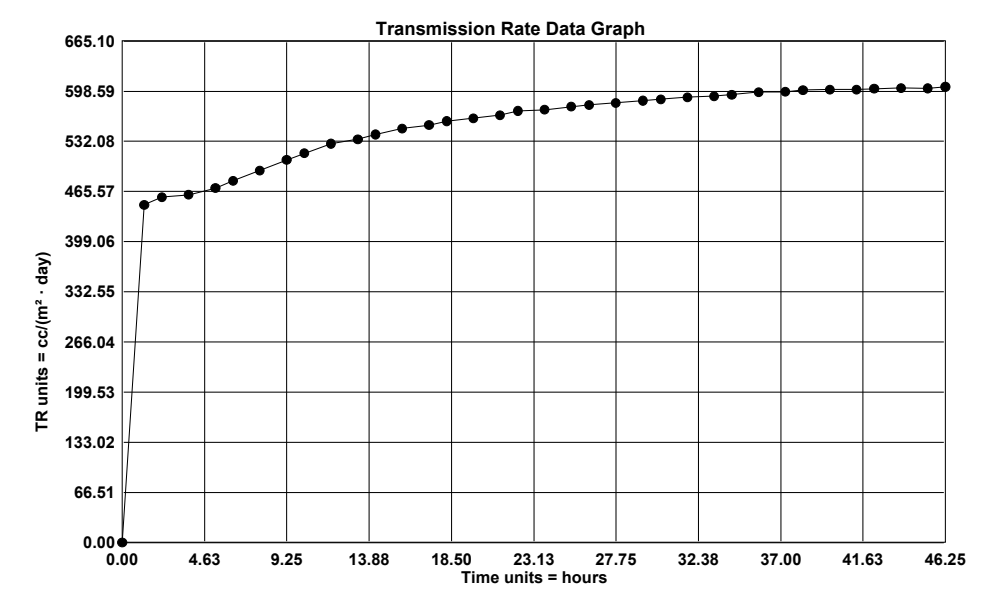
#### **TEST RESULTS**

IN SELECTED UNITS Transmission @100.0% 604.38 cc/(m<sup>2</sup> · day) Permeation @100.0% 15.109500 cc · mm/(m² · day) Rezero:

#### IN STANDARD UNITS

604.38 cc/(m<sup>2</sup> · day) 594.8622 cc · mil/(m² · day) 0.00201 cc/day

#### **OPERATOR COMMENTS:**



REFERENCES

#### REFERENCES

- [1] Hirasawa S, Saito Y, Nezu H, Ohashi N, Maruyama H. Analysis of drying shrinkage and flow due to surface tension of spin-coated films on topographic substrates. IEEE Trans Semicond Manuf 1997;10:438–44. doi:10.1109/66.641486.
- [2] Auras R, Harte B, Selke S. An Overview of Polylactides as Packaging Materials. Macromol Biosci 2004;4:835–64. doi:10.1002/mabi.200400043.
- [3] Hatui G, Dhibar S, Das CK, Bhattacharya P, Sahoo S. One Pot Synthesis of Graphene by Exfoliation of Graphite in ODCB. Graphene 2013;2:42–8. doi:10.4236/graphene.2013.21006.
- [4] Kumar A, Singh Negi Y, Choudhary V, Bhardwaj NK. Characterization of Cellulose Nanocrystals Produced by Acid-Hydrolysis from Sugarcane Bagasse as Agro-Waste " Characterization of Cellulose Nanocrystals Produced by Acid-Hydrolysis from Sugarcane Bagasse as Agro-Waste. J Mater Phys Chem 2014;2:1–8. doi:10.12691/jmpc-2-1-1.
- [5] Soni B, Hassan EB, Mahmoud B. Chemical isolation and characterization of different cellulose nanofibers from cotton stalks. Carbohydr Polym 2015;134:581–9. doi:10.1016/j.carbpol.2015.08.031.
- [6] Soni B, Hassan EB, Schilling MW, Mahmoud B. Transparent bionanocomposite films based on chitosan and TEMPO-oxidized cellulose nanofibers with enhanced mechanical and barrier properties. Carbohydr Polym 2016;151:779–89. doi:10.1016/j.carbpol.2016.06.022.
- [7] Huang H-D, Ren P-G, Xu J-Z, Xu L, Zhong G-J, Hsiao BS, et al. Improved barrier properties of poly(lactic acid) with randomly dispersed graphene oxide nanosheets. J Memb Sci 2014;464:110–8. doi:10.1016/J.MEMSCI.2014.04.009.
- [8] Liu H, Liu C, Peng S, Pan B, Lu C. Effect of polyethyleneimine modified graphene on the mechanical and water vapor barrier properties of methyl cellulose composite films. Carbohydr Polym 2018;182:52–60. doi:10.1016/j.carbpol.2017.11.008.
- [9] Park GT, Chang J-H, Park GT, Chang J-H. Comparison of Properties of PVA Nanocomposites Containing Reduced Graphene Oxide and Functionalized Graphene. Polymers (Basel) 2019;11:1–15. doi:10.3390/polym11030450.
- [10] Ren F, Tan W, Duan Q, Jin Y, Pei L, Ren P, et al. Ultra-low gas permeable cellulose nanofiber nanocomposite films filled with highly oriented graphene oxide nanosheets induced by shear field. Carbohydr Polym 2019;209:310–9. doi:10.1016/j.carbpol.2019.01.040.

- [11] Akhina H, Mohammed Arif P, Gopinathan Nair MR, Nandakumar K, Thomas S. Development of plasticized poly (vinyl chloride)/reduced graphene oxide nanocomposites for energy storage applications. Polym Test 2019;73:250–7. doi:10.1016/j.polymertesting.2018.10.015.
- [12] Ambrosio-Martín J, López-Rubio A, José Fabra M, Angel López-Manchado M, Sorrentino A, Gorrasi G, et al. Synergistic effect of lactic acid oligomers and laminar graphene sheets on the barrier properties of polylactide nanocomposites obtained by the in situ polymerization pre-incorporation method. J Appl Polym Sci 2016;133:1–11. doi:10.1002/app.42661.
- [13] Lee JH, Marroquin J, Rhee KY, Park SJ, Hui D. Cryomilling application of graphene to improve material properties of graphene/chitosan nanocomposites. Compos Part B Eng 2013;45:682–7. doi:10.1016/j.compositesb.2012.05.011.
- [14] Arul Jeya Kumar A, Srinivasan V. Thermal characteristics of chitosan dispersed poly lactic acid/basalt hybrid composites. Mater Express 2016;6:337–43. doi:10.1166/mex.2016.1310.
- [15] W. H. J. Fischer E, Sterzel H, K.-Z. Z. Wegner G. Investigation of the structure of solution grown crystals of lactide copolymers by means of chemical reactions. vol. 251. 1973. doi:10.1007/BF01498927.
- [16] Sonchaeng U, Iñiguez-Franco F, Auras R, Selke S, Rubino M, Lim LT. Poly(lactic acid) mass transfer properties. Prog Polym Sci 2018;86:85–121. doi:10.1016/j.progpolymsci.2018.06.008.
- [17] Helmke R. Oxygen-Barrier Packaging: How to Prevent Food Spoilage | Plastic Ingenuity. Plast Ingen 2017. https://www.plasticingenuity.com/blog/oxygen-barrier-packaging-methods (accessed April 11, 2019).
- [18] Jordá-Vilaplana A, Fombuena V, García-García D, Samper MD, Sánchez-Nácher L. Surface modification of polylactic acid (PLA) by air atmospheric plasma treatment. Eur Polym J 2014;58:23–33. doi:10.1016/j.eurpolymj.2014.06.002.
- [19] Banik I, Kim KS, Yun Y II, Kim DH, Ryu CM, Park CS, et al. A closer look into the behavior of oxygen plasma-treated high-density polyethylene. Polymer (Guildf) 2003;44:1163–70. doi:10.1016/S0032-3861(02)00847-9.
- [20] Auras R, Harte B, Selke S. Effect of water on the oxygen barrier properties of poly(ethylene terephthalate) and polylactide films. J Appl Polym Sci 2004;92:1790–803. doi:10.1002/app.20148.
- [21] Rocca-Smith JR, Pasquarelli R, Lagorce-Tachon A, Rousseau J, Fontaine S, Aguié-Béghin V, et al. Toward Sustainable PLA-Based Multilayer Complexes with Improved Barrier Properties. ACS Sustain Chem Eng 2019;7:3759–71. doi:10.1021/acssuschemeng.8b04064.

- [22] GONTARD N, GUILBERT S, CUQ J-L. Water and Glycerol as Plasticizers Affect Mechanical and Water Vapor Barrier Properties of an Edible Wheat Gluten Film. J Food Sci 1993;58:206–11. doi:10.1111/j.1365-2621.1993.tb03246.x.
- [23] Benbettaïeb N, Kurek M, Bornaz S, Debeaufort F. Barrier, structural and mechanical properties of bovine gelatin-chitosan blend films related to biopolymer interactions. J Sci Food Agric 2014;94:2409–19. doi:10.1002/jsfa.6570.
- [24] Giannakas A, Patsaoura A, Barkoula N-M, Ladavos A. A novel solution blending method for using olive oil and corn oil as plasticizers in chitosan based organoclay nanocomposites. Carbohydr Polym 2017;157:550–7. doi:10.1016/j.carbpol.2016.10.020.
- [25] Yan N, Capezzuto F, Lavorgna M, Buonocore GG, Tescione F, Xia H, et al. Borate cross-linked graphene oxide-chitosan as robust and high gas barrier films. Nanoscale 2016;8:10783–91. doi:10.1039/c6nr00377j.
- [26] Aulin C, Gällstedt M, Lindström T. Oxygen and oil barrier properties of microfibrillated cellulose films and coatings. Cellulose 2010;17:559–74. doi:10.1007/s10570-009-9393-y.
- [27] Ogawa K, Yui T, Okuyama K. Three D structures of chitosan. Int J Biol Macromol 2004;34:1–8. doi:10.1016/J.IJBIOMAC.2003.11.002.
- [28] Li N, Bai R. Copper adsorption on chitosan–cellulose hydrogel beads: behaviors and mechanisms. Sep Purif Technol 2005;42:237–47. doi:10.1016/J.SEPPUR.2004.08.002.
- [29] Ravi Kumar MN. A review of chitin and chitosan applications. React Funct Polym 2000;46:1–27. doi:10.1016/S1381-5148(00)00038-9.
- [30] Aulin C, Karabulut E, Tran A, Waisgberg L, Lindström T. Transparent nanocellulosic multilayer thin films on polylactic acid with tunable gas barrier properties. ACS Appl Mater Interfaces 2013;5:7352–9. doi:10.1021/am401700n.

#### 5. CONCLUSION AND RECOMMENDATIONS

## 5.1 Conclusions

In the preliminary study, oxygen permeability (OP) values of the in-house produced PLA films and PLA films coated with chitosan and chitosan-graphene were measured. Due to the variability of the OP results, these films were not used for further testing. Instead, LLDPE films were selected as a substrate to optimize the method of coating and as a proof of concept for the production of high oxygen barrier films. From OP tests on LLDPE and LLDPE coated films, we decided not to include hot pressing in sample preparation and to use commercial film as a substrate to minimize OP data variations. Then commercial PLA films were coated on both sides instead of on one side and tested for the OP. The OP results were compared with the theoretical oxygen barrier of multilayer films. Each section of the testing process is concluded below.

HPLA-coating-HPLA-HP films were prepared during the preliminary study and tested for OP at 23°C, 0% RH. The OP results showed unexpected high standard deviations. For example, an OP of 1254 kg m m<sup>-2</sup> s<sup>-1</sup> Pa<sup>-1</sup> for HPLA-HPLA-HP, and 943  $\pm$  1108 kg m m<sup>-2</sup> s<sup>-1</sup> Pa<sup>-1</sup> for HPLA-2chit-HPLA-HP, which could be attributed to the unevenness of the film thickness as well as the presence of cracks in the films due to processing conditions of the in-house laboratory extruder. Commercial LLDPE films were used to conduct the proof of concept of the coating study. No cracks were found in LLDPE-coating-LLDPE-HP films. The coated LLDPE films provided good transparency compared to the uncoated LLDPE films. OP was measured at 23°C and 0% RH and the results still showed high standard deviations and several data outliers due to the variability of the hot pressing. LLDPE-LLDPE-HP had an OP of 4670 kg m m<sup>-2</sup> s<sup>-1</sup> Pa<sup>-1</sup> and LLDPE-2chit-LLDPE-

HP had one for  $812 \pm 792$  kg m m<sup>-2</sup> s<sup>-1</sup> Pa<sup>-1</sup>. Hence, to better study the oxygen barrier mechanism of coated PLA films, commercial PLA films were used as a substrate for further studies, and hot pressing was not used for sample preparation.

PLA with 5 and 20 coating layers (PLA-5chit and PLA-20chit, respectively) were produced using a coating machine. SEM images of both films showed clearly distinguished interfaces between different coating layers, indicating the existence of individual deposited coating layer instead of a bulk one. Thicknesses of pure PLA film and the 20-layer coating part in PLA-20chit were 19  $\mu$ m and 16  $\mu$ m, respectively. The thickness of the 20-layer coating part was 10 times larger than the theoretical coating thickness (1.6  $\mu$ m for 20-layer coating) [1]. This was due to the curvature of the coating film, which was confirmed by the SEM image. Since the coating solutions were applied one by one on one side of the PLA film, this procedure enabled the surface of the coated solution as well as the coated side of PLA to shrink due to surface tension [2], creating cracks on the coating layers when the films were flattened after drying.

Thermal stability and transition stages were tested on PLA, chitosan, graphite, chiGRH, PLA-5chit, PLA-20chit, PLA-5chitGRH, and PLA-20chitGRH using TGA and DSC. Degradation of pure PLA started at 259°C and ended at 388°C, with a peak derivative weight at 360°C. Graphite only had 5% weight loss within the testing range (0-600°C). Chitosan had a major decomposition from 190°C and lasted to 600°C, with a peak at 289°C and started to have a stable weight change speed at 410°C. Then, decomposition stages of coated PLA films were characterized and analyzed. Weight percentage of PLA in PLA-5chit, PLA-20chit, PLA-5chitGRH, and PLA-20chitGRH were calculated as 91%, 82%, 94%, and 70%, respectively, using TGA results (% weight loss of each film and coating component, % residue of PLA, and % residue of chitGRH). Comparison of the

transition stages and the degrees of crystallinity showed that the coating layers did not affect the crystallinity of the PLA substrate, which means that the bulk structure of the PLA films remained unaltered.

OP tests were done on PLA, PLA-5chit and PLA-20chit at 23°C, 0% and 50% RH. Under both RH conditions, OP values of OP values of PLA-20chit and PLA-5chit were not significantly different. Large standard deviations of OP values were only found in films with coating layers. These were because of the existence of the cracks in coating layers as confirmed by SEM images.

Coating-PLA-coating films (3 or 10 layers of chitosan or chitGRH coating on each side of PLA film) were then produced to prevent curvature and cracks. OP tests were conducted at 23°C and various RH from 0% to 90%. Small standard deviations of OP values illustrated the success in choosing to do coating on both sides of the substrate film instead on one side. The OP data showed that: 1) chitosan is more hydrophilic than PLA; 2) RH only affected OP of the coated PLA films when they were tested at RH at 60% and 90% RH; 3) the more the coating layers, the better the oxygen barrier; 4) graphene is more effective in 20-layer coating than in 6 layers coating at 60% and 90% RH, and less effective at 0% and 30% RH; and 5) storage conditions are important factors that affected the permeation mechanism.

A high oxygen barrier packaging material need an OP that lower than 5 x  $10^{-20}$  kg m m<sup>-2</sup> s<sup>-1</sup> Pa<sup>-1</sup> with a thickness of 20  $\mu$ m at 23°C and 1 atm [3]. From this study, 10chit-PLA-10chit and 10chitGRH-PLA-10chitGRH without conditioning at 0% and 30% RH, 3chitGRH-PLA-3chitGRH at 0% RH without conditioning, and 3chit-PLA-3chit at 0% RH with conditioning can be considered high

oxygen barrier films, with potentials to future development of high oxygen barrier compostable polymeric films.

## 5.2 Recommendations

This study investigated the effects of chitosan and chitGRH coating on oxygen barrier properties of PLA film at 23°C and 0, 30, 60, and 90% RH. We suggest including more tests between 30% and 90% RH for better understanding effect of moisture on oxygen permeation. Also, it is important to understand the changes in properties of the coated films under different temperatures for commercial use. To better understand the oxygen permeation mechanism, OP measurements on PLA-coating-PLA films and PLA films with bulk single layer coating are needed. Since moisture content is one of the factors that affects most OP, we suggest all future samples being stored at dry conditions before testing.

RH did not show any significant effects on the OP values of all coated PLA films at 23°C, 0 and 30% RH, and no effect on 10chitGRH-PLA-10chitGRH at 0, 30, and 60% RH. OPs of 3chit-PLA-3chit, 3chitGRH-PLA-3chitGRH, and 10chit-PLA-10chit only increased significantly from 30% to 60% RH, and OP of 10chitGRH-PLA-10chitGRH started a significant increase from 60% to 90%. The clear transition of oxygen permeation behavior called for a future study between 30% to 60% RH for 3chit-PLA-3chit, 10chit-PLA-10chit, and 3chitGRH-PLA-3chitGRH, and between 60% to 90% RH for 10chitGRH-PLA-10chitGRH, and to understand the mechanism of OP variation as RH changes.

In this study, we tested the OP at 23°C between 0 and 90 %RH; however, commercial use of the films will require a high oxygen barrier at various temperatures depending on product

types and transportation methods. Therefore, future testing at 4°C (e.g., in a refrigerator) and 45°C (e.g., on a tarmac or in a truck with sun exposure) is needed.

For the effect of water plasticization, the interaction between water and chitosan and the effect on OP should be elucidated since this factor is more important than water plasticization affected OP. Thus, future work should also include PLA-coating-PLA films to check how PLA films can protect the chitosan and chitGRH layer inside.

We did not study the effect of multilayer coating method on oxygen permeation. Hence, it is important to understand if a multilayer coating and a single layer coating with same thickness will show a different OP value.

Most of the samples in this study were not kept in dry conditions before the OP tests. With the fact that storage conditions have an effect on OP values as shown in section 4.3.2.4, we suggest that all the film samples should be kept at dry conditions before testing.

**REFERENCES** 

## **REFERENCES**

- [1] RK PrintCoat Instruments Ltd. RK PrintCoat Instruments K303 Multicoater n.d. www.rkprint.com (accessed April 22, 2019).
- [2] Hirasawa S, Saito Y, Nezu H, Ohashi N, Maruyama H. Analysis of drying shrinkage and flow due to surface tension of spin-coated films on topographic substrates. IEEE Trans Semicond Manuf 1997;10:438–44. doi:10.1109/66.641486.
- [3] Helmke R. Oxygen-Barrier Packaging: How to Prevent Food Spoilage | Plastic Ingenuity. Plast Ingen 2017. https://www.plasticingenuity.com/blog/oxygen-barrier-packaging-methods (accessed April 11, 2019).